

2007

A Late Holocene Reconstruction of Ocean Climate Variability in the Gulf of Maine, USA, Based on Calibrated Isotope Records and Growth Histories from the Long-lived Ocean Quahog (*Arctica islandica* L.)

Alan D. Wanamaker

Follow this and additional works at: <http://digitalcommons.library.umaine.edu/etd>

 Part of the [Climate Commons](#)

Recommended Citation

Wanamaker, Alan D., "A Late Holocene Reconstruction of Ocean Climate Variability in the Gulf of Maine, USA, Based on Calibrated Isotope Records and Growth Histories from the Long-lived Ocean Quahog (*Arctica islandica* L.)" (2007). *Electronic Theses and Dissertations*. 101.

<http://digitalcommons.library.umaine.edu/etd/101>

This Open-Access Dissertation is brought to you for free and open access by DigitalCommons@UMaine. It has been accepted for inclusion in Electronic Theses and Dissertations by an authorized administrator of DigitalCommons@UMaine.

**A LATE HOLOCENE RECONSTRUCTION OF OCEAN CLIMATE VARIABILITY IN
THE GULF OF MAINE, USA, BASED ON CALIBRATED ISOTOPE RECORDS AND
GROWTH HISTORIES FROM THE LONG-LIVED
OCEAN QUAHOG (*ARCTICA ISLANDICA* L.)**

By

Alan D. Wanamaker Jr.

B.A. University of New Hampshire, 1997

M.A. University of New Hampshire, 1998

A THESIS

Submitted in Partial Fulfillment of the

Requirements for the Degree of

Doctor of Philosophy

(in Earth Sciences)

The Graduate School

The University of Maine

May, 2007

Advisory Committee:

Karl J. Kreutz, Associate Professor, Department of Earth Sciences, and Climate Change Institute, Advisor

Daniel F. Belknap, Professor, Department of Earth Sciences, School of Marine Sciences, and Climate Change Institute

Harold W. Borns Jr., Professor Emeritus, Department of Earth Sciences, and Climate Change Institute (Honorary Director)

Kirk A. Maasch, Professor, Department of Earth Sciences, and Climate Change Institute

Neal R. Pettigrew, Associate Professor, School of Marine Sciences

LIBRARY RIGHTS STATEMENT

In presenting this thesis in partial fulfillment for an advanced degree at The University of Maine, I agree that the Library shall make it freely available for inspection. I further agree that permission for “fair use” copying of this thesis for scholarly purposes may be granted by the Librarian. It is understood that any copying or publication of this thesis for financial gain shall not be allowed without my written permission.

Signature:

Date:

**A LATE HOLOCENE RECONSTRUCTION OF OCEAN CLIMATE VARIABILITY IN
THE GULF OF MAINE, USA, BASED ON CALIBRATED ISOTOPE RECORDS AND
GROWTH HISTORIES FROM THE LONG-LIVED
OCEAN QUAHOG (*ARCTICA ISLANDICA* L.)**

By

Alan D. Wanamaker Jr.

Thesis Advisor: Dr. Karl J. Kreutz

An Abstract of the Thesis Presented
in Partial Fulfillment of the Requirements for the
Degree of Doctor of Philosophy
(in Earth Sciences)
May, 2007

Understanding regional patterns of interannual to decadal-scale climate variability over the past 1000 years is critical for evaluating recently observed trends in atmosphere/ocean conditions, particularly in highly-productive ecosystems such as the Gulf of Maine (GOM) that are sensitive to minor changes in climate and/or changes in slope water input. To develop quantitative relationships between bivalve shell chemistry ($\delta^{18}\text{O}_c$) and growing conditions, aquaculture-based experiments were developed using *Mytilus edulis* collected in the GOM and Greenland. These experiments yielded a highly accurate and precise paleothermometer [e.g., $T\text{ }^\circ\text{C} = 16.28 (\pm 0.10) - 4.57 (\pm 0.15) \{ \delta^{18}\text{O}_c \text{ VPBD} - \delta^{18}\text{O}_w \text{ VSMOW} \} + 0.06 (\pm 0.06) \{ \delta^{18}\text{O}_c \text{ VPBD} - \delta^{18}\text{O}_w \text{ VSMOW} \}^2$; $r^2 = 0.99$; $N = 323$; $p < 0.0001$] for *M. edulis*, and the techniques were applied to the long-lived bivalve species *Arctica islandica*. To examine ocean variability in the Western GOM

during the last millennium, a 142-year-old living *A. islandica* and three fossil *A. islandica* shells (corrected $^{14}\text{C}_{\text{AMS}} = 1030 \pm 78 \text{ AD}$; $1320 \pm 45 \text{ AD}$; $1357 \pm 40 \text{ AD}$) were collected for $\delta^{18}\text{O}$ and growth increment analysis. The standardized annual growth index (SGI) of the modern shell is significantly correlated with continuous GOM plankton recorder data (1961 – 2003; *Calanus finmarchicus*; $r^2 = 0.55$; $p < 0.0001$), and SGIs during the late Holocene contain significant periods of 2-6 years, suggesting that slope water variability coupled with North Atlantic Oscillation (NAO) dynamics is primarily responsible for productivity variability. Mean shell-derived isotopic changes were $+0.47 \text{ ‰}$ from 1000 AD to present, and likely reflect a $2 \text{ }^\circ\text{C}$ cooling caused by an increase in Labrador Current (LC) transport of $\sim 0.7 \text{ Sv}$ ($1 \text{ Sv} = 10^6 \text{ m}^3 \text{ s}^{-1}$) and a corresponding decrease in Gulf Stream influence on GOM water temperatures during the past millennium. This hypothesis is consistent with modern observational relationships among the LC, GOM water temperatures, NAO, and Atlantic Multi-Decadal Oscillation (AMO). These results corroborate recent evidence of a large-scale cooling of slope waters and/or dynamical oceanographic changes outside the GOM during the Holocene, and suggest that a direct link exists between the GOM and Northwestern Atlantic.

ACKNOWLEDGEMENTS

This dissertation is dedicated to Jack and Jayna Wanamaker. May you both follow your passions and curiosities throughout life. To my wife Ellen, I thank you for supporting and encouraging me during these five years. Your selflessness and love is greatly appreciated. I thank my mother, Carol Vaughan, who taught me the value of hard work and dedication.

I thank my primary advisor, Dr. Karl Kreutz, who provided fantastic opportunities, countless hours of guidance, and helpful feedback throughout the entire project. To the other members of my dissertation committee, Dr. Daniel Belknap, Dr. Harold Borns, Dr. Kirk Maasch, and Dr. Neal Pettigrew, I thank you for the essential guidance and feedback during this work. The work presented here is greatly improved because of your constructive criticism and encouragement.

I thank Dr. Stephen Norton for his mentorship, and for inviting me to study at UMaine. I also thank Jeff Owen for encouraging me to come to UMaine. Dr. Bernd Schöne (University of Mainz) graciously hosted me at his lab in Germany, and taught me how to micromill and prepare *Arctica islandica* samples. Douglas “Cap” Introne spent a good portion of the last five years teaching me about mass spectrometry, and helping me run samples. Thank you, Cap. I thank Scott Feindel at the Darling Marine Center for his expertise, dedication, and help with all of the aquaculture work. I also thank family friends, Larry and Leah Marquis, for their support and inspiration to pursue my formal education. I thank Erich Osterberg for his friendship and many conversations about climate science. Bucky and Sue Owen warmly provided me with a place to stay for two years while I was commuting to UMaine.

I am very grateful for the financial support that I received during my tenure as a graduate student. All of the research presented here was supported by the National Science Foundation (NSF ATM-0222553). Additional support from the Department of Earth Sciences and the Center for Science and Mathematics Education Research was provided via Graduate Assistantships. In addition, multiple grants from the Association of Graduate Students at UMaine provided travel support for research and conferences.

The following acknowledgements refer to help and support I received for the research presented in chapters two through six. Chapter 2 is published in *Geochemistry, Geophysics, Geosystems* (2006, 7, Q09011, doi:10.1029/2005GC001189) with Karl J. Kreutz, Harold W. Borns Jr., Douglas S. Introne, Scott Feindel, and Bruce J. Barber. We thank Paul Rawson (University of Maine, School of Marine Sciences) for his advice on mussel cultivation, Nancy Raymond and Zachary von Hasseln (University of Maine students) for help maintaining the aquaculture systems, Timothy Miller (Darling Marine Center) for help with logistics and space, and Marty Yates for X-ray diffraction analysis (University of Maine, Earth Sciences). We also thank Mary Elliot and an anonymous reviewer for their insightful and constructive comments that improved this manuscript.

Chapter 3 is in press in *Paleoceanography* (2007) with Karl J. Kreutz, Harold W. Borns Jr., Douglas S. Introne, Scott Feindel, Svend Funder, Paul D. Rawson, and Bruce J. Barber. We thank Robin Abbott and colleagues from VECO Polar Resources for travel and accommodations while in Kangerlussuaq, Greenland, Fartato Olsen for providing boating and bivalve collecting logistics in Sisimiut, Greenland, 109th Air National Guard (Albany, NY) for transportation to and from Greenland, Zachary von Hasseln (University of Maine) for aquaculture set-up and maintenance, Timothy Miller (Darling Marine

Center) for help with logistics and space, Wendy Abdi for algal paste $\delta^{13}\text{C}$ analysis (University of Ottawa, G.G. Hatch Isotope Laboratories), and Erin Fisher Owen for $\delta^{13}\text{C}$ DIC/Salinity data (University of Maine). Bivalves collected in Greenland were transported into the USA and Maine with appropriate federal and state permits, in addition to written permission granted by the Denmark Directorate of Environment and Nature. We also thank David Dettman and David Gillikin for their insightful and constructive comments that greatly improved this manuscript.

Chapter 5 is in review at the International Journal of Earth Sciences with Karl J. Kreutz, Bernd R. Schöne, Kirk A. Maasch, Andrew Pershing, Harold W. Borns Jr., Douglas S. Introne, and Scott Feindel. We thank Dan Belknap and Joe Kelley (University of Maine) for the fossil shells from vibracore SBVC9609, David Rodland and Sven Baier for their help preparing shell samples (INCREMENTS Research Group, University of Frankfurt), NOSAMS at Woods Hole Oceanographic Institution for AMS analyses, and the Association of Graduate Students (AGS) at the University of Maine for travel funds to the University of Frankfurt. The NOAA (Ocean-Atmosphere Research/Earth System Research Laboratory/Physical Sciences Division, Boulder, Colorado, USA, [<http://www.cdc.noaa.gov/>]) provided the Kaplan SST V2 dataset. This study has been made possible in part by a German Research Foundation (DFG) grant (to BRS) within the framework of the Emmy Noether Program.

Chapter 6 is in review at Climate Dynamics with Karl J. Kreutz, Bernd R. Schöne, Neal R. Pettigrew, Harold W. Borns Jr., Douglas S. Introne, Daniel Belknap, Kirk A. Maasch, and Scott Feindel. We thank David Rodland and Sven Baier for their help preparing shell samples (INCREMENTS Research Group, University of Frankfurt),

NOSAMS at Woods Hole Oceanographic Institution for AMS analyses, Association of Graduate Students (University of Maine) for travel support, Lloyd Keigwin, David Lund, and Thomas Marchitto for providing proxy data for Figure 6.5, and Fei Chai (University of Maine) for early conversations that shaped this manuscript. Prince 5 station data were provided by Marine Environmental Data Services (Fisheries and Ocean Division of Canada; available at http://www.meds-sdmm.dfo-mpo.gc.ca/zmp/main_zmp_e.html). This study has been made possible in part by a German Research Foundation (DFG) grant (to BRS) within the framework of the Emmy Noether Program.

TABLE OF CONTENTS

ACKNOWLEDGEMENTS.....	ii
LIST OF TABLES.....	xii
LIST OF FIGURES.....	xiv
Chapter	
1. INTRODUCTION.....	1
2. AN AQUACULTURE-BASED METHOD FOR CALIBRATED BIVALVE ISOTOPE PALEOTHERMOMETRY.....	7
2.1. Introduction.....	8
2.2. Materials and Methods.....	10
2.2.1 Experimental Bivalve.....	10
2.2.2. Aquaculture Design and Implementation.....	11
2.2.3. Sample Preparation and Analysis.....	15
2.2.4. Calibration of Temperature and $\delta^{18}\text{O}$ Relationships.....	16
2.3. Results and Discussion.....	18
2.4. Improvements and Future Work.....	20
2.5. Summary.....	21

3. EXPERIMENTAL DETERMINATION OF SALINITY, TEMPERATURE, GROWTH, AND METABOLIC EFFECTS ON SHELL ISOTOPE CHEMISTRY OF <i>MYTILUS EDULIS</i> COLLECTED FROM MAINE AND GREENLAND.....	22
3.1. Introduction.....	23
3.2. Materials and Methods.....	26
3.2.1. Animal Collection and Genetic Identification.....	26
3.2.2. Aquaculture Design and Implementation.....	27
3.2.3. Growth Rate Determination.....	31
3.2.4. Sample Preparation and Analysis.....	31
3.2.5. Calibration of Temperature and $\delta^{18}\text{O}_c$ Relationships.....	33
3.3. Results and Discussion.....	34
3.3.1. Size and Shell Growth Rate Effects on $\delta^{18}\text{O}_c$	34
3.3.2. Possible Physiologic or Genetic Effects on $\delta^{18}\text{O}_c$ Based on Collection Location.....	34
3.3.3. Paleotemperature Relationship for <i>M. edulis</i>	36
3.3.4. Relationships Between $\delta^{18}\text{O}_c$ and $\delta^{13}\text{C}_c$, and Metabolic Carbon Isotope Effects.....	40
3.4. Conclusions.....	45

4. ASSESSING THE EFFECTS OF TEMPERATURE AND SALINITY ON SHELL CARBONATE OF THE LONG-LIVED BIVALVE <i>ARCTICA ISLANDICA</i> : AN AQUACULTURE-BASED STUDY.....	47
4.1. Introduction.....	48
4.2. Materials and Methods.....	49
4.2.1. Experimental Bivalve – <i>Arctica islandica</i>	49
4.2.2. Animal Collection.....	52
4.2.3. Aquaculture Design and Implementation.....	52
4.2.4. Sample Preparation and Analysis.....	54
4.3. Results and Discussion.....	55
4.3.1. Growth During Culture.....	55
4.3.2. Effects of Temperature and Salinity on Shell Carbonate ($\delta^{18}\text{O}_{\text{aragonite}}$).....	58
4.3.3. Previous Work- An <i>In situ</i> Study Using <i>A. islandica</i>	59
4.4. Improvements and Future Work.....	60
4.4.1. Growth Estimation.....	60
4.4.2. Aquaculture Design and Culture Duration.....	61
4.5. Conclusions.....	62

5. A LATE HOLOCENE PALEO-PRODUCTIVITY RECORD IN THE WESTERN GULF OF MAINE, USA INFERRED FROM GROWTH HISTORIES OF THE LONG-LIVED OCEAN QUAHOG (<i>ARCTICA ISLANDICA</i>).....	63
5.1. Introduction.....	63
5.2. Methods and Results.....	66
5.2.1. Animal Collection.....	66
5.2.2. Sample Preparation.....	66
5.2.3. Radiocarbon Dating.....	67
5.2.4. Sclerochronological Analyses.....	67
5.2.5. Detrending Age-Related Growth Patterns.....	68
5.2.6. Continuous Plankton Recorder (CPR) Data.....	69
5.2.6.1. Relationship between CPR Data and Shell Growth.....	70
5.2.7. Relationship between SST and Shell Growth.....	71
5.2.8. Relationship with the NAO and Shell Growth.....	71
5.2.9. Calibrated Late Holocene SGI Time-Series.....	72
5.2.10. Spectral Analyses.....	73

5.3. Discussion.....	77
5.3.1. A Paleo-productivity Proxy - SGI and <i>Calanus finmarchicus</i> abundance levels.....	77
5.3.2. North Atlantic Climate Variability and Ecosystem Dynamics in the Gulf of Maine.....	78
5.3.2.1. Relationship between the NAO and Shell Growth.....	80
5.3.3. Interannual-to-Decadal SGI Variations.....	81
5.4. Conclusions and Future Work.....	82
6. COUPLED NORTH ATLANTIC SLOPE WATER FORCING ON GULF OF MAINE TEMPERATURES OVER THE PAST MILLENNIUM.....	83
6.1. Introduction.....	83
6.2. Experimental Methods.....	88
6.2.1. Sample Collection.....	88
6.2.2. Sclerochronological and Isotope Analyses.....	88
6.2.3. Calculation of Sea Water Temperatures and Shell $^{14}\text{C}_{\text{AMS}}$ Dating.....	89
6.2.4. Instrumental Data.....	90
6.3. Results and Discussion.....	90
6.3.1. Relationship between Air Temperatures and Sea Water Temperatures.....	90
6.3.2. Labrador Current Influence on GOM Water Temperatures.....	91
6.3.3. NAO and AMO Forcing of GOM Water Temperatures.....	93

6.3.4. Shell-Derived Isotope Record and Reconstructed GOM Water Temperatures During the Last Millennium.....	94
6.3.5. Independent Evidence for late Holocene Cooling in the Northwestern Atlantic based on Multiple Marine and Terrestrial Records.....	96
6.4. Conclusions and Future Work.....	100
7. CONCLUDING REMARKS.....	101
REFERENCES CITED.....	106
APPENDICES.....	130
Appendix A. Supplementary Data for Chapter 2.....	131
Appendix B. Supplementary Data for Chapter 3.....	134
Appendix C. Supplementary Text and Figures for Chapter 6.....	140
BIOGRAPHY OF THE AUTHOR.....	144

LIST OF TABLES

Table 3.1.	Culture data for this study including temperature (± 0.5 °C, 1 σ), salinity (± 0.1 PSU), and oxygen isotopic composition of water ($\delta^{18}\text{O}_w$ ‰ [VSMOW], N = # of weeks that weekly samples were collected and analyzed, and 1 σ).....30
Table A.1.	Information for each column [1-13] is shown here: sample identification [1], shell oxygen isotopic values ‰ (VPDB) [2], shell carbon isotopic values ‰ (VPDB) [3], salinity (ppt) [4], shell length (mm) [5], water isotopic composition ‰ (VSMOW) [6], calcite - water (VPBD - VSMOW) [7], measured temperature (°C) [8], predicted temperature (°C) [9], temperature deviation (°C) [10], months grown [11], estimated growth rates (mm/month) [12], and estimated new linear growth (mm) [13].....131
Table B.1.	Information for each column [1-16] is shown here: collection location / age class [1], sample ID [2], culture temperature (°C) [3], culture salinity (PSU) [4], shell $\delta^{13}\text{C}$ ‰ (VPDB) [5], shell $\delta^{18}\text{O}$ ‰ (VPDB) [6], water $\delta^{18}\text{O}$ ‰ (VSMOW) [7], $\delta^{18}\text{O}$ ‰ shell – water (VPBD-VSMOW) [8], shell length (mm) [9], growth rate (mm/month) [10], linear shell removed

(mm) [11], predicted temperature (°C) [12], temperature deviation (°C) [13], estimated $\delta^{13}\text{C}$ DIC ‰ (VPDB) [14], predicted shell equilibrium $\delta^{13}\text{C}$ ‰ (VPDB) [15], estimated shell disequilibrium $\delta^{13}\text{C}$ ‰ (VPDB) [16].....134

LIST OF FIGURES

Figure 2.1.	Schematic diagram of the experimental design.....	12
Figure 2.2.	Temperatures for each of the four freshwater baths are shown with the 8-month mean and standard deviation.....	13
Figure 2.3.	The oxygen isotopic composition ($\delta^{18}\text{O}_w$) for each of the 24 growing environments is shown for a 5-month period.....	14
Figure 2.4.	The <i>M. edulis</i> (Maine juveniles) paleotemperature relationship is compared to the calcite equations of Epstein et al. (1953), Horibe and Oba (1972) and Kim and O'Neil (1997).....	19
Figure 3.1.	Location of <i>M. edulis</i> samples collected in Maine and western Greenland.....	27
Figure 3.2.	Schematic diagram of the experimental design.....	29
Figure 3.3.	Temperature offset is compared to shell length and average growth rates	35
Figure 3.4.	Paleotemperature relationships from this study, Wanamaker et al. (2006), Epstein et al. (1953), and Kim and O'Neil (1997).....	37
Figure 3.5.	Linear correlations between biogenic $\delta^{18}\text{O}_c$ and $\delta^{13}\text{C}_c$ from adult <i>M. edulis</i> collected in Maine and Greenland and juvenile <i>M. edulis</i> from Greenland	40

Figure 3.6.	Relationship between estimated dissolved inorganic carbon ($\delta^{13}\text{C}_c$ DIC; related to salinity) during culture and shell $\delta^{13}\text{C}_c$	42
Figure 3.7.	Relationship between ambient isotopic composition of water ($\delta^{18}\text{O}_w$) during culture and estimate of shell $\delta^{13}\text{C}_c$ disequilibrium, where $\delta^{13}\text{C}_c$ of 0 ‰ represents isotopic equilibrium is shown.....	43
Figure 4.1.	<i>Arctica islandica</i> (ocean quahog) being measured for shell length.....	51
Figure 4.2.	Temperatures for each of the four freshwater baths are shown with the 5-month mean and standard deviation.....	53
Figure 4.3.	The oxygen isotopic composition ($\delta^{18}\text{O}_w$) for each of the 12 growing environments is shown for the 5-month period.....	54
Figure 4.4.	Growth of tagged animals as a function of growing temperature.....	56
Figure 4.5.	Growth of tagged animals as a function of shell height.....	57
Figure 4.6.	Oxygen isotope results for <i>A. islandica</i> during culture compared to the mollusk equation of Grossman and Ku (1986).....	59
Figure 5.1.	The general geographic map for the Gulf of Maine, noting Casco Bay, shell location, and Boothbay Harbor is shown.....	65
Figure 5.2.	Annual growth of shell SF1 and ontogenetic age.....	69
Figure 5.3.	Time-series of shell SF1 SGI and zooplankton <i>Calanus finmarchicus</i> relative abundance is shown.....	70
Figure 5.4.	The late Holocene SGI time-series is illustrated.....	72
Figure 5.5.	Wavelet spectrums for shells SF1 and SBVC9609-30cm using the Morlet wavelet.....	74

Figure 5.6.	Spectral analysis for 142-year-old shell SF1 using MTM and SSA using KSpectra is shown.....	75
Figure 5.7.	Spectral analysis for 114-year-old shell SBVC9609-30cm using MTM and SSA using KSpectra is shown.....	76
Figure 6.1.	The general bathymetric map for the Gulf of Maine region and Eastern Canada, noting long-term climate stations and the shell collection location in the Western Gulf of Maine are shown.....	86
Figure 6.2.	Shell isotope-derived 30 m water temperature and BBH SST record are illustrated.....	91
Figure 6.3.	The relationship between Labrador Current (LC) transport (Han and Li, 2004) from the Eastern Newfoundland Slope (NE Track 096) and water temperatures in the Gulf of Maine with a 1-year lag are shown.....	92
Figure 6.4.	Late Holocene shell-derived water temperatures with a fixed salinity and $\delta^{18}\text{O}_c$ record, and late Holocene shell-derived salinity values with fixed mean water temperatures are shown.....	95

Figure 6.5.	Late Holocene shell-derived water temperatures with a fixed salinity and $\delta^{18}\text{O}_c$ record (this study), part of the Mg/Ca ratio derived bottom water temperatures from the Laurentian Slope (1854 m) (Marchitto and deMenocal, 2003), part of the alkenone-based SST record (Keigwin et al., 2003) from Emerald Basin (Scotian Shelf), and estimated Gulf Stream Transport in the Straits of Florida with 95 % confidence intervals (Lund et al., 2006) are shown for comparison.....	97
Figure 6.6.	Correlation (r) between winter (DJFM) NAO index and NCEP reanalysis precipitation rates during the same season from 1950-2003.....	99
Figure C.1.	High-resolution oxygen isotope profiles for shells SBVC9609-48cm and SBVC9609-40cm are shown with an approximate calendar age.....	142
Figure C.2.	High-resolution oxygen isotope profiles for shells SBVC9609-30cm and SF1 are shown with an approximate calendar age.....	143

1. Introduction

Climate results from the interaction of incoming solar radiation with many systems (lithosphere, hydrosphere, atmosphere, biosphere) and sub-systems (oceans, continents, cryosphere). There are many interactions and feedbacks within the climate system that are poorly understood. In order to fully understand Earth's climate history, records that span multiple time scales (daily-to-tectonic) and represent each sub-system must be utilized to elicit more than 4.5 billion years of climate history into the Holocene Epoch. In this dissertation, ocean variability in the Gulf of Maine is the major sub-system that will be explored, particularly during the last millennium, where few long-term oceanographic records exist prior to the 1950s.

Understanding climate variability during the Holocene (~ last 10,000 years) is crucial to developing a context for modern and future climate change, because climate during the Holocene represents a time during Earth's history that has climatic boundary conditions similar to those experienced now and in the near future (e.g., Mayewski et al., 2004). Further, the late Holocene experienced abrupt climate shifts (e.g., Medieval Warm Period [MWP] and the Little Ice Age [LIA]) on relatively short time scales (decadal-to-centennial). The magnitude, timing and spatial distribution of these late Holocene climate events are still poorly understood (e.g., Lamb, 1965; Fagan, 2000). Thus, documenting the spatial and temporal patterns of the MWP and LIA is an essential goal of paleoclimatology. Because the MWP and LIA have been primarily documented in Europe, less is known about the global extent of these climate modes (e.g., Bradley et al., 2003). It appears that the LIA was a global event (e.g., Kreutz et al., 1997; Mayewski et al., 2004; Maasch et al., 2005), but far less is known about the magnitude, and spatial extent of the warming signal during the MWP (e.g., Bradley and Jones, 1993). Currently, global climate change is happening at a rapid rate (IPCC, 2007). Because the MWP and the LIA climate events are considered primarily natural (prior to significant human impact

on greenhouse gases) and they represent both an anomalously warm and cold climate-state, an understanding of the magnitude, timing, and spatial extent of these events could dramatically help our understanding of present climate change, which now involves a human-induced component (IPCC, 2007). The instrumental period is short (generally less than 100 - 150 years) and is spatially limited (biased to Europe and N. America). Thus proxy climate records are used to elucidate past climate variability. Proxy records have dramatically improved the documentation of the climate on multiple time scales (e.g., ice-age cycles recorded in marine sediments [Raymo, 1994] and ice cores [Petit et al., 1999]; the El Niño Southern Oscillation recorded in corals [Cole et al., 1993]).

In order to develop a context of Holocene climate variability, proxy records must be globally distributed and diverse (e.g., different types of proxies that represent multiple climate sub-systems) (Mayewski et al., 2004). Further, proxy records need to accurately represent climate, therefore proxy records that are calibrated (with instrumental records or experimentally) offer a more complete representation of climate system (e.g., temperature, precipitation, atmospheric strength, productivity, etc.), and result in paleoclimatic reconstructions that are better constrained. The use of oxygen isotopes in biogenic carbonates has greatly improved our understanding of global climate change on 10,000 – 100,000 year time scales (temperature and ice-volume changes during ice-age cycles [Emiliani, 1966; Shackleton, 1967]). In addition, because biogenic carbonates (bivalves, corals, foraminifera) are globally distributed (both temporally and spatially) they provide an opportunity to reconstruct past ocean environments on time scales from interannual-to-decadal (bivalves and corals) to centennial-to-millennial (bivalves, corals, foraminifera).

Although climate during the Holocene is generally considered relatively stable compared to glacial periods (e.g., Petit et al., 1999), there is recent and substantial evidence for dramatic changes in North Atlantic climate, including increased Arctic air temperatures (Thompson and Wallace, 1998), decreased extent of sea ice (Johannessen

et al., 1999), decreased extent of permafrost (Smith et al., 2005; Zimov et al., 2006), increased melting of the Greenland Ice Sheet (Krabill et al., 2004; Chen et al., 2006), freshening of the North Atlantic (Dickson et al., 2002; Curry and Mauritzen, 2005), and slowing of the sub-polar gyre (Häkkinen and Rhines, 2004). Further, the observed freshening of the North Atlantic could cause instability in the thermohaline circulation, because a freshwater “cap” or layer in the Greenland and Labrador Seas would impede the formation of North Atlantic Deep Water (NADW) (Dickson et al., 2002). Curry and Mauritzen (2005) even suggested that an abrupt climate shift (cooling) could result from disrupting the formation of NADW, and the warm return current (Gulf Stream) would diminish and possibly shut down, causing significant and abrupt climate shifts in N. America and Europe. Variability in NADW formation in the Labrador Sea would also impact the transport of the cold Labrador Current, which flows along the eastern coasts of Canada and the United States (Lazier and Wright, 1993). Recently, Sachs (2007) suggested that Northwest Atlantic slope waters cooled by 4-10°C during the Holocene Epoch from Canada to the mid-US coast, possibly related to a shift in the Gulf Stream. Understanding the mechanisms responsible for the recently observed climate change, and interannual to decadal-scale climate variability in the North Atlantic sector therefore remains a fundamental research problem (e.g., Hurrell, 1995; Dickson et al., 1996; Griffies and Bryan, 1997; Tourre et al., 1999; Marshall et al., 2001; Sutton and Hodson, 2003).

The Gulf of Maine is a mid-latitude, semi-enclosed sea in the Northwestern Atlantic situated along the boundary of an Arctic water mass (Labrador Current) and a temperate water mass (Gulf Stream). Thus, the Gulf of Maine is sensitive to minor changes in climate and/or changes in slopewater input (MERCINA, 2001). Few studies have investigated the Holocene climate history of the Gulf of Maine (e.g., Schnitker, 1975), thus the paleoceanography of this region is poorly documented and understood. Further, it is unclear if the Gulf of Maine responds to and follows the oceanographic

conditions in the North Atlantic. The focus of the research presented in this dissertation is to develop calibrated aquaculture-based methods for isotope paleothermometry with bivalves, and to apply these methods to live and fossil bivalves collected from the Gulf of Maine to better understand the mechanisms responsible for interannual to decadal-scale ocean variability during the past millennium. A major goal of this work is to estimate local (within the Gulf of Maine) and regional (North Atlantic) controls on the oceanography of the Gulf of Maine. Hypotheses that link the spatial and temporal patterns of the North Atlantic Oscillation (NAO) and the Atlantic Multi-Decadal Oscillation (AMO) with the modern oceanography in the Gulf of Maine will be tested with instrumental and shell-derived records. This will be accomplished by analyzing shell carbonate isotope geochemistry and developing standardized growth increments (SGIs) (much like dendrochronology) from shells of *Arctica islandica* previously collected from the Gulf of Maine that span intervals of time during the past 1000 years. In addition, a 142-year-old animal was collected alive in 2004, which has produced a 140-year bottom water temperature record in the Western Gulf of Maine 1864-2003. This modern record will allow a comparison to be made with shells from the paleo-record, which were collected within 3 km of the modern shell in the same water depth. Because all *Arctica islandica* shells used in this study were collected from a similar location and water depth in the Gulf of Maine, changes in shell chemistry and growth histories have the potential to elicit important aspects of how the physical environment in the Gulf of Maine has changed during the past 1000 years.

The body of this dissertation consists of five sections (II through VI), and each section of the dissertation contains its own abstract, introduction, methods, presentation and review of results, and conclusions. A complete reference list is provided at the end of the dissertation. Combined, these papers deal with the development of improved aquaculture-based methods for calibrated isotope paleothermometry, the development of calibrated isotope proxies, and applications of these methods in the Gulf of Maine, to

better understand the ocean variability for periods of the late Holocene up to the present.

Section II (An aquaculture-based method for calibrated bivalve isotope paleothermometry) reviews the use of bivalves as paleoceanographic indicators (proxies), illustrating the need to better constrain (calibrate) the variables (temperature and oxygen isotopic composition of the water – related to salinity) that primarily control the oxygen isotope composition of bivalve shells. I present culture-based methods that greatly improve the development of paleotemperature relationships that are well constrained, accurate, and species-specific. Further, these methods can be exported and modified to carry out similar experiments with other biogenic carbonates (corals, foraminifera, etc.), which ultimately can improve paleoceanographic reconstructions.

Section III (Experimental determination of salinity, temperature, growth, and metabolic effects on the shell isotope chemistry of *Mytilus edulis* collected from Maine and Greenland) develops a context to further test and improve methods from section II, as well as specifically addressing factors that may influence the isotopic chemistry of the intertidal bivalve *Mytilus edulis* (common blue mussel). In this section, we test and validate the usefulness of the experimental design and demonstrate that *M. edulis* is a valid paleoceanographic proxy. I present a rigorously tested, calibrated ocean proxy (*M. edulis*) and determine if life process (age, size, growth rates, metabolism) or geographic location (Maine and Greenland, near end-member environmental conditions for *M. edulis*) affect isotope-equilibrium during biomineralization.

Section IV (Assessing the effects of temperature and salinity on shell carbonate of the long-lived bivalve *Arctica islandica*: an aquaculture-based study) addresses the need to develop calibrated isotope proxies that are long-lived, and distributed in high-to-mid latitudes, where relative few marine paleo-records exist compared to the tropics. Because *Arctica islandica* (ocean quahog) is a long-lived (commonly 100 years or older), deep-water bivalve, this animal provides a unique opportunity to assess ocean variability from

interannual-to-centennial time scales.

Section V (A late Holocene paleo-productivity record in the Western Gulf of Maine, USA inferred from growth histories of the long-lived ocean quahog [*Arctica islandica*]) investigates if growth records from the shells of *Arctica islandica* can be used to document changes in productivity (related to ambient growing conditions) in the Western Gulf of Maine. Shell growth records are calibrated with continuous plankton recorder (CPR) data in the Gulf of Maine for several decades. Based on this modern calibration, estimates of productivity based on shell growth records are given for periods of the last 1000 years. Further, this study corroborates the influence of the NAO on trophic conditions (and hence shell growth) in the Gulf of Maine.

Section VI (Coupled North Atlantic Slopewater forcing on Gulf of Maine temperatures over the past millennium) develops a context for modern ocean variability in the Gulf of Maine. Further, this research provides the first annualized paleo-record (water temperature) for the Gulf of Maine for intervals during the last millennium. Slopewater currents (Labrador Current and Gulf Stream) and dominant modes of climate (NAO and AMO) are investigated in detail to determine to what extent these forcing mechanisms impact the oceanography in the Gulf of Maine.

Section VII (Concluding remarks) provides an overall interpretation of the dissertation results, and highlights the importance and contribution of the research presented here to the scientific community. Further, this concluding section illustrates how small shifts in slopewater positions and slopewater input (Labrador Current derived and Gulf Stream derived) may affect water temperatures and productivity levels in the Gulf of Maine. In addition, section VII includes a context for the observed shell-derived changes (geochemistry and SGIs) from the Western Gulf of Maine in relation to other oceanographic records from the Northwest Atlantic during the last millennium.

2. An aquaculture-based method for calibrated bivalve isotope paleothermometry

To quantify species-specific relationships between bivalve carbonate isotope geochemistry ($\delta^{18}\text{O}_c$) and water conditions (temperature and isotopic composition [$\delta^{18}\text{O}_w$]; related to salinity), an aquaculture-based methodology was developed and applied to *Mytilus edulis* (blue mussel). The four-by-three factorial design consisted of four circulating temperature baths (7, 11, 15 and 19 °C), and three salinity ranges (23, 28, and 32 parts per thousand [ppt]; monitored for $\delta^{18}\text{O}_w$ weekly). In mid-July of 2003, 4800 juvenile mussels were collected in Salt Bay, Damariscotta, Maine and were placed in the configuration. The size distribution of harvested mussels, based on 105 specimens, ranged from 10.9 mm to 29.5 mm with a mean size of 19.8 mm. The mussels were grown in controlled conditions for up to 8.5 months, and a paleotemperature relationship based on juvenile *M. edulis* from Maine was developed from animals harvested at months 4, 5, and 8.5. This relationship [$T \text{ } ^\circ\text{C} = 16.19 (\pm 0.14) - 4.69 (\pm 0.21) \{ \delta^{18}\text{O}_c \text{ VPBD} - \delta^{18}\text{O}_w \text{ VSMOW} \} + 0.17 (\pm 0.13) \{ \delta^{18}\text{O}_c \text{ VPBD} - \delta^{18}\text{O}_w \text{ VSMOW} \}^2$; $r^2 = 0.99$; $N = 105$; $p < 0.0001$] is nearly identical to the Kim and O'Neil (1997) abiogenic calcite equation over the entire temperature range (7 - 19 °C), and it closely resembles the commonly used paleotemperature equations of Epstein et al. (1953) and Horibe and Oba (1972). Further, the comparison of the *M. edulis* paleotemperature equation with the Kim and O'Neil (1997) equilibrium-based equation indicates that *M. edulis* specimens used in this study precipitated their shell in isotopic equilibrium with ambient water within the experimental uncertainties of both studies. The aquaculture-based methodology described here allows similar species-specific isotope paleothermometer calibrations to be performed with other bivalve species, and thus provides improved quantitative paleoenvironmental reconstructions.

2.1. Introduction

Oxygen isotopic analysis of marine biogenic carbonates ($\delta^{18}\text{O}_c$) is a standard paleoceanographic method used to reconstruct seawater temperature and/or changes in the isotopic composition of seawater ($\delta^{18}\text{O}_w$), when other independent methods can constrain either water temperature or salinity (Mg/Ca ratios, alkenones, etc.). $\delta^{18}\text{O}_c$ is a function of seawater temperature (Urey, 1947; Epstein et al., 1953; Craig, 1965; O'Neil et al., 1969), isotopic composition of the seawater (related to salinity) (Emiliani, 1966; Shackleton, 1967), and any species-specific fractionation that occurs during biomineralization (Erez, 1978; Shackleton et al., 1973; Swart, 1983; Gonzalez and Lohmann, 1985; McConnaughey, 1989a; McConnaughey, 1989b; Owen et al., 2002a; Lorrain et al., 2004). Substantial information about marine paleoenvironments can be elicited from stable isotope profiles ($\delta^{18}\text{O}_c$) from living and fossil bivalves (e.g., Williams et al., 1982; Arthur, et al., 1983; Krantz, et al., 1987; Romanek et al., 1987; Wefer and Berger, 1991; Weidman et al., 1994; Klein et al., 1997; Purton et al., 1999; Ivany et al., 2003; Schöne et al., 2004, Carre et al., 2005). However, several factors have been recognized that complicate the understanding of biogenic carbonates, which have been described, in part, by previous workers. These factors include carbonate precipitation in equilibrium with ambient water (Shackleton et al., 1973; McConnaughey, 1989b), pH effects (Spero et al., 1997; Zeebe et al., 2003), ontogeny (Bijma et al., 1998), diagenesis (e.g., Grossman et al., 1993), seasonal timing and duration of shell growth, and large-scale geographic trends in temperature and productivity gradients on shell growth (Jones, 1981; Harrington, 1989; Goodwin et al., 2001; Owen et al., 2002b; Schöne et al., 2003b; Goodwin et al., 2004; De Ridder et al., 2004; Schöne et al., 2005a).

In the past, the interpretation of $\delta^{18}\text{O}_c$ has been based upon theoretical studies of chemical equilibrium and kinetics (Urey, 1947; Usdowski and Hoefs, 1993), or laboratory experiments involving inorganic precipitation of CaCO_3 from solution (e.g., McCrea, 1950; O'Neil et al., 1969; Tarutani et al., 1969; Kim and O'Neil, 1997; Zhou

and Zheng, 2003). Other methods have employed an empirical calibration of bivalves, done by measuring $\delta^{18}\text{O}_c$ of collected shells from the natural setting and/or from shells grown in a controlled setting and by measuring or estimating $\delta^{18}\text{O}_w$ (Epstein et al., 1953; Craig, 1965; Horibe and Oba, 1972; Grossman and Ku, 1986; Owen et al., 2002a; Chauvaud et al., 2005). However, previous oxygen isotope bivalve calibrations have one or several potential limitations: (1) Estimates of temperature and/or $\delta^{18}\text{O}_w$ were used in the development of paleotemperature equations; (2) a limited number of environmental conditions, such as a single temperature or a single salinity, were utilized during culturing; (3) a limited number of bivalves (as few as one) were grown at a particular temperature and salinity range; and (4) a limited suite of bivalve species was used.

The general isotope calibrations for calcite and aragonite (Epstein et al., 1953; Grossman and Ku, 1986) have been applied to a wide variety of organisms precipitating carbonate skeletons, which were not cultured in their calibrations, over timescales ranging from seasonal to glacial/interglacial. Also, these isotope calibrations were not designed to assess factors such as “life processes” that complicate the interpretation of $\delta^{18}\text{O}_c$. Recognition of these limitations has led to the development of aquaculture-based techniques for selected foraminifera species (e.g., Erez and Luz, 1983; Spero and Lea, 1993; 1996; Bemis et al., 1998; Bijma et al., 1998), bivalves (e.g., Owen et al., 2002a), and corals (e.g., Al-Horani et al., 2003). We present here a methodology for growing a wide-range of bivalve species in which key environmental conditions are well constrained and monitored, and represent reasonable growing conditions similar to the natural environment. Our goal is to develop a reproducible aquaculture-based method for use with a wide range of bivalve species, particularly from mid-to-high latitudes where few high-resolution (seasonal) paleo-oceanographic records exist. This method facilitates the study of shell chemistry, including biologically induced effects as a function of growing conditions.

2.2. Materials and Methods

2.2.1. Experimental Bivalve

The relative abundance in coastal environments and broad geographical distribution of the intertidal bivalve *M. edulis* makes it an ideal species for paleo-environmental reconstructions. *M. edulis* has a current geographic range that extends from Greenland to North Carolina in the western Atlantic Ocean (Wells and Gray, 1960; Read and Cumming, 1967). *M. edulis* also occurs on the east and west coasts of South America, the Falkland Islands, and along the European coasts from the western border of the Kara Sea south to the Mediterranean (Tebble, 1966; Seed, 1992), and fossils are found in many late-glacial sediments in the circum-Arctic. It is absent from the Pacific coast of North America (Seed, 1992). The southern distribution of this species appears to be limited by an inability to tolerate water temperatures exceeding 27 °C (Read and Cumming, 1967). The environmental optimum for this species is a salinity range of > 20 - 35 ppt (parts per thousand) and a temperature range of 10 - 20 °C (Bayne et al., 1973), but it will tolerate and commonly inhabits colder waters. Because *M. edulis* is an intertidal to shallow subtidal organism, the shell of this species has the potential to record nearshore sea surface temperature (SST). In addition, it appears to be an appropriate organism to monitor hydrographic changes over time, because it is found in estuaries and at river mouths. Although Theisen (1973) has reported that *M. edulis* may live up to 18 to 24 years, *M. edulis* is commonly short-lived (6-7 years old). *M. edulis* deposits annual growth rings (Lutz, 1976) and micro-growth rings (Richardson, 1989). An adult blue mussel (> 2 years) can grow to about 8 – 10 cm shell length allowing for a high-resolution environmental reconstruction (sub-monthly). Growth rates in their natural settings are variable, depending on environmental conditions (Incze et al., 1980). The shell of temperate *M. edulis* is two layered, with an outer calcitic layer and an aragonitic inside layer (Taylor et al., 1969). The aragonitic growth layer lags the calcitic layer

substantially, thus all new outer-edge growth is calcitic. As the organism continues to grow, the aragonitic layer follows outward toward the mantle.

In mid-July of 2003, 4800 juvenile *M. edulis*, ~15 mm shell length on average, were collected in Salt Bay, Damariscotta, Maine, USA. These animals were transported to the Darling Marine Center in Walpole, Maine and were kept moist in storage containers. Animals were sorted to ensure that a similar distribution of size fractions were equally distributed in each temperature/salinity configuration. Animals were acclimated to the culture temperature gradually for a period of one week. Based on 100 random samples, their size range was 9.8 – 20.2 mm, with a mean of 15.3 mm ($1\sigma = 2.4$ mm).

2.2.2. Aquaculture Design and Implementation

An aquaculture system was designed at the Darling Marine Center to achieve four temperature settings (7, 11, 15 and 19 ± 0.5 °C) and three salinity settings (23, 28, and 32 ± 0.1 ppt). This four by three factorial design allowed 12 different growing conditions to be maintained simultaneously. Each experiment has been duplicated (buckets A and B). The system consists of three large containers (500-liter) connected to a heating/cooling system (Aquanetics Systems), in which four 20-liter buckets were placed into the fresh water bath (Fig. 2.1). The temperature of each bath was measured with a HOBO® H8 data logger every 30 minutes with an accuracy of ± 0.5 °C (Fig. 2.2), and each HOBO® H8 data logger was calibrated in an ice-water bath to ensure accuracy. The average water exchange in each recirculating bath was approximately 10 liters per minute.

Seawater was collected via the flowing seawater laboratory at the Darling Marine Center, and was pumped from the Damariscotta River at - 10m below mean low tide. Seawater was mixed for desired salinity (23, 28, and 32 ± 0.1 ppt) and stored in 2,460-liter containers and sealed. Salinity measurements were made via a YSI model 85 oxygen, conductivity, salinity, and temperature system with an accuracy of ± 0.1 ppt. We used a simple mixing line based on the mean $\delta^{18}\text{O}_w$ values (see below) of well water

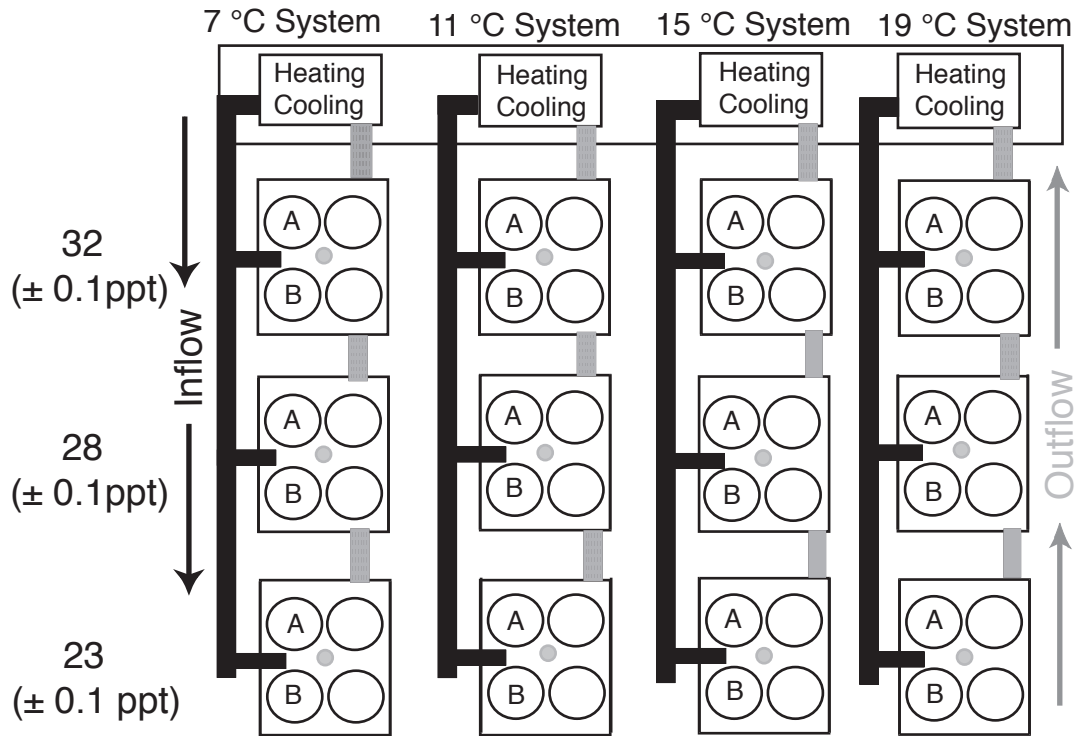


Figure 2.1. Schematic diagram of the experimental design. Each temperature condition is shown vertically, and each salinity condition is shown horizontally. Black indicates inflow and gray indicates outflow. Buckets A and B are replicates. Buckets to the right of A and B are for water changes. All buckets are in a fresh water bath to maintain desired temperature setting to within ± 0.5 °C.

and seawater (desired $\delta^{18}\text{O}_w = [0.0029 \cdot x] - 8.6$; where $x = \#$ of salt water liters added to the 2,460-liter container) to achieve the desired isotopic composition and salinity. Adjustments were made by adding small volumes of either well water or seawater to the containers to achieve the desired salinity of 23 and 28 ± 0.1 ppt. The highest salinity (32ppt) was limited by the seasonal cycle in the Damariscotta River system, and had a mean oxygen isotopic composition ($\delta^{18}\text{O}_w$) of -1.40 ‰ Vienna Standard Mean Ocean Water (VSMOW) ($N=8$; $1\sigma = 0.11$ ‰) during June, 2003. For 23 and 28 ppt mixtures, seawater was mixed with well water from the Darling Marine Center, which had a mean $\delta^{18}\text{O}_w$ of -8.62 ‰ (VSMOW) ($N=12$; $1\sigma = 0.14$ ‰) during June, 2003. The above procedure was repeated in October, 2003 to replenish seawater that was used through

March, 2004 (mean seawater $\delta^{18}\text{O}_w$ of -1.46‰ VSMOW; $N = 10$; $1\sigma = 0.08\text{‰}$ and mean well water $\delta^{18}\text{O}_w$ of -8.59‰ VSMOW; $N = 10$; $1\sigma = 0.09\text{‰}$).

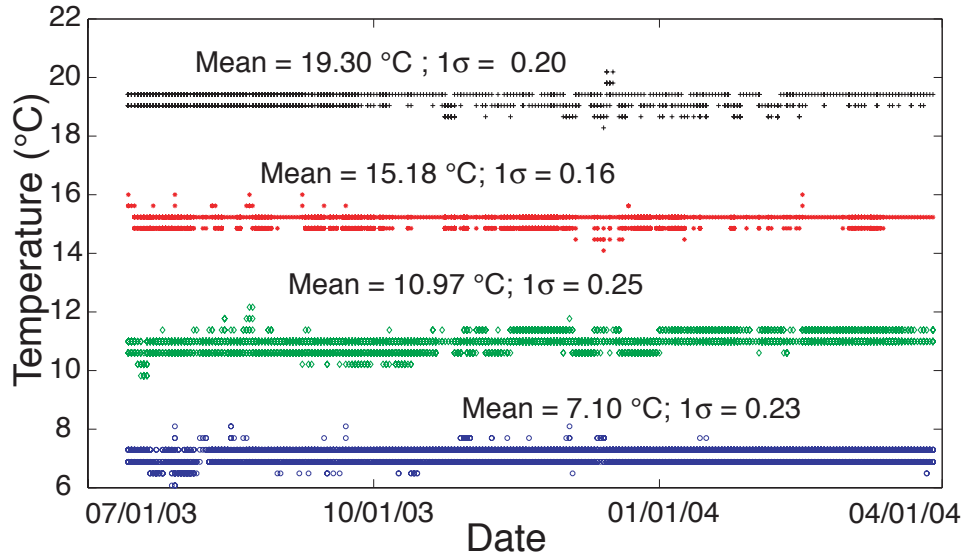


Figure 2.2. Temperatures for each of the four freshwater baths are shown with the 8-month mean and standard deviation. The HOBO® H8 data logger digitally measured water temperature with an error of $\pm 0.5\text{ °C}$, and the appearance of two lines for each temperature is an artifact of the digital measurement.

Two hundred blue mussels were placed in each 20-liter temperature/salinity environment, for a total of 4800 animals. The animals were cultured for a total of 8.5 months (Mid-July 2003 through March 2004) with five animals being removed from each configuration monthly for analysis. Ten animals in each temperature and salinity configuration were tagged on July 14, 2003 with a numbered shellfish tag ($\sim 3\text{mm}$) directly adhered to each animal. The shell length for each these mussels were determined with digital calipers ($\pm 0.01\text{ mm}$) by measuring along the maximum growth axis, and monitored monthly. Average linear growth rates (mm/month) were 0.10, 0.08, 0.09, and 0.14 for 7° , 11° , 15° and 19° °C temperature ranges respectively. In their natural

setting, *M. edulis* has growth rates of ~ 3 mm/month, with considerable variation among individuals (Incze et al., 1980). Overall, there were no noticeable trends in growth rate versus salinity or temperature.

Complete water changes for each temperature/salinity environment were made weekly, to remove metabolic waste. The aquaculture design allowed for one extra 20-liter bucket to be in place with identical water (isotopic composition and temperature) (Fig. 2.1). Mussels were fed twice daily (total of 10 ml) a concentrated spat formula

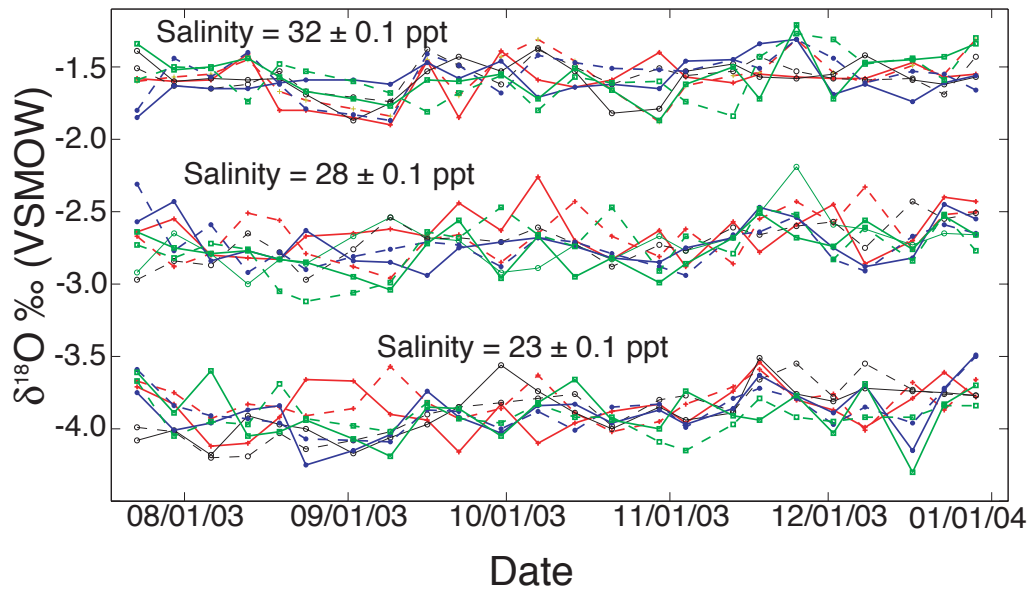


Figure 2.3. The oxygen isotopic composition ($\delta^{18}\text{O}_w$) for each of the 24 growing environments is shown for a 5-month period* (* only one group of animals were used in the final paleotemperature relationship beyond 5 months, and complete $\delta^{18}\text{O}_w$ values are listed in Appendix A.). The salinities are 32 ppt (top), 28 ppt (middle), and 23 ppt (bottom). Temperatures are 19 °C (red), 15 °C (black), 11 °C (blue), and 7 °C (green). For the replicate environments, the solid lines represent bucket A, while the dashed lines represent bucket B. The average standard deviations for $\delta^{18}\text{O}_w$ are (1σ) = 0.18 ‰, 0.19 ‰, and 0.17 ‰ for 32 ppt, 28 ppt, and 23 ppt respectively. The observed variabilities are 3-4 times larger than the analytical error of the measurement, and may be caused by the addition of food/water that was isotopically different from the growing conditions, although it was made from the same salinity water. Some evaporation from buckets also could account for a small amount of the variability.

(Innovative Aquaculture Products, Ltd.) where 5ml of spat was diluted in 1 liter of identical isotopic composition water in which they grew. Water samples for each of the twenty-four buckets were collected weekly, after water changes were made, to monitor $\delta^{18}\text{O}_w$ (Fig. 2.3). There was no isotopic difference noted when water was collected prior to and after water changes. Throughout the experiment mortality was low (< 10%) for all temperature and salinity configurations for the first five months. Mortality rates were higher (~ 20 - 25 %) for animals grown at 20 °C for the remainder of the experiment, while all others remained low.

2.2.3. Sample Preparation and Analysis

Weekly water samples ($\delta^{18}\text{O}_w$) were measured via a dual-inlet VG/Micromass SIRA, which has a long-term precision of $\pm 0.05 \text{‰}$ (Fig. 2.3). Weekly $\delta^{18}\text{O}_w$ from each temperature/salinity environments were averaged over the growing interval (4, 5, and 8.5 months), and used in the isotope calibration (Appendix A). All $\delta^{18}\text{O}_w$ (δ in ‰ = $[(R_{\text{sample}}/R_{\text{standard}}) - 1] * 1000$; $[R = ^{18}\text{O}/^{16}\text{O}]$) values are reported with respect to Vienna Standard Mean Ocean Water (VSMOW).

Animals were cleaned and air-dried. Shell samples were further oven dried at 40 °C overnight. The periostracum was removed with a razor blade along the ventral margin. Prior to sampling, each animal's shell length was recorded. The outer edge of each valve was micro-milled using a variable speed mounted drill and binocular microscope with 6.5x to 40x magnification. To ensure that only new shell carbonate material was used for the isotope calibration, mussels from each month were sampled and standard deviations of isotopic variability ($\delta^{18}\text{O}_{\text{calcite}} - \delta^{18}\text{O}_{\text{water}}$) were calculated. These standard deviations (1σ) for months 1 and 2 were on the order of 0.32 ‰ – 0.52 ‰, thus these animals were not used in the study. Standard deviations of isotopic variability ($\delta^{18}\text{O}_{\text{calcite}} - \delta^{18}\text{O}_{\text{water}}$) for months 4, 5, and 8.5 were on the order of $1\sigma = 0.09 \text{‰} - 0.12 \text{‰}$, and remained constant. In addition, growth rate data (Appendix A) was used to estimate how much linear shell

material could be removed during sampling, without mixing previously grown shell with controlled growth. X-ray diffraction was performed on a limited number of samples from shell edges to rule out a mixed matrix of calcite and aragonite. This method is extremely accurate in detecting the presence of polymorphs, because of the return signal generated from the different crystal habits of calcite (hexagonal) and aragonite (orthorhombic) during the X-ray diffraction analysis. All measurements indicate that there was no aragonite present near the ventral margin, and furthermore by visually inspecting the shells the pearly aragonitic layer lagged the calcitic outer shell layer substantially (> 1cm). Shell carbonate analysis ($\delta^{18}\text{O}_c$) was performed on a dual-inlet VG/Micromass Prism, via a 30-place carousel and common acid bath without chromium oxide (CrO_3) at 90°C , which has a long-term precision of $\pm 0.10 \text{ ‰}$. Average shell samples weighed approximately 100 μg . Samples were calibrated using NBS-19 standards at the beginning and end of each run, with a standard to sample ratio of 1:3. All shell carbonate values ($\delta^{18}\text{O}_c$) are reported with respect to Vienna Pee-Dee Belemnite (VPBD).

2.2.4. Calibration of Temperature and $\delta^{18}\text{O}$ Relationships

Least squares regression was used to generate the *M. edulis* paleotemperature relationship. Root mean squared error (RMSE) were calculated at the 95 % confidence interval (C.I.), and quoted errors on the slope and intercepts are reported at the 95 % C.I. Our shell data ($\delta^{18}\text{O}_c$) are reported against the international VPBD scale and our water data ($\delta^{18}\text{O}_w$) are reported against the international VSMOW scale, which minimizes approximations and multiple corrections. However, in order to compare our results to the Epstein et al. (1953), Horibe and Oba (1972) and Kim and O'Neil (1997) calcite equations, corrections had to be made to each of their data sets or equations, because Epstein et al. (1953) and Horibe and Oba (1972) report the $\delta^{18}\text{O}_c - \delta^{18}\text{O}_w$ versus [PDB],

while Kim and O'Neil (1997) report the $\delta^{18}\text{O}_c - \delta^{18}\text{O}_w$ versus [SMOW]. The water data of Epstein et al. (1953) was converted to the VSMOW scale using the following relationship:

$$\delta^{18}\text{O}_w (\text{VSMOW}) = 1.00022 * \delta^{18}\text{O}_w (\text{PDB}) + 0.22 \quad (\text{Friedman and O'Neil, 1977}),$$

and least squares regression of their data yielded a paleotemperature relationship in the following form:

$$T \text{ } ^\circ\text{C} = 15.51 (\pm 0.48) - 4.25 (\pm 0.31) [\delta^{18}\text{O}_c \text{ VPBD} - \delta^{18}\text{O}_w \text{ VSMOW}] + 0.14 (\pm 0.21) [\delta^{18}\text{O}_c \text{ VPBD} - \delta^{18}\text{O}_w \text{ VSMOW}]^2; r^2 = 0.98; \text{RMSE } \pm 0.79 \text{ } ^\circ\text{C}. \quad (2.1)$$

Similarly, the calcite equation of Horibe and Oba (1972) was converted to the VPDB - VSMOW scale using the following relationship:

$$\delta^{18}\text{O}_w (\text{VSMOW}) = 1.00022 * \delta^{18}\text{O}_w (\text{PDB}) + 0.22 \quad (\text{Friedman and O'Neil, 1977}),$$

and the conversion of their equation yielded a paleotemperature relationship in the following form:

$$T \text{ } ^\circ\text{C} = 16.10 - 4.27 [\delta^{18}\text{O}_c \text{ VPBD} - \delta^{18}\text{O}_w \text{ VSMOW}] + 0.16 [\delta^{18}\text{O}_c \text{ VPBD} - \delta^{18}\text{O}_w \text{ VSMOW}]^2. \quad (2.2)$$

The calcite data (5 mM solution) of Kim and O'Neil (1997) were corrected (+ 0.25 ‰) to account for differences in acid fractionation factors used in their work (1.01050) and then converted to the VPDB scale using the following equation:

$$\delta^{18}\text{O}_c (\text{VPBD}) = 0.97006 * \delta^{18}\text{O}_w (\text{SMOW}) - 29.94 \quad (\text{Friedman and O'Neil, 1977}),$$

and least squares regression of their data yielded a paleotemperature relationship in the following form:

$$T \text{ } ^\circ\text{C} = 15.07 (\pm 0.86) - 4.60 (\pm 0.59) [\delta^{18}\text{O}_c \text{ VPBD} - \delta^{18}\text{O}_w \text{ VSMOW}] + 0.09 (\pm 0.13) [\delta^{18}\text{O}_c \text{ VPBD} - \delta^{18}\text{O}_w \text{ VSMOW}]^2; r^2 = 0.99; \text{RMSE} \pm 0.72 \text{ } ^\circ\text{C}. \quad (2.3)$$

2.3. Results and Discussion

A paleotemperature relationship for *M. edulis* was derived during this study from 7 ° - 19 °C, including three salinity settings (23, 28, and 32 ± 0.1 ppt):

$$T \text{ } ^\circ\text{C} = 16.19 (\pm 0.14) - 4.69 (\pm 0.21) [\delta^{18}\text{O}_c \text{ VPBD} - \delta^{18}\text{O}_w \text{ VSMOW}] + 0.17 (\pm 0.13) [\delta^{18}\text{O}_c \text{ VPBD} - \delta^{18}\text{O}_w \text{ VSMOW}]^2; r^2 = 0.99; N = 105; p < 0.0001; \text{RMSE} \pm 0.54 \text{ } ^\circ\text{C}. \quad (2.4)$$

Equation (2.4) is compared to equations (2.1, 2.2, and 2.33) (Fig. 2.4). *M. edulis* (Eq. 2.4) is slightly offset relative to the Kim and O’Neil (1997) (Eq. 2.3) abiogenic calcite equation over the entire temperature range (7 - 19 °C), and it closely resembles the commonly used paleotemperature equations of Epstein et al. (1953) (Eq. 2.1) and Horibe and Oba (1972) (Eq. 2.2). The comparison of the *M. edulis* paleotemperature equation with the Kim and O’Neil (1997) equilibrium-based model indicates that *M. edulis* specimens used in this study precipitated their shell in isotopic equilibrium with ambient water within the experimental uncertainties of both studies (Fig. 2.4).

There is similar isotopic variability ($\delta^{18}\text{O}_c - \delta^{18}\text{O}_w$) for *M. edulis* over the upper temperature ranges ($1\sigma = 0.12 \text{ } \text{‰}$ at 19 °C; 0.13 ‰ at 15 °C; 0.12 ‰ at 11°C), and slightly less at the lowest temperature ($1\sigma = 0.09 \text{ } \text{‰}$ at 7 °C) (Fig. 2.4). The observed variability is slightly higher or within the range of combined random analytical errors for water and carbonate analyses ($\pm 0.11 \text{ } \text{‰}$; Miller and Miller, 1993). We determined that

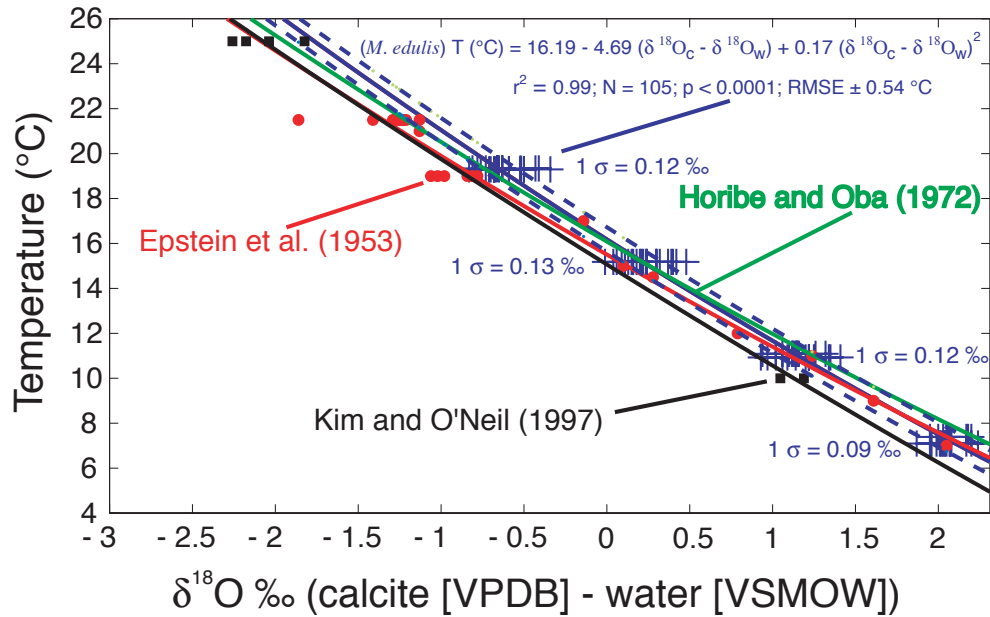


Figure 2.4. The *M. edulis* (Maine juveniles) paleotemperature relationship (this study; [blue line and blue data points]) is compared to the calcite equations of Epstein et al. (1953; [red line and red data points]), Horibe and Oba (1972; [green line]) and Kim and O'Neil (1997; [black line and black data points]). Standard deviations for this study are reported for each temperature range in which animals grew. The RMSE ± 0.54 °C is reported for this study at 95 % C.I. [dashed blue lines].

approximately 0.09 ‰ of the variability is shell-derived for all temperature and salinity conditions, however this is less than the analytical error during measurement of $\delta^{18}\text{O}_c$. We attribute the remainder of the variability to minor changes in the isotopic composition of the water during culture. Owen et al. (2002a) reported isotopic variability of *Pecten maximus* (Great Scallop) at any one temperature of $1\sigma = 0.05$ ‰ – 0.18 ‰. The Kim and O'Neil (1997) inorganic calcite experiment yielded isotopic variability of $1\sigma = 0.06$ ‰, 0.19 ‰, and 0.10 ‰ for 40 °, 25 °, and 10 °C respectively. Epstein et al. (1953) included temperature-controlled conditions and multiple animals for only 21.5 °C and 19 °C (Fig. 2.4), where the isotopic variability was 1σ [‰] = 0.22 ‰ and 0.11 ‰ respectively. The isotopic variability from Epstein et al. (1953) was equal to, or nearly twice as great as the isotopic variability noted in this study for *M. edulis*. All other data from Epstein et

al. (1953) had only a single bivalve grown for each temperature range, and estimates of temperature and $\delta^{18}\text{O}_w$ were used (Fig 2.4). Unfortunately, it is not possible to assess the isotopic variability ($\delta^{18}\text{O}_c - \delta^{18}\text{O}_w$) where only one bivalve was grown. Based on the isotopic variability noted in *M. edulis*, it is likely that similar or greater variability would have been noted if Epstein et al. (1953) had multiple animals at all temperature ranges.

The size (shell length) distribution of mussels, based on 105 animals harvested in the experiment, ranged from 10.9 mm to 29.5 mm with a mean size of 19.8 mm. This variation in shell length (related to the age of the animal) allowed for quantification of potential vital effects. A comparison of shell length and temperature deviation (measured temperature minus predicted temperature; [predicted temperatures from this study]) is made to determine if there is any shell length-related isotope disequilibrium. There is a weak positive correlation ($r^2 = 0.03$) between the shell length of the animal and temperature deviation, but the relationship is not statistically significant. This result suggests that *M. edulis* did not exhibit age/size-related disequilibrium during biomineralization over the culture period.

2.4. Improvements and Future Work

Improvements in this aquaculture-based system that are being considered focus on improving constraints on growth rates, including bio-marking (Kaehler and McQuaid, 1999; Day et al., 1995; Pirker and Schiel, 1993), entire batch measuring, and tagging or etching every individual animal. In addition, because mortality rates were relatively low, it is likely that fewer animals can be grown. Because most of the animals used in this study were juveniles (less than 2 years old), we are currently culturing adults to further refine the *M. edulis* paleotemperature relationship. Ongoing work includes growing *M. edulis* juveniles and adults from western Greenland to determine if there are any large-scale geographic trends in shell carbonate as a function of growing conditions. Other work may include similar aquaculture-based experimentation to evaluate the effects of

temperature and salinity on trace metal uptake in bivalve shell carbonate, provided the trace element ratios in the water can be adequately controlled. A potential benefit of this work would be to eliminate an unknown in the paleotemperature relationship, thus allowing a well-constrained paleoenvironmental reconstruction to be made.

2.5. Summary

During this study we have addressed several limitations associated with past aquaculture-based isotope calibrations including: (1) Precisely measured water temperature and $\delta^{18}\text{O}_w$ values were used in the development of a paleotemperature equation; (2) a wide-range of salinity and temperatures were utilized during culture; (3) multiple bivalves (23-28) were grown at each temperature to assess shell isotopic variability; and (4) a species-specific bivalve isotope paleothermometer was developed. The relationships among water temperature, shell carbonate ($\delta^{18}\text{O}_c$), and water isotopic composition ($\delta^{18}\text{O}_w$) have been thoroughly examined for *M. edulis*, hence we are confident in using this bivalve for reconstructing paleoenvironments. Still, past water temperatures are unknown, and values for the oxygen isotopic composition of ocean waters, especially coastal zones, are not well constrained and need to be estimated (e.g., Rye and Sommer, 1980). If $\delta^{18}\text{O}_w$ can be estimated, or determined independently, this species-specific aquaculture-based methodology can improve environmental reconstructions. Further, this experimental design offers the opportunity to assess many growth-related isotope effects (age, growth rates, life processes, etc.) in a relatively short time, and to determine if shell carbonate is precipitated in equilibrium with ambient water.

Additional information is provided in Appendix A, including all shell data used in this study (isotopic values, shell length, growth), culture conditions (isotopic composition of water, salinity, temperature), as well as predicted temperatures based on the paleotemperature relationship for *M. edulis*.

3. Experimental determination of salinity, temperature, growth, and metabolic effects on shell isotope chemistry of *Mytilus edulis* collected from Maine and Greenland

To study the effects of temperature, salinity, and life processes (growth rates, size, metabolic effects, and physiological/genetic effects) on newly precipitated bivalve carbonate, we quantified shell isotopic chemistry of adult and juvenile animals of the intertidal bivalve *Mytilus edulis* (Blue mussel) collected alive from western Greenland and the central Gulf of Maine coast and cultured under controlled conditions. Data for juvenile and adult *M. edulis* bivalves cultured in this study, and previously (Wanamaker et al., 2006), yielded statistically identical paleotemperature relationships. Based on these experiments, we have developed a species-specific paleotemperature equation for the bivalve *M. edulis* [$T\text{ }^{\circ}\text{C} = 16.28 (\pm 0.10) - 4.57 (\pm 0.15) \{ \delta^{18}\text{O}_c \text{ VPBD} - \delta^{18}\text{O}_w \text{ VSMOW} \} + 0.06 (\pm 0.06) \{ \delta^{18}\text{O}_c \text{ VPBD} - \delta^{18}\text{O}_w \text{ VSMOW} \}^2$; $r^2 = 0.99$; $N = 323$; $p < 0.0001$]. Compared to the Kim and O'Neil (1997) inorganic calcite equation, *M. edulis* deposits its shell in isotope equilibrium ($\delta^{18}\text{O}_{\text{calcite}}$) with ambient water. Carbon isotopes ($\delta^{13}\text{C}_{\text{calcite}}$) from sampled shells were substantially more negative than predicted values, indicating an uptake of metabolic carbon into shell carbonate, and $\delta^{13}\text{C}_{\text{calcite}}$ disequilibrium increased with increasing salinity. Sampled shells of *M. edulis* showed no significant trends in $\delta^{18}\text{O}_{\text{calcite}}$ based on size, cultured growth rates, or geographic collection location, suggesting that vital effects do not affect $\delta^{18}\text{O}_{\text{calcite}}$ in *M. edulis*. The broad modern and paleogeographic distribution of this bivalve, its abundance during the Holocene, and the lack of an intra-species physiologic isotope effect demonstrated here, makes it an ideal near-shore paleoceanographic proxy throughout much of the North Atlantic Ocean.

3.1. Introduction

Climate models require ocean data that are long-term, high-resolution, and from a variety of locations, especially from mid-to-high latitudes. Because relatively few such records exist and historical observational records are temporally short and spatially limited, proxy records are needed to supplement our knowledge of past environments. Shells of bivalve mollusks serve as important archives of paleoenvironmental information, and can provide high-resolution records of past and present ocean climate variability (e.g., Schöne et al., 2005a). Species-specific bivalve proxies that have been experimentally calibrated (e.g., Owen et al., 2002a; Owen et al., 2002b; Chauvaud et al., 2005; Wanamaker et al., 2006) provide the means to reconstruct paleoenvironments with accuracy, because the isotopic variability of the biogenic carbonate has been thoroughly examined during the culture period and hence the uncertainties are better constrained than non-species-specific isotope calibrations (e.g., Epstein et al., 1953; Grossman and Ku, 1986). The fidelity of any proxy, however, is limited when it has not been calibrated. For example, some biogenic species do not precipitate their skeletons in equilibrium with ambient water (e.g., Spero et al., 1997; McConnaughey, 1989a; McConnaughey, 1989b; Owen et al., 2002a; Owen et al., 2002b; Adkins et al., 2003), so that carbonate samples from these organisms may provide inaccurate estimations of water temperature if a generic calcite or aragonite paleotemperature equation is used (e.g., Epstein et al., 1953; Grossman and Ku, 1986).

The relative composition of two commonly studied isotopes ($\delta^{18}\text{O}_c$ and $\delta^{13}\text{C}_c$) in biogenic carbonates may be affected differently by environmental conditions. The oxygen isotopic chemistry of biogenic carbonates ($\delta^{18}\text{O}_c$) is primarily controlled by water temperature and the isotopic composition of water ($\delta^{18}\text{O}_w$; related to salinity) (Urey, 1947; Epstein et al., 1953; Craig, 1965; Emiliani, 1966; Shackleton 1967; O'Neil et al.,

1969). In contrast, the carbon isotopic chemistry ($\delta^{13}\text{C}_c$) during shell precipitation may be related to dissolved inorganic carbon (DIC) (Mook and Vogen, 1968; Mook, 1971; Killingley and Berger, 1979; Arthur et al., 1983), metabolic carbon (Klein et al., 1996b; Geist et al., 2005), or some combination of both (Tanaka et al., 1986; McConnaughey et al., 1997; Dettman et al., 1999; Vander Putten et al., 2000; Furla et al., 2000; Lorrain et al., 2004; Gillikin et al., 2006b). Thus, $\delta^{13}\text{C}_c$ profiles from biogenic carbonates have the potential to be indicators of paleoproductivity, paleo-DIC, paleo- pCO_2 , or paleoecology (e.g., Shanahan et al., 2005), while $\delta^{18}\text{O}_c$ profiles have the potential to reflect basic hydrographic conditions (temperature and salinity). The interpretation of $\delta^{18}\text{O}_c$ and $\delta^{13}\text{C}_c$ data can be complicated by life processes (e.g., growth rates, metabolism, ontogeny), which often play an important role during biomineralization (Erez, 1978; Shackleton et al., 1973; Swart, 1983; Gonzalez and Lohmann, 1985; McConnaughey, 1989a; McConnaughey, 1989b; Owen et al., 2002a; Owen et al., 2002b). Further, life processes may influence whether biogenic organisms produce calcium carbonate (CaCO_3) in isotopic equilibrium with ambient water, and because most CaCO_3 secreting animals experience growth deceleration with increasing age, ontogenetic isotope effects may influence shell chemistry (Krantz et al., 1987; 1989; Harrington, 1989; Freitas et al., 2005).

Although isotope paleothermometry is a powerful tool in paleoclimate studies and bivalves are extremely valuable proxies (e.g., Schöne et al., 2005a), there are still some confounding issues that need to be considered. Bemis et al. (1998) demonstrated that temperature reconstructions based on “paleotemperature relationships” vary by as much as 2 °C. Further, previous aquaculture-based studies evaluated shell isotopic chemistry of calcite at relatively warm temperature ranges only (~ 7 - 30 °C) (Epstein et al., 1953; Craig, 1965; Horibe and Oba, 1972). Hence, sub-polar to temperate paleoceanographic reconstructions using these experimental relationships are limited because they are not constrained by culture data at low temperatures. Another potential problem associated

with isotope paleothermometry at relatively low temperatures is determining “isotope equilibrium” during biomineralization. Kim and O’Neil (1997) revisited the work of O’Neil et al. (1969) and recommend a new mineral-specific fractionation factor ($\alpha = 1.01050$) for calcite at 10 °C, which is preferred for low temperature environments (Kim and O’Neil, 1997). However, their “equilibrium-based-model” is only constrained by two measurements of inorganic calcite at 10 °C, and temperature estimates based on this new relationship differ by more than 1 °C from the O’Neil et al. (1969) equation at 10 °C. These discrepancies suggest that individual bivalve species should be cultured to determine if they deposit their shell in isotopic equilibrium, particularly at low but ecologically relevant temperatures, and caution must be employed when choosing an equilibrium-based model to compare culture-based data (e.g., McCrea, 1950; O’Neil et al., 1969; Tarutani et al., 1969; Kim and O’Neil, 1997; Zhou and Zheng, 2003).

Harrington (1989) suggested that large-scale geographic trends in temperature and productivity may affect shell isotope chemistry, because shell production gaps and secular trends in isotopic profiles may be linked to these environmental conditions. It is assumed that the isotopic chemistry of shell material for bivalves of the same species that live in different climate regimes (e.g., sub-polar, temperate) would not be affected by physiology during the biomineralization process. In other words, one would not expect a bivalve (of the same species) from one climate regime to precipitate its shell in disequilibrium with ambient water, while the same bivalve precipitates its shell in equilibrium in another climate regime, unless there was a physiologic or genetic effect present. Few experimental studies have investigated the effects of life processes (i.e., age, size, growth rates; metabolic effects, etc.) on molluscan shell isotopic chemistry (e.g., Owen et al., 2002a; Owen et al., 2002b; Chauvaud et al., 2005; Wanamaker et al., 2006), and to our knowledge no previous workers have investigated the physiologic or genetic effects on shell isotope chemistry based on collecting bivalves from different climate regimes.

Previously, we quantified the shell isotopic variability of juvenile *M. edulis* bivalves (collected from Maine) cultured under controlled conditions (Wanamaker et al., 2006). Here, we build upon our previous work and quantify shell isotopic variability of adult and juvenile animals of the intertidal bivalve *M. edulis* based on growing conditions that are comparable to sub-polar to temperate ocean climates, and we develop a paleotemperature relationship for *M. edulis* that is well constrained experimentally. Further, we investigate how life processes (size, growth rates, metabolism, and physiology) impact shell isotope chemistry during culturing. Finally, we present a calibrated paleoceanographic proxy, *M. edulis*, which is a common intertidal bivalve with a wide-geographic distribution that will allow for the development of high-resolution paleoceanographic records throughout much of the North Atlantic Ocean.

3.2. Materials and Methods

3.2.1. Animal Collection and Genetic Identification

Approximately 1,000 adult and juvenile sized *M. edulis* were collected alive in western Greenland (Sisimiut; 66° 55' 59.9" N, 53° 40' 59.9" W) during July 2004 and transported in moist storage containers to the Darling Marine Center in Walpole, Maine. Greenland bivalves were quarantined while at the Darling Marine Center. Adult *M. edulis* were collected alive from the western coast of Maine (Damariscotta River; 43° 56' 42.7" N, 69° 33' 4.3" W) (Fig. 3.1) during December 2004 and transported to the Darling Marine Center.

A sub sample (N = 32) of adult mussels from Sisimiut, Greenland was sampled for genetic identification to ensure that mussels from this location were *Mytilus edulis* instead of the congener, *M. trossulus*. These ranges of two ecologically and morphologically similar species overlap throughout the north Atlantic so that specimens

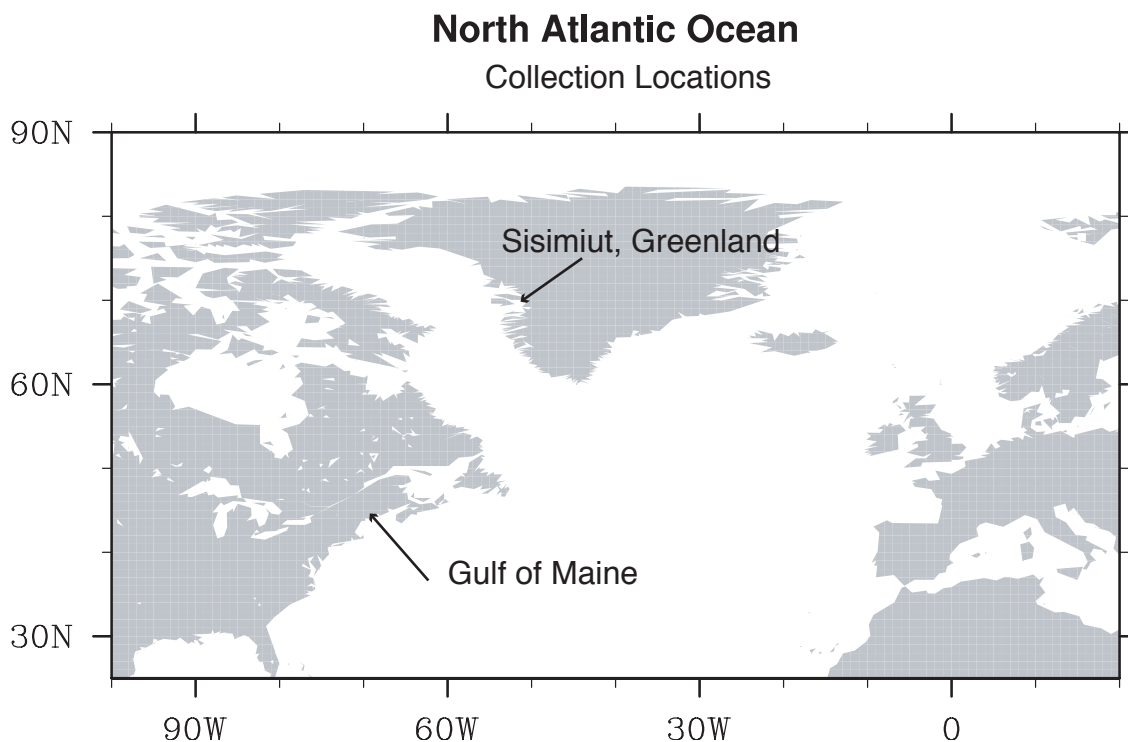


Figure 3.1. Location of *M. edulis* samples collected in Maine and western Greenland.

of *M. trossulus* can easily be confused with *M. edulis*. For genetic identification, a small portion (~10 mg) of mantle tissue was sampled from of each the mussels and DNA isolated using a Qiagen DNA Mini Kit following manufacturer’s protocol. The isolated DNA was used as template in three nuclear DNA PCR-based markers that are diagnostic for *M. edulis* and *M. trossulus*. Application of these markers, Glu-5’, ITS, and Mal-I, followed the methods of Rawson et al. (1996), Heath et al. (1995) and Rawson et al. (2001), respectively. All 32 individuals were identified as *M. edulis* at all three markers. Given the sample size this result suggests that the frequency of *M. trossulus* at Sisimiut is less than 5% ($P = 0.0375$).

3.2.2. Aquaculture Design and Implementation

We used a recirculating water bath system at the Darling Marine Center to achieve four temperature settings (4, 8, 12 and 15 ± 0.5 °C) and three salinity settings (23, 28, and

32 ± 0.1 PSU) (Wanamaker et al., 2006). This four by three factorial design allowed 12 different growing conditions to be maintained simultaneously. The system consisted of three large containers (500-liter) connected to an Aquanetics heat pump for temperature control. Water of each specified temperature was then delivered to a set of three 250-liter tanks that served as individual water baths. In each tank we placed four 20-liter buckets as shown in Figure 3.2. Two buckets (A and B) contained experimental replicates for each temperature by salinity treatment while the other two buckets contained water for subsequent water changes (Fig. 3.2). The temperature of each bath was measured with a HOBO® H8 data logger every hour with an accuracy of ± 0.5 °C, and the temperature of one bucket in each bath was measured via StowAway® Tidbit® every hour with an accuracy of ± 0.5 °C (Table 3.1). Seawater was collected via the flowing seawater laboratory at the Darling Marine Center, and was pumped from the Damariscotta River at 10 m depth below mean low tide. Seawater was mixed with well water for desired salinity (23, 28, and 32 ± 0.1 PSU) and stored in 2,460-liter containers indoors and sealed. Salinity measurements were made via a YSI® model 85 oxygen, conductivity, salinity, and temperature system with an accuracy of ± 0.1 PSU. We used a simple mixing line (Wanamaker et al., 2006) to achieve the desired isotopic composition and salinity. Adjustments were made by adding small volumes of either well water or seawater to the containers to achieve the desired salinity of 23 and 28 ± 0.1 PSU.

Thirty juvenile blue mussels (shell length 14 – 24 mm) from Greenland were placed in each 20-liter temperature/salinity environment ($N_{\text{tot}} = 720$). The animals were cultured for a total of 5 months (August 3, 2004 through January 5, 2005). Six adult blue mussels collected in Maine and five adult blue mussels collected in Greenland were placed in each 20-liter temperature/salinity environment (without replicates), for a total of 132 animals and cultured for 6 months (January 24, 2005 through July 29, 2005). The water in each experimental bucket was changed completely once a week to remove metabolic waste. Mussels were fed a shellfish diet (Instant Algae Marine Microalgae

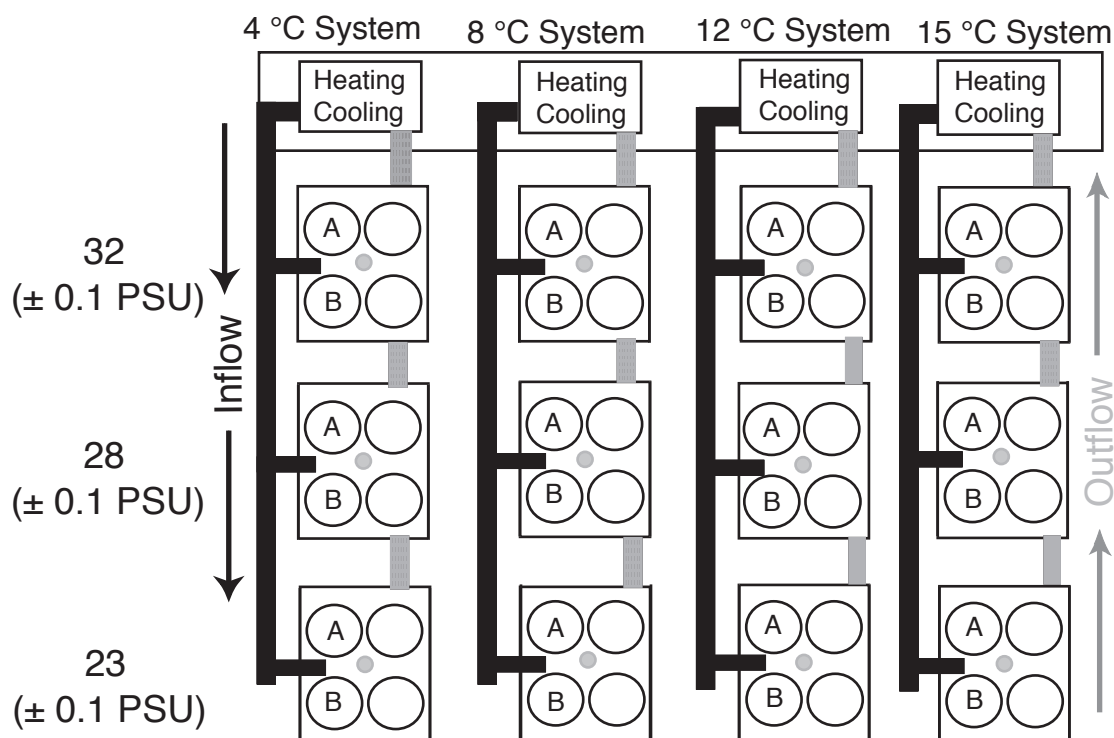


Figure 3.2. Schematic diagram of the experimental design. Each temperature condition is shown vertically, and each salinity condition is shown horizontally. Black indicates inflow and gray indicates outflow. Buckets A and B are replicates. Buckets to the right of A and B are for water changes. All buckets are in a fresh water bath to maintain desired temperature setting to within ± 0.5 °C.

Concentrate, Reed Mariculture, Inc.) twice daily (total of 8×10^9 cells/day) of diluted algal paste made from water with which they grew (identical isotopic composition).

Water samples (60 ml) from each bucket were collected weekly to monitor $\delta^{18}\text{O}_w$ prior to water changes, although there was no isotopic difference noted when water was collected prior to and after water changes. Water samples were stored in glass vials and refrigerated prior to $\delta^{18}\text{O}_w$ analysis.

Greenland Juvenile Aquaculture Temperatures

Temperature (± 0.5 °C)	(1 σ)
4.0	0.2
8.0	0.2
11.9	0.3
15.2	0.4

Growing Conditions	Salinity	Average ($\delta^{18}\text{O}_w$ ‰), N = 22	Average ($\delta^{18}\text{O}_w$ ‰), N = 22
Temperature (°C)	(± 0.1 PSU)	Bucket A (1 σ $\delta^{18}\text{O}_w$)	Bucket B (1 σ $\delta^{18}\text{O}_w$)
4.0	23	-3.12 (0.14)	-3.10 (0.15)
4.0	28	-1.94 (0.12)	-1.93 (0.11)
4.0	32	-1.40 (0.12)	-1.35 (0.12)
8.0	23	-3.07 (0.14)	-3.12 (0.15)
8.0	28	-1.93 (0.12)	-1.96 (0.11)
8.0	32	-1.37 (0.10)	-1.36 (0.12)
11.9	23	-3.10 (0.11)	-3.13 (0.12)
11.9	28	-2.03 (0.13)	-1.97 (0.11)
11.9	32	-1.39 (0.09)	-1.41 (0.09)
15.2	23	-3.09 (0.12)	-3.17 (0.16)
15.2	28	-1.95 (0.13)	-1.97 (0.14)
15.2	32	-1.37 (0.12)	-1.34 (0.10)

Greenland and Maine Adults Aquaculture Temperatures

Temperature (± 0.5 °C)	(1 σ)
4.1	0.3
8.0	0.2
11.5	0.2
15.0	0.4

Growing Conditions	Salinity	Average ($\delta^{18}\text{O}_w$ ‰), N = 23
Temperature (°C)	(± 0.1 PSU)	Bucket A (1 σ $\delta^{18}\text{O}_w$)
4.1	23	-3.10 (0.13)
4.1	28	-1.94 (0.11)
4.1	32	-1.42 (0.13)
8.0	23	-3.02 (0.13)
8.0	28	-1.98 (0.13)
8.0	32	-1.57 (0.09)
11.5	23	-3.05 (0.16)
11.5	28	-1.95 (0.09)
11.5	32	-1.58 (0.09)
15.0	23	-3.02 (0.09)
15.0	28	-1.89 (0.13)
15.0	32	-1.54 (0.09)

Table 3.1. Culture data for this study including temperature (± 0.5 °C, 1 σ), salinity (± 0.1 PSU), and oxygen isotopic composition of water ($\delta^{18}\text{O}_w$ ‰ [VSMOW], N = # of weeks that weekly samples were collected and analyzed, and 1 σ).

3.2.3. Growth Rate Determination

To accurately determine the start of experimental shell growth, juvenile *M. edulis* from Greenland were treated with a biomarker where animals were immersed in a calcein solution (160 mg/l) for 24-hours (modified from Kaehler and McQuaid, 1999). In addition, the shell length for each animal was determined with digital calipers (± 0.01 mm) by measuring along the maximum growth axis, and averaged to determine a bulk shell length per temperature/salinity condition. The average initial shell length (based on 720 individual animals) was 15.88 mm \pm 1.54 mm. This was repeated monthly to determine average bulk linear growth rates (mm/month).

Similarly, adult *M. edulis* from Maine and Greenland (shell length 26 – 70 mm) were immersed in a calcein solution to mark the onset of experimental growth, and each individual animal was marked by etching a number in its shell near the umbo. Individual monthly growth rates were determined by measuring starting and ending shell lengths.

3.2.4. Sample Preparation and Analysis

The $\delta^{18}\text{O}_w$ weekly water samples were measured via a dual-inlet VG/Micromass SIRA ($\text{CO}_2 - \text{H}_2\text{O}$ equilibration method at 30 °C for 12 hours), with a precision of ± 0.06 ‰ based on replicate International Atomic Energy Agency (IAEA) laboratory standards [Vienna Standard Mean Ocean Water (VSMOW, 0.0 ‰), Standard Light Antarctic Precipitation (SLAP, -55.5 ‰), IAEA OH-1 (-0.1 ‰), IAEA OH-2 (-3.3 ‰), IAEA OH-3 (-8.7 ‰), IAEA OH-4 (-15.3 ‰), and internal laboratory standards Big Bear Brook (BBB, -8.5 ‰), Light Antarctic Precipitation (LAP, -40.3 ‰), Antarctic Surface Snow (ASS; -25.8 ‰)], where one standard was run for every five samples. All $\delta^{18}\text{O}_w$ (δ in ‰ = $[(R_{\text{sample}}/R_{\text{standard}}) - 1] * 1000$; $[R = ^{18}\text{O}/^{16}\text{O}]$) values are reported with respect to VSMOW. Weekly $\delta^{18}\text{O}_w$ from each temperature/salinity environments were averaged over the growing intervals, and used in the isotope calibration (Table 3.1).

To measure shell $\delta^{18}\text{O}_c$ and $\delta^{13}\text{C}_c$ the animals were first cleaned (removed soft tissues) and air-dried. Shell samples were further oven dried at 40 °C overnight. The periostracum was removed with a razor blade along the ventral margin. Prior to sampling, the shell length of each animal was recorded. The outer-edge of each valve was micro-milled using a variable speed mounted drill and binocular microscope with 6.5x to 40x magnification. Next, the sample size (linear shell removed) was determined by measuring each animal's shell length after sampling and subtracting it from the initial measurement. Shell carbonate analysis ($\delta^{18}\text{O}_c$ and $\delta^{13}\text{C}_c$) was performed on a dual-inlet VG/Micromass Prism, via a 30-place carousel and common acid bath without chromium oxide (CrO_3) at 90°C, with precision of $\pm 0.10 \text{ ‰}$ ($\delta^{18}\text{O}_c$) and $\pm 0.07 \text{ ‰}$ ($\delta^{13}\text{C}_c$) based on laboratory standards. Results are reported relative to Vienna Pee-Dee Belemnite (VPBD) by calibration to the NBS-19 reference standard ($\delta^{18}\text{O}_c = -2.20 \text{ ‰}$ and $\delta^{13}\text{C}_c = 1.95 \text{ ‰}$) at the beginning and end of each run, with a standard to sample ratio of 1:3. Average shell samples weighed approximately 100 μg .

To determine the isotopic composition ($\delta^{13}\text{C}$) of the food (algal paste) used in this study, we dried 30 ml of paste at 50 °C for 24 hours. The dried samples were weighed into tin capsules. The dried samples were flash combusted at 1800 °C in an elemental analyzer (EA) [EA 1110 (CE Instruments) + Conflo III + DeltaPlus Advantage IRMS (ThermoFinnigan)] and resulting gases were carried via helium through the EA to purify and separate into N_2 and CO_2 . Gases were carried from the EA into an isotope ratio mass spectrometer (IRMS) for isotope analysis via a Conflo interface. Based on replicate standard analyses, the analytical precision (2σ) is $\pm 0.2 \text{ ‰}$. Results are reported relative to VPBD by calibration to the NBS-19 reference standard ($\delta^{18}\text{O}_c = -2.20 \text{ ‰}$ and $\delta^{13}\text{C}_c = 1.95 \text{ ‰}$).

3.2.5. Calibration of Temperature and $\delta^{18}\text{O}_c$ Relationships

Least squares regression was used to investigate the relationship between culture conditions and shell carbonate isotope values and to develop a paleotemperature relationship for *M. edulis*. The root mean squared error (RMSE) was calculated at the 95 % confidence interval (C.I.), and quoted errors on the slope and intercepts are reported at the 95 % C.I. Our shell data ($\delta^{18}\text{O}_c$) are reported against the international VPBD scale and our water data ($\delta^{18}\text{O}_w$) are reported against the international VSMOW scale, which minimizes approximations and multiple corrections. However, in order to compare our results to the Epstein et al. (1953) and the Kim and O'Neil (1997) calcite equations, corrections had to be made to each of their data sets, because they report the $\delta^{18}\text{O}_c - \delta^{18}\text{O}_w$ versus [PDB] and $\delta^{18}\text{O}_c - \delta^{18}\text{O}_w$ versus [SMOW] respectively. In addition, Kim and O'Neil (1997) use an acid fractionation factor of 1.01050 whereas other studies used 1.01025. The modified equations are shown below for Epstein et al. (1953) (Eq. 3.1) and Kim and O'Neil (1997) (Eq. 3.2) respectively reported by Wanamaker et al. (2006):

$$T \text{ } ^\circ\text{C} = 15.51 (\pm 0.48) - 4.25 (\pm 0.31) [\delta^{18}\text{O}_c \text{ VPBD} - \delta^{18}\text{O}_w \text{ VSMOW}] + 0.14 (\pm 0.21) [\delta^{18}\text{O}_c \text{ VPBD} - \delta^{18}\text{O}_w \text{ VSMOW}]^2; r^2 = 0.98; \text{RMSE} \pm 0.79 \text{ } ^\circ\text{C}; \quad (3.1)$$

$$T \text{ } ^\circ\text{C} = 15.07 (\pm 0.86) - 4.60 (\pm 0.59) [\delta^{18}\text{O}_c \text{ VPBD} - \delta^{18}\text{O}_w \text{ VSMOW}] + 0.09 (\pm 0.13) [\delta^{18}\text{O}_c \text{ VPBD} - \delta^{18}\text{O}_w \text{ VSMOW}]^2; r^2 = 0.99; \text{RMSE} \pm 0.72 \text{ } ^\circ\text{C}. \quad (3.2)$$

In order to compare our results to the paleotemperature relationship for juvenile *M. edulis* (Maine) cultured from 7 - 19 $^\circ\text{C}$ (Wanamaker et al., 2006), the equation is listed below:

$$T \text{ } ^\circ\text{C} = 16.19 (\pm 0.14) - 4.69 (\pm 0.21) [\delta^{18}\text{O}_c \text{ VPBD} - \delta^{18}\text{O}_w \text{ VSMOW}] + 0.17 (\pm 0.13) [\delta^{18}\text{O}_c \text{ VPBD} - \delta^{18}\text{O}_w \text{ VSMOW}]^2; r^2 = 0.99; \text{RMSE} \pm 0.54 \text{ } ^\circ\text{C}. \quad (3.3)$$

3.3. Results and Discussion

3.3.1. Size and Shell Growth Rate Effects on $\delta^{18}\text{O}_c$

We found no evidence for a significant relationship between temperature offset [based on predicted temperatures of measured $\delta^{18}\text{O}_{\text{calcite}} - \delta^{18}\text{O}_{\text{water}}$ from Wanamaker et al. (2006) (Eq. 3.3) and actual culture temperatures] and either shell length or shell growth in this study. The shell length of mussels used in the experiments spanned some 60 mm and included adults and juveniles.

Bulk growth measures for juveniles (Greenland) for each temperature/salinity treatment were used, because biomarking with calcein was ineffective for *M. edulis* during this experiment. Although we viewed the shell material with a blue light, the lack of a distinct fluorescence mark is puzzling, as other workers have been successful using this method on *M. edulis* (e.g., Gillikin et al., 2006). Growth rates were dissimilar between adults and juveniles (Fig. 3.3, bottom). As expected, juveniles grew faster than adults. Shell growth was low relative to other studies and may be due to a culture effect (food, confined growing environment, etc.). However, we fed mussels algal paste instead of live cultures to reduce $\delta^{18}\text{O}_w$ variability. Live cultures could have added larger quantities of seawater with very different isotopic composition. Across the growth rates observed in the experiments there was no apparent relationship between temperature offset and shell growth. This result signifies that there are no growth related vital effects on $\delta^{18}\text{O}_c$.

3.3.2. Possible Physiologic or Genetic Effects on $\delta^{18}\text{O}_c$ Based on Collection Location

There is no evidence of a physiologic or genetic isotopic effect on $\delta^{18}\text{O}_c$ based on *M. edulis* specimens collected in Greenland or Maine (Fig. 3.3). Although mussels collected in Maine and Greenland were grown under identical conditions (Gulf of Maine), we are confident that mussels collected from Greenland deposited their shells

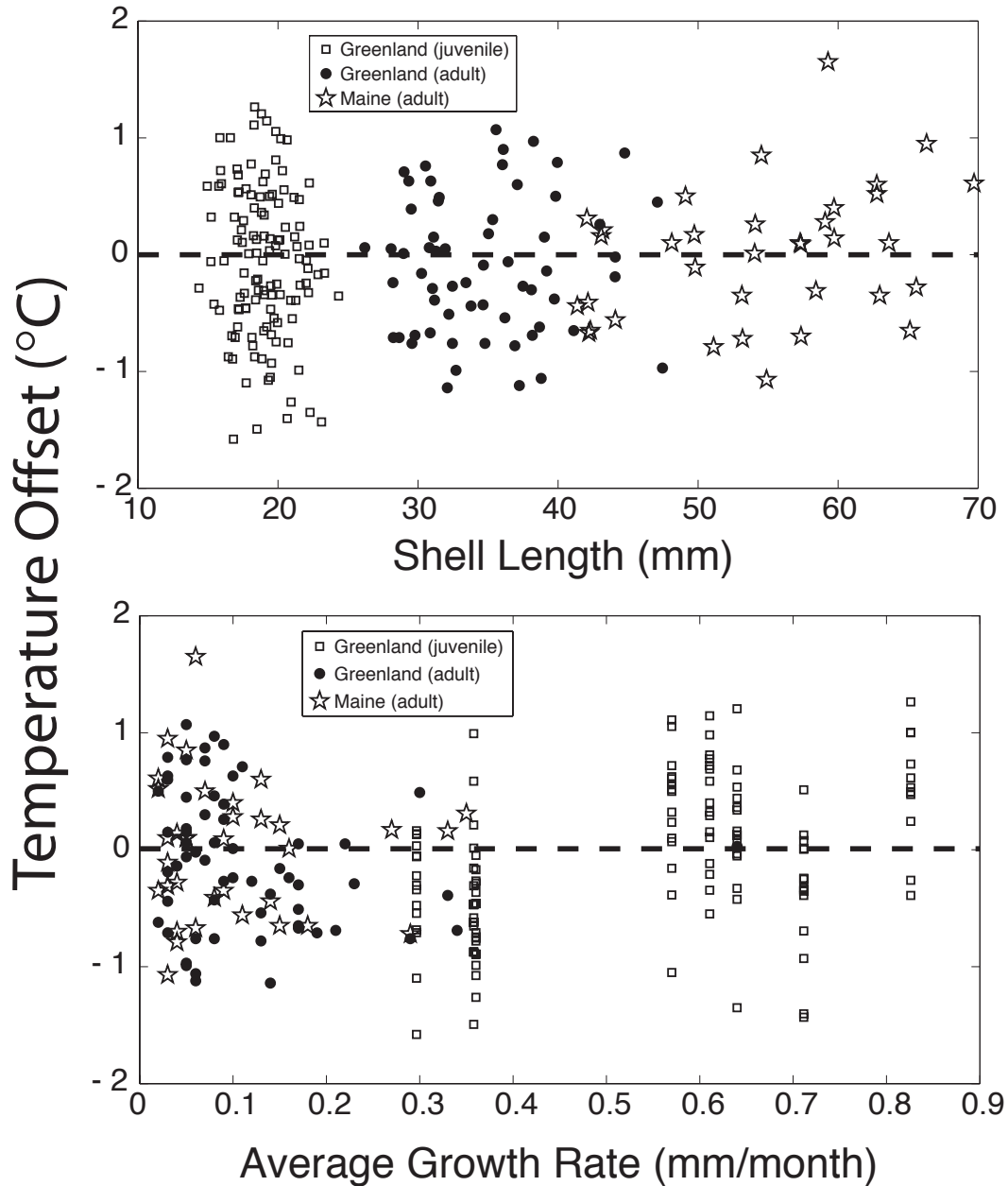


Figure 3.3. Temperature offset [based on predicted temperatures of measured $\delta^{18}\text{O}_{\text{calcite}} - \delta^{18}\text{O}_{\text{water}}$ from Wanamaker et al. (2006) (Eq. 3.3 in this paper) and actual culture temperatures] is compared to shell length (top) and average growth rates (individual for adults and bulk for juveniles) (bottom). The dashed horizontal line represents a temperature offset of 0 °C.

isotopically ($\delta^{18}\text{O}_c$) identical (within analytical uncertainties) to animals collected from Maine. An aquaculture experiment based on Greenland conditions would include an isotopically depleted freshwater end-member ($\delta^{18}\text{O}_w = \sim -25 \text{‰ VSMOW}$ at 0 PSU)

(Wanamaker, unpublished data, 2006) compared to the conditions we used in the Gulf of Maine ($\delta^{18}\text{O}_w = -8.6\text{‰}$ VSMOW at 0 PSU) (Wanamaker et al., 2006). It is likely that if mussels were also cultured under Greenland conditions, similar results would be obtained. Because mussels from Maine and Greenland did not illustrate isotope effects based on physiology or slight genetic variations between the two populations, *M. edulis* is a highly suitable bivalve for paleoceanographic studies. This result indicates that it is appropriate to apply paleotemperature relationships for this species over wide-geographic locations.

3.3.3. Paleotemperature Relationship for *M. edulis*

An updated paleotemperature relationship for *M. edulis* (juveniles and adults) collected from different climate and environmental regimes (Maine and Greenland) was derived from this study and from previous work (Wanamaker et al., 2006), thereby including animals cultured from 4 ° - 19 °C, including three salinity conditions (23, 28, and 32 ± 0.1 PSU):

$$T \text{ } ^\circ\text{C} = 16.28 (\pm 0.10) - 4.57 (\pm 0.15) [\delta^{18}\text{O}_c \text{ VPBD} - \delta^{18}\text{O}_w \text{ VSMOW}] + 0.06 (\pm 0.06) [\delta^{18}\text{O}_c \text{ VPBD} - \delta^{18}\text{O}_w \text{ VSMOW}]^2; r^2 = 0.99; N= 323; p < 0.0001; \text{RMSE} \pm 0.57 \text{ } ^\circ\text{C}. \quad (3.4)$$

We also used bivariate least squares regression (Model II) because there is an error associated with both the x and y measurements in Eq. 3.4. This method yielded a statistically identical relationship compared to Eq. 3.4 in the following form:

$$T \text{ } ^\circ\text{C} = 16.33 - 4.48 [\delta^{18}\text{O}_c \text{ VPBD} - \delta^{18}\text{O}_w \text{ VSMOW}]; r^2 = 0.99. \quad (3.5)$$

Additionally we derived the fractionation factor $\alpha_{\text{calcite-water}} \left(\frac{[1000 + \delta^{18}\text{O}_c]}{[1000 + \delta^{18}\text{O}_w]} \right)$ (relative to VSMOW; T is in Kelvin) for the *M. edulis* animals sampled above:

$$1000 \ln \alpha_{\text{(calcite-water)}} = 18.02 (10^3 T^{-1}) - 31.84. \quad (3.6)$$

Our results (Eq. 3.4) are compared to Kim and O’Neil (1997) (Eq. 3.2) and Epstein et al. (1953) (Eq. 3.1) in Figure 3.4. The updated paleotemperature relationship for *M. edulis* (Eq. 3.4) is slightly offset (less than 0.2 ‰) relative to Kim and O’Neil (1997) (Eq. 3.2) over the entire temperature range, however this isotopic offset is not statistically significant (within analytical errors). Based on a comparison with the abiogenic calcite equation of Kim and O’Neil (1997) (Eq. 3.2) and the uncertainties associated with

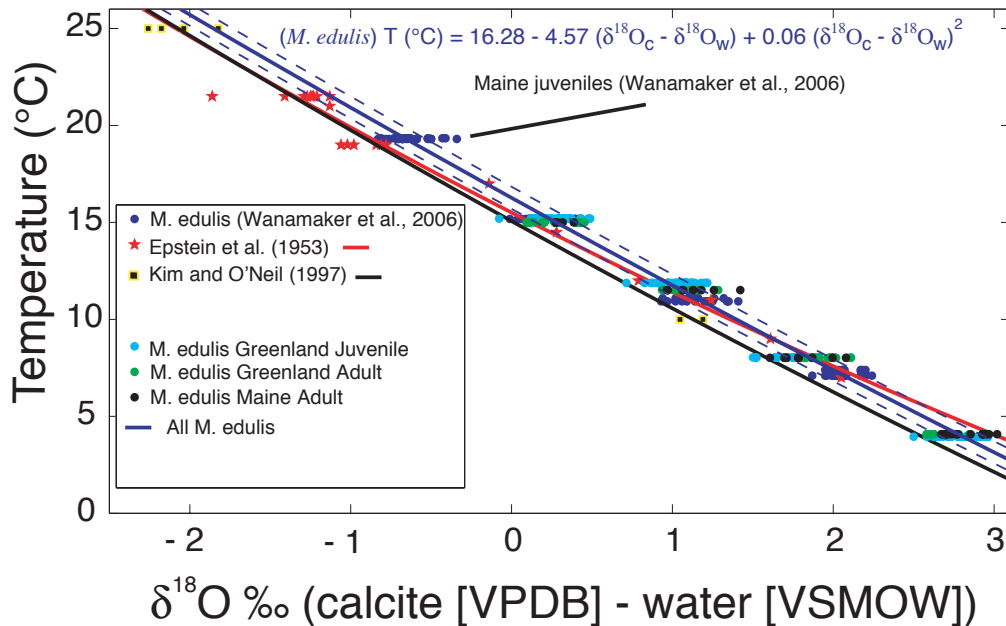


Figure 3.4. Paleotemperature relationships from this study (turquoise circles = Greenland juveniles; green circles = Greenland adults; black circles = Maine adults) (solid blue line = Eq. 3.4; dashed blue lines = upper and lower error of 0.57 °C), Wanamaker et al. (2006) [blue circles; Eq. 3.3], Epstein et al. (1953) [red stars and red line; Eq. 3.1] and Kim and O’Neil (1997) [black and yellow squares and solid black line; Eq. 3.2].

this study and the Kim and O'Neil (1997) study, *M. edulis* (both juveniles and adults, and from Maine and Greenland) precipitated its shell calcite in isotopic equilibrium with ambient water. The animals cultured below ~ 17 °C from the Epstein et al. (1953) (Eq. 3.1) experiment agree rather well with our derived calcite equation for *M. edulis* (Fig. 3.4). Above that temperature (~ 17 °C), only about half of the data from Epstein et al. (1953) (Eq. 3.1) fall within the experimental errors (± 0.57 °C) of this study. Because this study included many more bivalves cultured at each temperature compared to the pioneering work of Epstein et al. (1953), we are more confident with this paleotemperature relationship than those previously published (e.g., Epstein et al., 1953; Craig et al., 1965).

There were no noticeable trends or deviations in shell isotopic variability ($\delta^{18}\text{O}_c$ VPBD – $\delta^{18}\text{O}_w$ VSMOW) based on an animal's size (shell length), growth rates, or geographic origin (Figs. 3.3 and 3.4). Further, the variance in isotopic composition is relatively constant across temperatures (± 0.11 ‰ - 0.14 ‰), and is roughly equal to the combined analytical errors associated with measuring $\delta^{18}\text{O}_c$ and $\delta^{18}\text{O}_w$ of ± 0.12 ‰ (Miller and Miller, 1993). The isotopic variability noted here ($\delta^{18}\text{O}_c$ VPBD – $\delta^{18}\text{O}_w$ VSMOW) is less than or about equal to similar experimental studies that grew multiple bivalves at one temperature (e.g., Epstein et al., 1953; Owen et al., 2002a; Owen et al., 2002b; Wanamaker et al., 2006).

Based on these results, *M. edulis* bivalves are an accurate and reliable proxy for water temperature if $\delta^{18}\text{O}_w$ can be determined independently. *M. edulis* deposit their shell ($\delta^{18}\text{O}_c$) in isotope equilibrium with seawater, and do not show any apparent vital effect based on age/size, growth rates, or geographic origin (physiologic or genetic effect). Because *M. edulis* deposits distinct growth bands (Lutz, 1976; Richardson, 1989) high-resolution (sub-monthly to annual) isotope records are possible, and the broad geographic distribution and the occurrence of *M. edulis* through the Holocene make this bivalve an ideal proxy of environmental conditions. Further, this study complements trace-element

work conducted by Vander Putten et al. (2000) and Gillikin et al. (2006a) on the calcitic shell layer of *M. edulis*, where environmental and biologic controls on shell chemistry were assessed. Although no evident trace metal ratio paleothermometer (Mg/Ca or Sr/Ca) resulted from the work of Vander Putten et al. (2000) for *M. edulis*, other trace metals (Ba and Mn) seem to be related to productivity. Gillikin et al. (2006a) found that Ba/Ca ratios in the calcitic shell material may be used to reconstruct paleo-Ba/Ca ratios of ambient water. Thus a multi-proxy (isotopes and trace metals) approach to reconstructing past ocean environments is possible with *M. edulis*. Donner and Nord (1986) reported stable isotope results from *M. edulis* fossils from Holocene raised beaches in Norway, and presented paleotemperature estimates based on the calcite equations of Craig (1965) and Shackleton (1974) with estimated $\delta^{18}\text{O}_w$ values. Donner and Nord (1986) considered these paleotemperature estimates to be too high, and concluded that coastal mixing of less saline waters must be taken into account for the elevated temperature estimates. However, now that a comprehensive paleotemperature relationship for *M. edulis* (including low temperatures during culture [4°C]) has been established, this work can be reevaluated. Other studies have used the absence or presence of *M. edulis* as a “guide” fossil or climatic indicator to reveal general oceanic conditions (warm or cold) during periods of the Holocene (e.g., Hjort and Funder, 1974; Salvigsen et al., 1992). Also, the modern occurrence of *M. edulis* is used to mark the mid-arctic/high arctic boundary, because *M. edulis* is not found at the 0 °C isotherm (Feyling-Hanssen, 1955). Now these relationships can be further refined with the results presented here for *M. edulis*, and new problems can be investigated using this calibrated proxy. For example, the abundance of fossil *M. edulis* shells in circum N. Atlantic glaciomarine muds (e.g., Presumpscot Formation in Maine) from the most recent deglaciation and the lack of a geographic isotope effect will allow for improved paleoenvironmental constructions along the southeast Laurentide ice sheet, which is not well understood (Borns et al., 2004; Borns, pers. com.).

3.3.4. Relationships Between $\delta^{18}\text{O}_c$ and $\delta^{13}\text{C}_c$, and Metabolic Carbon Isotope Effects

A comparison of shell $\delta^{18}\text{O}_c$ and $\delta^{13}\text{C}_c$ from this study is shown in Figure 3.5. The linear correlations between $\delta^{18}\text{O}_c$ and $\delta^{13}\text{C}_c$ are relatively weak, but significant ($y_1 = 0.47*x + 2.01$; $r^2 = 0.35$; $N = 97$; $p < 0.0001$; [Maine and Greenland Adults] and $y_2 = 0.44*x + 2.24$; $r^2 = 0.19$; $N = 121$; $p < 0.0001$; [Greenland Juveniles]) (Fig. 3.5). A strong correlation between biogenic $\delta^{18}\text{O}_c$ and $\delta^{13}\text{C}_c$ may represent a vital effect during biomineralization (e.g., McConnaughey, 1989a). The two leading hypotheses that attempt to explain this effect are the “kinetic” model (McConnaughey, 1989a; McConnaughey, 1989b) and the “carbonate” model (Adkins et al., 2003) both of which are reviewed in detail by Cohen and McConnaughey (2003) and Shanahan et al. (2005). Both the “kinetic” and “carbonate” models link calcification rates to coupled $\delta^{18}\text{O}$ and $\delta^{13}\text{C}_c$ isotope fractionation, but by different processes in the extracellular calcifying fluid (ECF) (see Shanahan et al., 2005). Only a weak correlation (but significant at 95 %

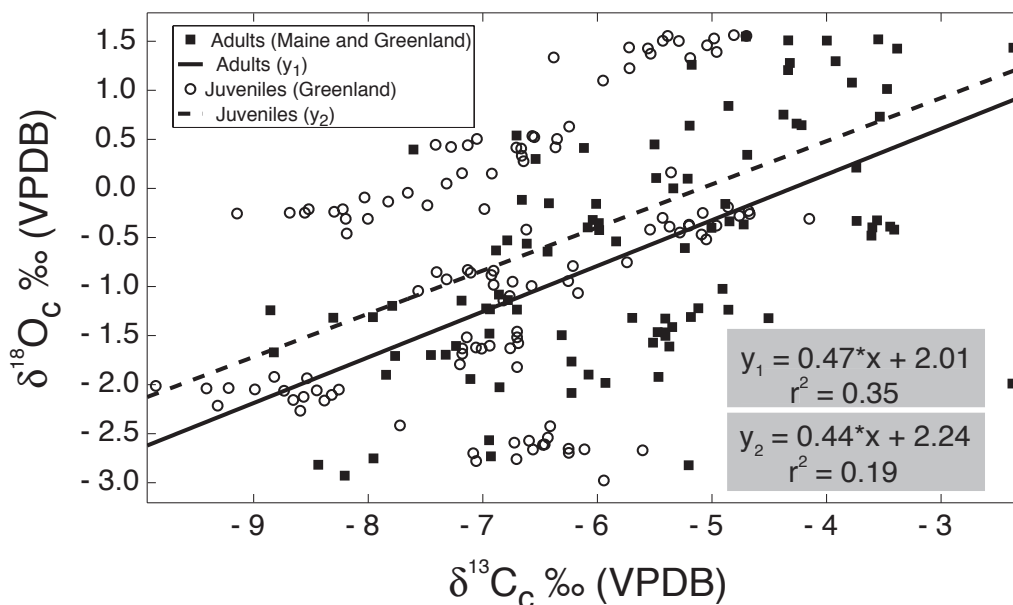


Figure 3.5. Linear correlations between biogenic $\delta^{18}\text{O}_c$ and $\delta^{13}\text{C}_c$ from adult *M. edulis* collected in Maine and Greenland (black squares) and juvenile *M. edulis* from Greenland (open circles).

C.I.) between growth rates (GR) and $\delta^{13}\text{C}_c$ is noted ($\text{GR} = 0.01 * \delta^{13}\text{C}_c + 0.01$; $r^2 = 0.05$; $p < 0.03$, [adults] and $\text{GR} = 0.04 * \delta^{13}\text{C}_c + 0.28$; $r^2 = 0.07$; $p < .004$, [juveniles]), and no correlation exists between growth rates and temperature offset (derived from $\delta^{18}\text{O}$) (Fig. 3.3). Because our data indicates that *M. edulis* deposits its shell in oxygen isotope equilibrium with respect to ambient water (Fig. 3.4), these proposed “vital effect” models (McConnaughey, 1989a; McConnaughey, 1989b; Adkins et al., 2003) do not appear to be valid for this bivalve. Further, Gillikin et al. (2006b) suggested that coupled isotope ($\delta^{18}\text{O}$ and $\delta^{13}\text{C}$) disequilibrium fractionation does not impact bivalves, because bivalves generally precipitate shell material in oxygen isotope equilibrium with ambient water (e.g., Epstein et al., 1953; Chauvaud et al., 2005).

It has been shown that many biogenic organisms do not deposit their skeletons in ($\delta^{13}\text{C}_c$) equilibrium with DIC (e.g., Wefer and Berger, 1991). In order to determine if *M. edulis* deposits its shell in carbon isotope equilibrium with ambient water, we used a $\delta^{13}\text{C}$ DIC/Salinity mixing line from seawater collected at the Darling Marine Center during the summer of 2006 ($\delta^{13}\text{C} \text{ ‰ DIC} = -19.5 + 0.62 * \text{salinity}$; $N = 24$; $r^2 = 0.99$; $p < 0.0001$; [Owen et al., unpublished data, 2006]) to estimate our $\delta^{13}\text{C}$ DIC values. We realize that the estimated $\delta^{13}\text{C}$ DIC values reported here are poorly constrained because we did not monitor $\delta^{13}\text{C}$ DIC continuously throughout the experiment, and that metabolic and atmospheric derived CO_2 , and freshwater input can make $\delta^{13}\text{C}$ DIC values more negative. However, can we rule out significant changes in salinity and/or fresh water input based on the stability of weekly $\delta^{18}\text{O}_w$ measurements (Appendix B). Further, periodic (~ 1 per week) measurements of water pH showed that the water used during culture experiments was highly buffered with an average pH of 8.0 ± 0.1 for all salinity treatments. Therefore, we believe our data remains useful. The relationship between $\delta^{13}\text{C}$ and the DIC of water used during the culture period ($\delta^{18}\text{O}_w$) is depicted in Figure 3.6. The predicted equilibrium values for shell $\delta^{13}\text{C}_c$ is $\delta^{13}\text{C} \text{ ‰ DIC} + 1 \pm 0.2 \text{ ‰}$ (Romanek et al., 1992) for newly formed calcite derived solely from DIC (Fig. 3.6). Based on the data in

Figure 3.6, it appears that *M. edulis* did not deposit its shell in carbon isotope equilibrium with respect to DIC during this culture period. The mean $\delta^{13}\text{C}_c$ values are -4.73‰ ($1\sigma = 1.13\text{‰}$; $N = 36$), -6.21‰ ($1\sigma = 1.38\text{‰}$; $N = 61$), and -6.77‰ ($1\sigma = 1.25\text{‰}$; $N = 121$) for adults (Maine), adults (Greenland), and juveniles (Greenland) respectively. On average *M. edulis* $\delta^{13}\text{C}_c$ values are in disequilibrium by -4.61‰ ($1\sigma = 2.57\text{‰}$; $N = 218$) with respect to ambient DIC (Fig. 3.6). The degree of carbon disequilibrium (deviation from $\delta^{13}\text{C}_c \text{‰ DIC} + 1$; Romanek et al., 1992) increases with increasing $\delta^{18}\text{O}_w$ values (related to salinity) [mean shell carbon disequilibrium values are -1.96‰ (23 PSU), -5.43‰ (28 PSU) and -7.06‰ (32 PSU)] (Fig. 3.7). Nearly 70 % of the carbon isotope disequilibrium (corrected for ambient DIC) is explained by $\delta^{18}\text{O}_w$ values ($r^2 = 0.69$; $N = 218$; $p < 0.0001$) (Fig. 3.7). The increased carbon isotope disequilibrium with increasing salinity may be caused by the activity of the enzyme carbonic anhydrase (CA), which

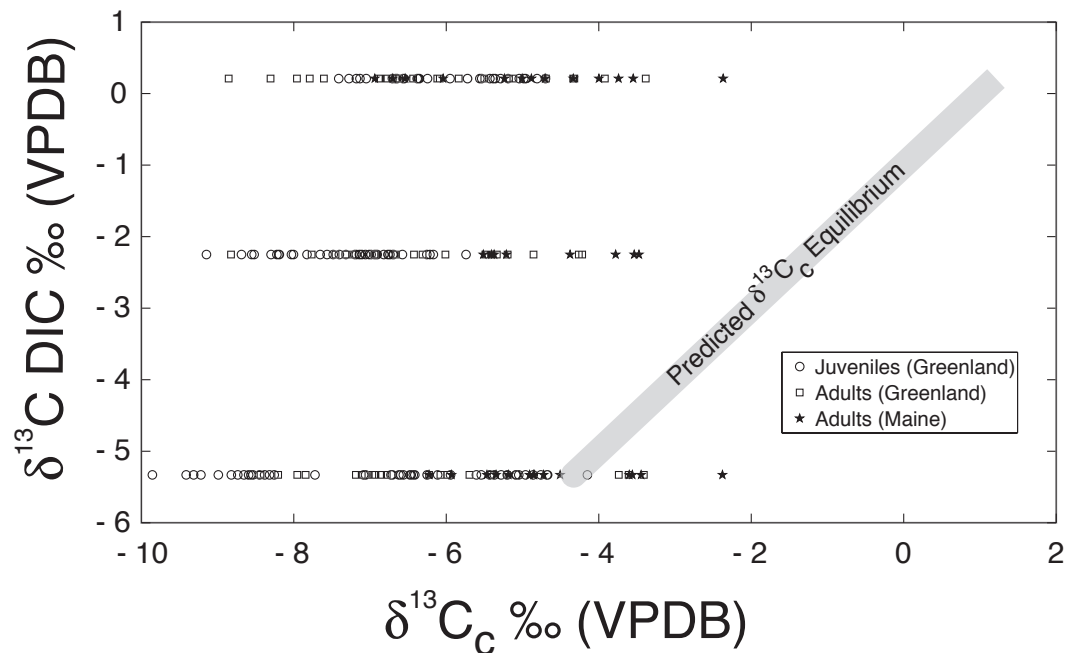


Figure 3.6. Relationship between estimated dissolved inorganic carbon ($\delta^{13}\text{C}_c$ DIC; related to salinity) during culture and shell $\delta^{13}\text{C}_c$. The gray area represents the predicted range of $\delta^{13}\text{C}_c$ values in carbon isotope equilibrium with DIC (Equilibrium = $\delta^{13}\text{C}_c \text{ DIC} \text{‰} + 1.0 \pm 0.2 \text{‰}$ from Romanek et al., 1992). DIC values from Owen et al. [unpublished data, 2006].

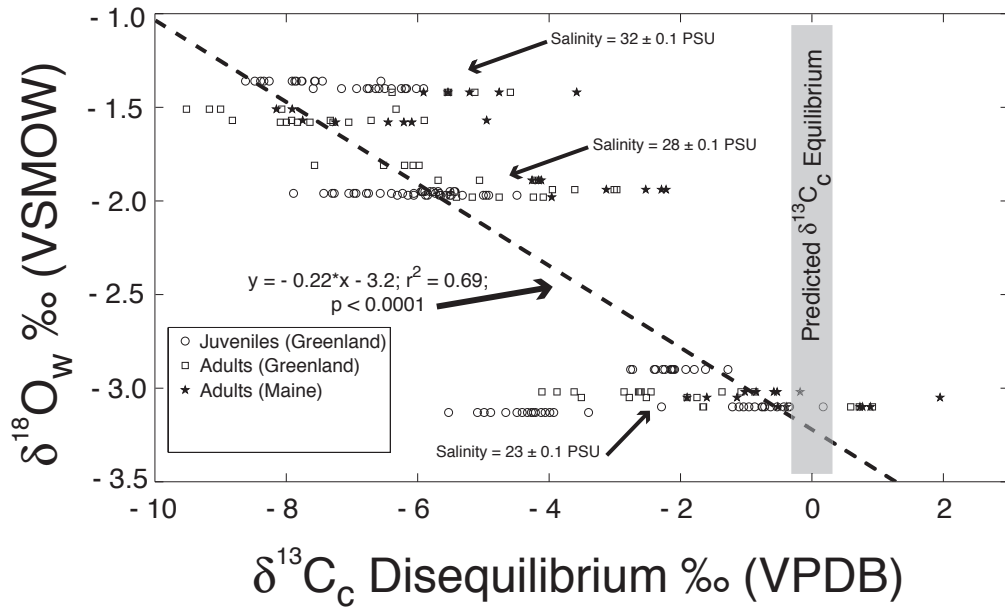


Figure 3.7. Relationship between ambient isotopic composition of water ($\delta^{18}\text{O}_w$) during culture (related to salinity) and estimate of shell $\delta^{13}\text{C}_c$ disequilibrium, where $\delta^{13}\text{C}_c$ of 0 ‰ represents isotopic equilibrium (Equilibrium = $\delta^{13}\text{C}_c$ DIC ‰ + 1.0 ± 0.2 ‰ from Romanek et al., 1992) is shown. The gray area represents the predicted range of $\delta^{13}\text{C}_c$ values in carbon equilibrium with DIC.

catalyzes the reaction between the bicarbonate phase to CO_2 , and facilitates the diffusion of DIC into the calcifying fluid (e.g., Paneth and O’Leary, 1985). CA activity has been linked to the concentration of ambient Cl^- ions, which inhibit the activity of this enzyme (e.g., Pocker and Tanaka, 1978). Therefore at increased salinities (elevated $[\text{Cl}^-]$) a reduction in CA activity may cause a reduction in ambient DIC that is incorporated into the biogenic carbonate, and an increased amount of metabolic carbon may be utilized during biomineralization, which will deplete the calcifying fluid with respect to the DIC pool (e.g., Gillikin et al., 2006b). Because metabolic carbon originates from ingested food it typically has lower $\delta^{13}\text{C}$ values than DIC (DeNiro and Epstein, 1978). The food used during this study primarily was composed of marine phytoplankton, and the $\delta^{13}\text{C}$ values were -35.23 ± 0.18 ‰ ($N = 2$) thus the food has likely influenced the overall shell $\delta^{13}\text{C}_c$ values. Using end-member carbon reservoir conditions (food $\delta^{13}\text{C} = -35.23$ ‰ and ambient $\delta^{13}\text{C}$ DIC values), mean shell $\delta^{13}\text{C}_c$ values (-5.85 ‰ at $\text{DIC} = 0.21$ ‰, -6.68

‰ at DIC = - 2.25 ‰, - 6.29 ‰ at DIC = - 5.33 ‰) (Fig. 3.6), and assuming that $\delta^{13}\text{C}$ food values approximate $\delta^{13}\text{C}$ tissue values (Gillikin et al., 2006), it is estimated that *M. edulis* incorporated ~ 7 % metabolic carbon at 23 PSU, ~ 16 % metabolic carbon at 28 PSU, and ~ 20 % metabolic carbon at 32 PSU based on the metabolic carbon contribution equation of McConnaughey et al. (1997). The increased metabolic contribution to shell $\delta^{13}\text{C}_c$ at higher salinities supports a biologically induced vital effect possibly related to CA activity. Klein et al. (1996b) suggested that high mantle metabolic activity incorporates a greater amount of metabolic derived carbon, whereas low mantle activity would allow more DIC to be incorporated into the shell material. We found no evidence to support greater carbon isotope disequilibrium based on where the animals were collected (Maine or Greenland), culture temperature, growth rates, or shell length (related to the age of the animal). Our results corroborate earlier work by Tanaka et al. (1986) (modified by McConnaughey et al., 1997), Vander Putten et al. (2000), and Gillikin et al. (2006b) that investigated the mechanisms responsible for $\delta^{13}\text{C}$ incorporation into *M. edulis* shells collected *in situ*. In these studies, it was determined that a significant portion of shell $\delta^{13}\text{C}_c$ was derived from metabolic carbon, because $\delta^{13}\text{C}_c$ values were depleted with respect to ambient DIC conditions where the animals lived. Although Gillikin et al. (2006b) estimated that *M. edulis* incorporated less than 10% metabolic carbon into its shell they suggested that environmental reconstructions using $\delta^{13}\text{C}_c$ profiles from *M. edulis* would be limited to extreme changes in ambient $\delta^{13}\text{C}$ DIC/salinity conditions.

Based on previous studies and the results presented here, we suggest that the $\delta^{13}\text{C}_c$ shell values from *M. edulis* are not generally suitable for environmental reconstructions (paleo-DIC or paleo- pCO_2). However, in a low-salinity environment (e.g., upper estuary) $\delta^{13}\text{C}_c$ values from *M. edulis* may be suitable to reconstruct paleo-DIC conditions, because $\delta^{13}\text{C}_c$ values approach equilibrium with respect to ambient DIC (Fig. 3.7). In order for this methodology ($\delta^{13}\text{C}_c$ as a paleo-indicator) to be valid and reliable on biogenic carbonates, it is crucial to develop a better understanding of the mechanisms responsible for the

partitioning of $\delta^{13}\text{C}_c$ during biomineralization. Certainly, the applicability and reliability of $\delta^{13}\text{C}_c$ from bivalves (and other biogenic carbonates) as paleo-indicators could be improved with similar isotope calibration work presented here, especially if $\delta^{13}\text{C} \text{‰}$ DIC is continuously monitored. It is likely that many biogenic organisms precipitate their tests in equilibrium with ambient DIC, but this cannot be readily assumed. Further isotope calibration work coupled with trace metal studies have the potential for unlocking promising biogenic archives that do in fact record important paleoenvironmental conditions.

3.4. Conclusions

In this study, we show that *M. edulis* deposits its shell in isotopic equilibrium with ambient water with respect to oxygen. We have developed a rigorous paleotemperature relationship for *M. edulis* including juveniles and adults from Maine and Greenland grown from 4 ° - 19 °C in three salinity conditions (23, 28, and 32 ± 0.1 PSU). The error associated with this paleothermometer at the 95 % C.I. is only ± 0.57 °C when $\delta^{18}\text{O}_w$ values can be determined independently. We have demonstrated that the shell chemistry of *M. edulis* ($\delta^{18}\text{O}_c$) is not influenced by growth rates, the size of the animal (related to age), or where the animal was collected. The broad modern and paleo-geographic distribution of this bivalve, its abundance during the Holocene, and the lack of intra-species geographic variability in isotope fractionation demonstrated here, makes it an ideal near-shore paleoceanographic proxy throughout much of the North Atlantic Ocean. Based on the $\delta^{13}\text{C}$ DIC/Salinity mixing line used in this study, we have verified that *M. edulis* incorporates a significant portion (7 – 20 %) of metabolic carbon into its shell, and determined that carbon isotope disequilibrium increased with increasing salinity during the culture period. Thus $\delta^{13}\text{C}_c$ profiles from the bivalve *M. edulis* are not generally suitable for reconstructing paleo-DIC or paleo- pCO_2 . However, it may be possible to use $\delta^{13}\text{C}_c$ values from *M. edulis* in low-salinity environments to reconstruct paleo-DIC where

$\delta^{13}\text{C}_c$ values of shell material is nearly in carbon isotope equilibrium with ambient DIC, however this needs to be further investigated. All data associated with this study can be found in Appendix B.

4. Assessing the effects of temperature and salinity on shell carbonate of the long-lived bivalve *Arctica islandica* L.: an aquaculture-based study

The geochemical (stable isotope) signature from shells of the long-lived bivalve *Arctica islandica* Linné (ocean quahog) has been widely used to reconstruct past ocean environments. These reconstructions rely on the assumption that *A. islandica* deposits its shell in isotope equilibrium with ambient water. To test this assumption, we studied the effects of temperature and salinity on newly precipitated bivalve carbonate (CaCO_3 - aragonite), by quantifying shell isotopic chemistry ($\delta^{18}\text{O}_{\text{aragonite}}$) of adult (N = 61) bivalves *A. islandica* collected alive in the northern Gulf of Maine and cultured under controlled conditions. Adult *A. islandica* bivalves (of two size/age classes ~ 36.5 mm [12-15 years old] and ~ 46.8 mm [~20 years old]) from Maine were cultured for 5 months at four temperature ranges (7°, 11°, 15°, and 19°C) and three salinity ranges (23, 28, and 32 parts per thousand [ppt]; related to isotopic composition [$\delta^{18}\text{O}_w$]). Results from this study are compared to the mollusk aragonite equation developed by Grossman and Ku (1986). Based on this comparison, either: 1) *A. islandica* does not deposit its shell in isotope equilibrium with ambient water, or 2) the sampled shells contained a mixture of new (from this study) and old (prior to culture) carbonate material. Because growth rates were low (0.0 – 0.24 mm/month) and the $\delta^{18}\text{O}_w$ of the reservoirs varied substantially (0.22 – 0.43 ‰) during the culture period, it is likely that sampled shell used for the calibration contained a mixture of new and old carbonate rather than *A. islandica* depositing its shell in isotope disequilibrium. In addition, previous work by Weidman et al. (1994) suggests that *A. islandica* deposits its shell in isotope equilibrium with seawater. We therefore assume that our calibration attempt was ineffective. Future isotope calibration work with *A. islandica* should include 1-2 years of culture time to ensure sufficient new growth to assess if this bivalve deposits its shell in isotope equilibrium.

4.1. Introduction

Stable isotope profiles (mostly oxygen) and growth histories from the shells of *Arctica islandica* (Linnaeus 1767) (ocean quahog) have been widely used in paleoceanography (Weidman and Jones, 1993a; Weidman et al., 1994; Witbaard et al., 1994; Marsh et al., 1999; Marchitto et al., 2000; Schöne et al., 2003a; 2004; 2005a; 2005b). *A. islandica* is a long-lived, slow-growing bivalve that is commonly over 100 years old. Further, extremely old *A. islandica* individuals have been reported to be 225, 268 and 374 years old by Ropes and Murawski (1983), Forsythe et al. (2003) and Schöne et al. (2005a) respectively. The longevity and the sub-arctic to mid-latitude distribution of *A. islandica* in the northern hemisphere make it an extremely useful proxy of past ocean environments. Because *A. islandica* deposits distinct annual lines in its shell, it is possible to reconstruct past ocean environments at sub-annual resolution (Thompson et al., 1980; Jones, 1980; Jones, 1983; Ropes, et al., 1984; Kraus et al., 1992; Kennish et al., 1994). If the collection date is known, paleoenvironmental reconstructions with an absolute chronology can be created (e.g., Jones, 1983, Jones et al., 1989; Schöne et al., 2005a; 2005b).

Thus far, it has been assumed that *A. islandica* deposits its shell in isotope equilibrium (carbon and oxygen) with ambient water (e.g., Weidman et al., 1994). In addition, paleotemperature reconstructions using this bivalve have been primarily based on the empirical relationship developed by Grossman and Ku (1986) for mollusks (10 species of Gastropods and 2 species of Scaphopods; N = 28) that form an aragonitic shell layer. The Grossman and Ku (1986) mollusk paleotemperature relationship has been extremely helpful in estimating past ocean temperatures based on oxygen isotope profiles ($\delta^{18}\text{O}_c$) when the isotopic composition of the water ($\delta^{18}\text{O}_w$) was known or could be estimated reliably. However several uncertainties still exist from these reconstructions, including: 1) knowing if a generic paleotemperature relationship is suitable for other

aragonitic organisms (i.e., *A. islandica* may exhibit vital effects during biomineralization, or may not deposit its shell in equilibrium with the ambient water); 2) some key environmental parameters were estimated ($\delta^{18}\text{O}_w$ and water temperature) for some of the mollusks used in the paleotemperature equation; and 3) the root mean squared error (RMSE) associated with the Grossman and Ku (1986) mollusk equation is ± 1.5 °C at the 95% confidence interval, making it difficult to decipher water temperature changes that may only be 1-3 °C. Recent work by Wanamaker et al. (2006) demonstrated that species-specific (*Mytilus edulis*- common blue mussel) isotope calibrations are feasible and offer many benefits over generic isotope calibrations (e.g., Epstein et al., 1953; Grossman and Ku, 1986), including highly controlled culture conditions (e.g., temperature, $\delta^{18}\text{O}_w$, growth), multiple bivalves grown at each temperature, and a paleotemperature equation that is rigorous ($N > 300$) with a small error (RMSE ± 0.57 °C). Also, because the isotopic variability of shell material (blue mussel) was thoroughly examined during culture, isotope reconstructions that utilize the Wanamaker et al. (2006) equation for the blue mussel have fewer uncertainties than generic isotope calibrations.

To address these issues in the ocean quahog, we quantified the variability of shell isotope chemistry of the bivalve *A. islandica* cultured under controlled temperature and salinity conditions for five months.

4.2. Materials and Methods

4.2.1. Experimental Bivalve- *Arctica islandica*

Arctica islandica (ocean quahog) is a long-lived bivalve with a wide geographic distribution throughout the northern North Atlantic Ocean. *A. islandica* has been recognized as an important marine geochemical biorecorder (e.g., Weidman *et al.*, 1994). Further, growth histories (similar to dendrochronology) from this bivalve have proven

to record environmental ocean conditions (e.g., productivity, temperature, circulation changes) (Jones, 1980; Witbaard et al, 1997; Schöne et al., 2003a). It is abundantly distributed along the eastern and western Atlantic ocean at depths from 10 to 244 m (in full-ocean salinity conditions) in sand and mud/sand sediments, where summer temperatures remain below 20 °C (Cargnelli et al., 1999). In the western Atlantic, *A. islandica* is found from St. George's Bay, Newfoundland to north of Cape Hatteras. South of Cape Cod, beds occur progressively farther offshore (Feindel et al., 2003). The ocean quahog is a filter feeder, primarily relying on phytoplankton that settle into the benthic zone. It is an extremely long-lived bivalve with low natural mortality (Weinberg, 1993). In addition, 100-year-old individuals were fairly common on federal survey cruises on the Mid-Atlantic shelf (Cargnelli et al., 1999). Growth rates of young animals are variable. Reports on the mean age of quahogs at 50 mm shell length range from 12 years (Kennish et al., 1994) to 30 years (Kraus et al., 1992). These variations in growth rates are attributed to different environmental conditions. The growth rate decreases with age, and generally a maximum size is reached at approximately 140 mm (Ropes et al., 1984). Shell growth appears to be primarily related to food quality and availability (e.g., depth of the water column, horizontal advection) as well as water temperature (Beal and Kraus, 1989; Witbaard, 1996; Witbaard et al., 1999). The shell of *A. islandica* is composed of an inner and outer layer, both of which are aragonitic (Ropes et al., 1984) (Fig. 4.1). The outer shell layer contains annual layers (bands) and carbonate material removed from this part of the shell reflects ambient ocean conditions (Weidman et al., 1994).

The age at which ocean quahogs reach sexual maturity is highly variable (Cargnelli et al., 1999). Rowell et al. (1990) reported individuals reaching maturity at approximately 13 years old for animals near Nova Scotia. Thompson et al. (1980) found animals reached sexual maturity around 9 years old for Middle Atlantic Bight populations. The spawning of the ocean quahog is quite long, sometimes lasting from

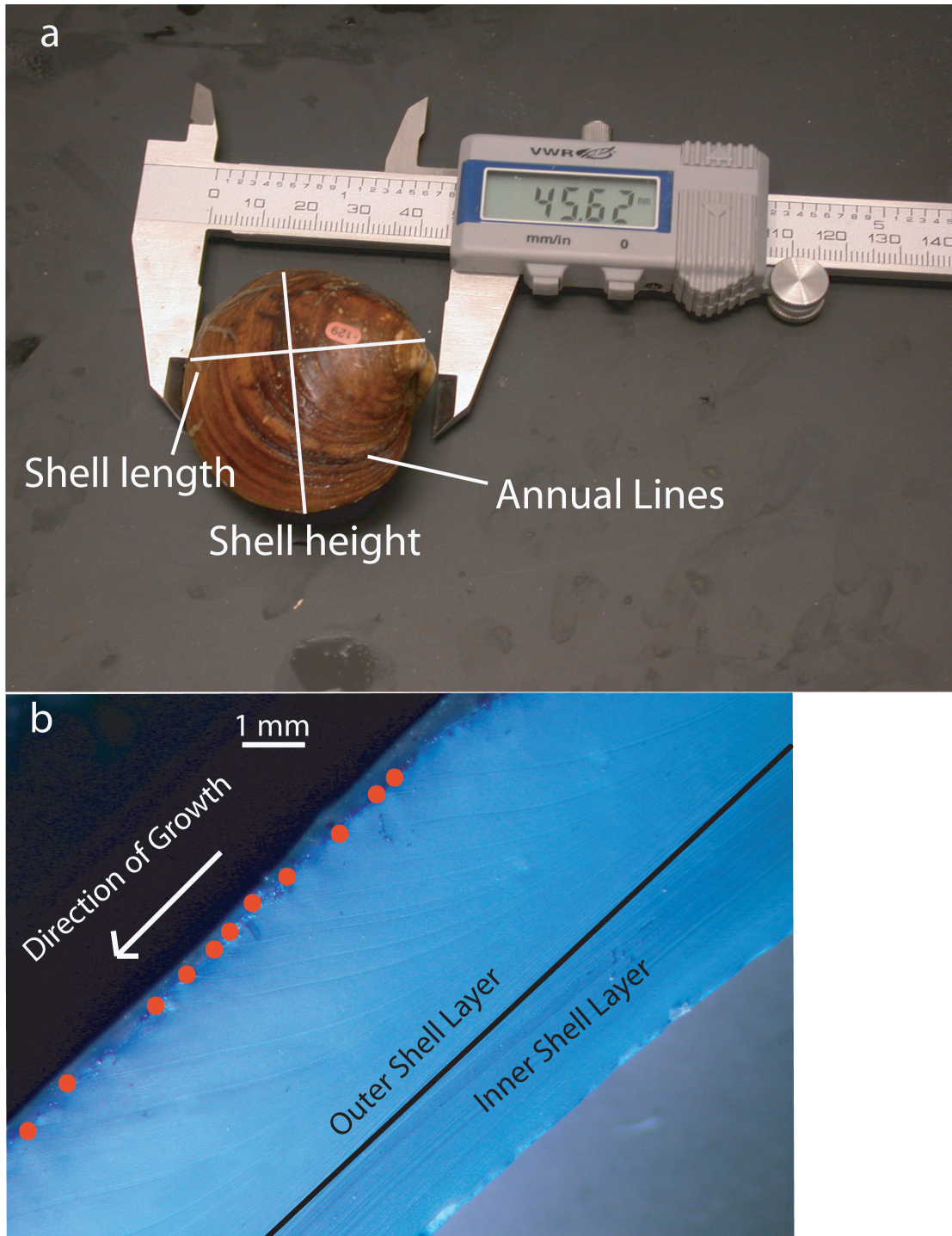


Figure 4.1. (a) *Arctica islandica* (ocean quahog) being measured for shell length. Note the evidence of annual lines on the shell surface. (b) Polished and stained (Mutvei solution, methods detailed in Schöne et al., 2005c) section of *A. islandica*. Note the two-layered shell and the appearance of annual lines (marked by red dots).

spring to fall (Cargnelli et al., 1999). The environmental conditions for spawning are not clearly known yet (Cargnelli et al., 1999), but Jones (1981) and Mann (1982) believe that spawning is coincident with the highest seasonal water temperatures (usually occurring in fall). Further, some other environmental stimuli such as food availability, pH change, or increases in dissolved oxygen may work in conjunction with warmer water to initiate spawning (Mann, 1982).

4.2.2. Animal Collection

Approximately 200 live *A. islandica* individuals were collected from the Gulf of Maine, USA by the Maine Department of Marine Resources during a stock assessment in 2003. Animals were transported to the Darling Marine Center in Walpole, Maine, where they were kept in the flowing seawater laboratory receiving ambient conditions from the Damariscotta River, until they were placed in the aquaculture system.

4.2.3. Aquaculture Design and Implementation

An aquaculture system was designed at the Darling Marine Center to achieve four temperature settings (7, 11, 15 and 19 ± 0.5 °C) (Fig. 4.2) and three salinity settings (23, 28, and 32 ± 0.1 ppt) (see section II and III for details). This four by three factorial design allowed 12 different growing conditions to be maintained simultaneously.

Fifteen ocean quahogs were placed in each 20-liter temperature/salinity environment, for a total of 180 animals. Five quahogs in each temperature and salinity configuration were tagged on October 29, 2003 with a numbered shell fish tag (~3mm) directly adhered to each animal. The shell length for each these quahogs were determined with digital calipers (± 0.01 mm) by measuring along the maximum growth axis (Fig. 4.1), and monitored monthly. The quahogs used during this study were of two age classes

(12-15 and ~ 20 years old) based on counting of external bands on the shell. The mean size of the tagged animals ($N = 60$) was 42.71 ± 4.32 mm. The animals were cultured for a total of 5 months (November 2003 through March 2004).

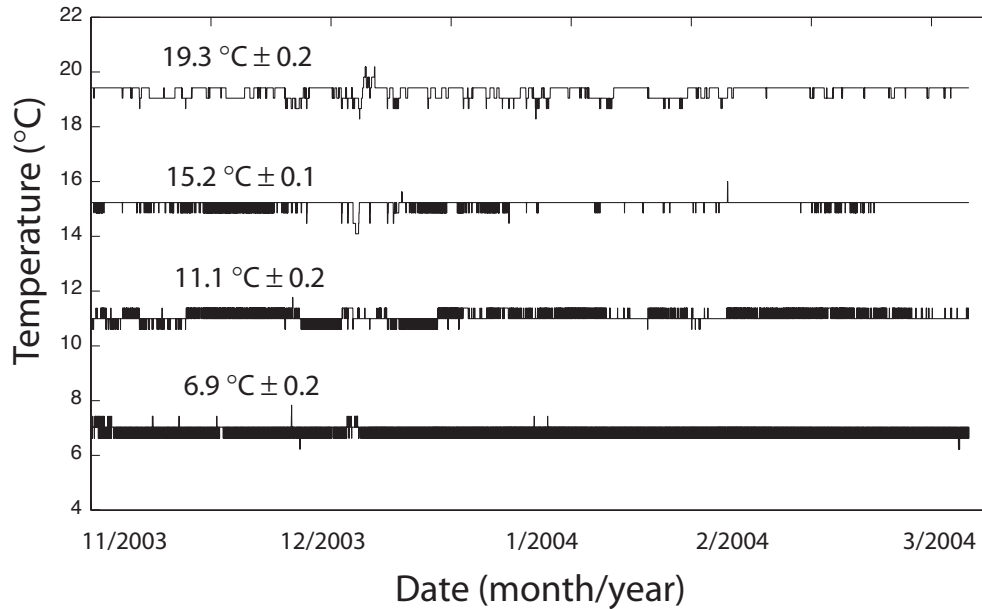


Figure 4.2. Temperatures for each of the four freshwater baths are shown with the 5-month mean and standard deviation. The HOBO® H8 data logger digitally measured water temperature with an error of ± 0.5 °C, and the appearance of two lines for each temperature is an artifact of the digital measurement.

Complete water changes for each temperature/salinity environment were made weekly, to remove metabolic waste. The aquaculture design allowed for one extra 20-liter bucket to be in place with identical water (isotopic composition and temperature). Quahogs were fed twice daily (total of 10 ml) a concentrated spat formula (Shellfish Diet; Innovative Aquaculture Products, Ltd.) where 5 ml of spat was diluted in 1 liter of water identical in isotopic composition to that in which they grew. Water samples for each of the twelve buckets were collected weekly, after water changes were made, to monitor $\delta^{18}\text{O}_w$ (Fig. 4.3). There was no isotopic difference noted when water was collected prior to and after water changes. Throughout the experiment mortality was low (7.2 %) for

all temperature and salinity configurations, except for one bucket (20 °C; 23 ppt) that experienced a 33 % (5 of 15) mortality rate. This is likely attributed to an inability of *A. islandica* to tolerate both warm water (20 °C) and low salinity conditions (23 ppt) for an extended time.

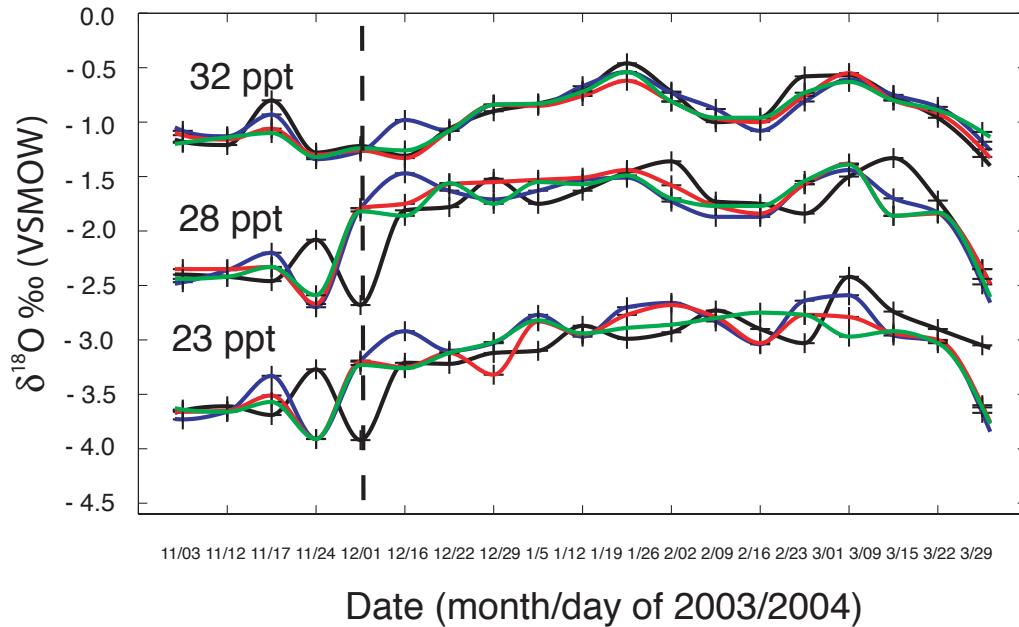


Figure 4.3. The oxygen isotopic composition ($\delta^{18}\text{O}_w$) for each of the 12 growing environments is shown for the 5-month period. The salinities are 32 ppt (top), 28 ppt (middle), and 23 ppt (bottom). Temperatures are 19 °C (green), 15 °C (red), 11 °C (blue), and 7 °C (black). The dashed vertical line represents the onset of reservoirs freezing. The analytical error associated with the measurement is ± 0.10 ‰ (VSMOW).

4.2.4. Sample Preparation and Analysis

Weekly water samples ($\delta^{18}\text{O}_w$) were measured via a dual-inlet VG/Micromass SIRA, with a precision of ± 0.10 ‰ based on replicate International Atomic Energy Agency (IAEA) laboratory standards [Vienna Standard Mean Ocean Water (VSMOW), Standard Light Antarctic Precipitation (SLAP), IAEA OH-1, IAEA OH-2, IAEA OH-3, IAEA OH-4, and internal laboratory standards Big Bear Brook (BBB), Light Antarctic

Precipitation (LAP), Antarctic Surface Snow (ASS)], where one standard was run for every five samples. All $\delta^{18}\text{O}_w$ (δ in ‰ = $[(R_{\text{sample}}/R_{\text{standard}}) - 1] * 1000$; $[R = ^{18}\text{O}/^{16}\text{O}]$) values are reported with respect to VSMOW. Weekly $\delta^{18}\text{O}_w$ from each temperature/salinity environments were averaged over the growing intervals, and used in the isotope calibration (Fig. 4.3).

Animals were cleaned and air-dried. Shell samples were further oven dried at 40 °C overnight. The periostracum was removed with a razor blade along the ventral margin. Prior to sampling, the shell length of each animal was recorded. The outer edge of each valve was micro-milled using a variable speed mounted drill and binocular microscope with 6.5x to 40x magnification.

Shell carbonate analysis ($\delta^{18}\text{O}_c$ and $\delta^{13}\text{C}_c$) was performed on a dual-inlet VG/Micromass Prism, via a 30-place carousel and common acid bath without chromium oxide (CrO_3) at 90°C, with precision of ± 0.20 ‰ ($\delta^{18}\text{O}_c$) and ± 0.17 ‰ ($\delta^{13}\text{C}_c$) based on laboratory standards. Samples were calibrated using NBS-19 standards at the beginning and end of each run, with a standard to sample ratio of 1:3. Average shell samples weighed approximately 100 μg . All shell carbonate values are reported with respect to Vienna Pee-Dee Belemnite (VPBD).

4.3. Results and Discussion

4.3.1 Growth During Culture

New linear shell growth during the five-month culture period was low (0.0 mm – 1.2 mm) and highly variable (Fig. 4.4). There was a significant relationship between growth and temperature, with animals growing faster in colder water than in warmer water (Fig. 4.4). The data were fit with a power model ($\text{Growth} = a * x^b$; $a = 41.39$; $b = -2.07$; $r^2 = 0.56$; $p < 0.0001$), and the temperature may explain 56 % of the observed variance in growth. Fourteen tagged quahogs of 58 that lived (~ 24%) showed no

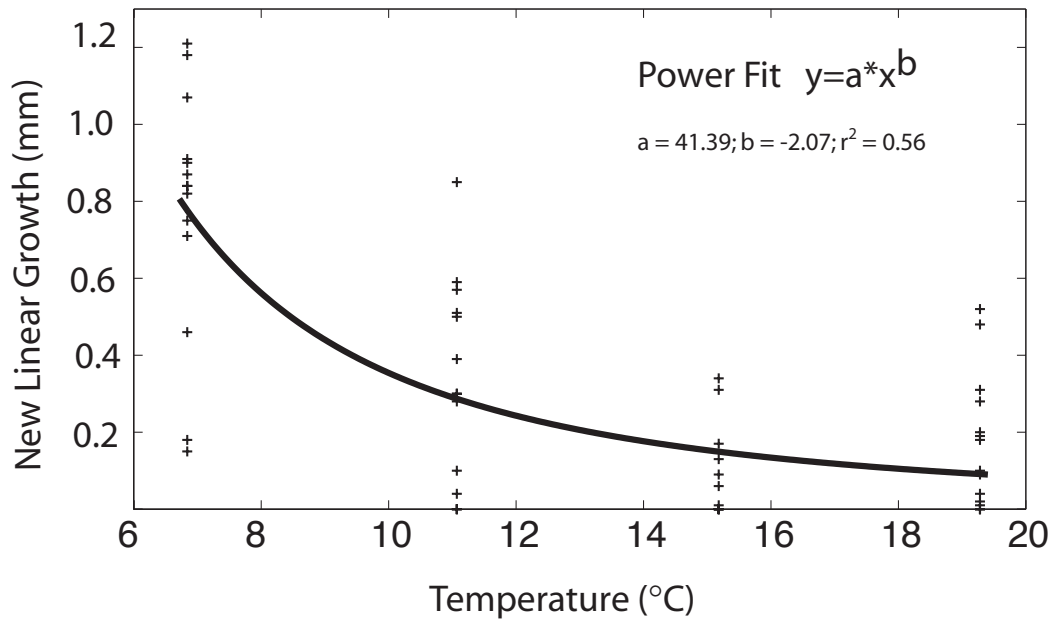


Figure 4.4. Growth of tagged animals as a function of growing temperature.

measurable growth during the experiment. Of these, four were in 11 °C, seven were in 15 °C, and three were in 19 °C. All animals in the 7 °C temperature setting showed measurable growth. There was no apparent trend in growth based on salinity (Growth = $0.42 - 0.0004*x$; $r = 0.04$). A weak relationship between growth and shell length is noted in Figure 4.5. Larger animals grew more on average than smaller animals (Growth = $-1.63 + 0.05*x$; $r^2 = 0.31$; $p < 0.0001$). Animals in colder water grew faster than animals in warmer water, which was reasonable because *A. islandica* has an upper thermal tolerance of ~ 20°C (e.g., Cargnelli et al., 1999), and they are commonly found in Arctic-like environments. However, the fact that larger animals grew faster than smaller ones was not expected. This contradicts the many published reports that juveniles (i.e., small quahogs) grow faster than adults (e.g., Thompson et al., 1980; Ropes et al., 1984; Kennish et al., 1994). One possible explanation for this anomalous result is that the larger animals were healthier than the smaller ones, but that is difficult to confirm. All quahogs experienced extremely low and highly variable growth during culture at each temperature. Kraus et

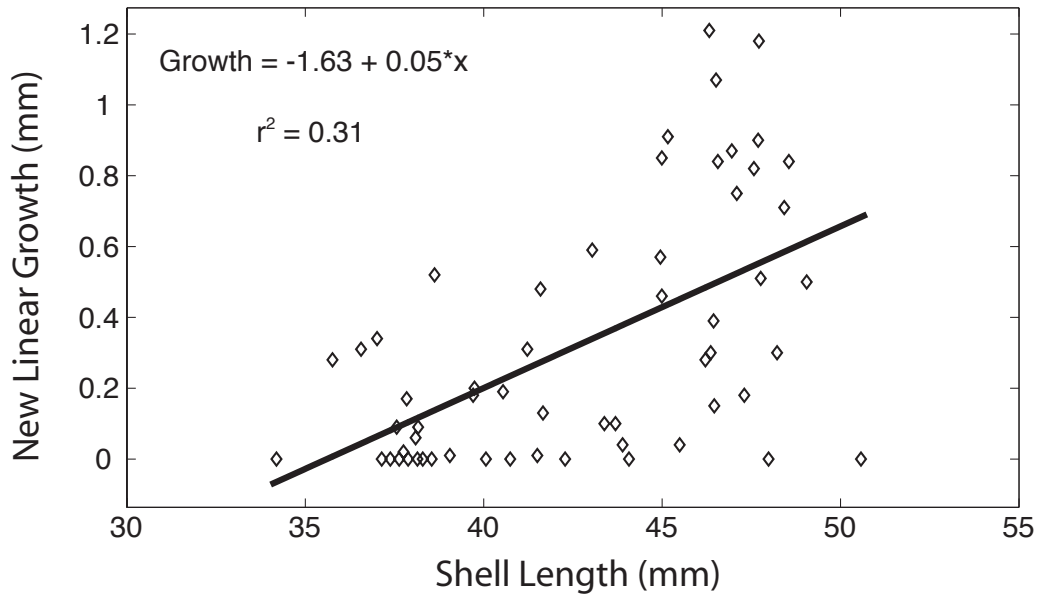


Figure 4.5. Growth of tagged animals as a function of shell height.

al. (1992) reported average growth rates of 0.61 mm/month for laboratory reared adult *A. islandica* individuals (average shell length of 53.9 mm [N = 43]), which received ambient conditions from the Damariscotta River, Walpole, ME. Further, Lutz et al. (1983) reported growth rates for juvenile *A. islandica* of ~ 1.7 mm/month grown *in situ* (predator-exclusion containers suspended from a dock near Boothbay Harbor, ME). In this experiment, growth rates for *A. islandica* ranged from 0.0 – 0.24 mm/month. These rates are 2.5 to 7 times lower than Kraus et al. (1992) and Lutz et al. (1983) reported, respectively. The largest difference between our experimental design and previous ones (Lutz et al., 1983; Kraus et al., 1992) is that the quahogs in their experiments experienced ambient ocean conditions, which included seasonal variations in food and temperature. We suggest that animals in our experimental design grew less because there was very little environmental change (constant temperature and salinity) to trigger growth, which might be needed for this species. Kraus et al. (1992) noted that growth in quahogs decreased from September to December, which may be related to reproduction cycles. Once again, growth in our experiment could have been affected by reproduction, because

of the timing of culture (November through March). Further, Beal and Kraus (1989) reported that growth rates might be reduced at high quahog densities. Alternatively, the experimental design was not suitable (e.g., processed food, 20-liter containers, size of quahogs, etc.) for quickly growing animals. Further, if animals were grown longer (1-2 years), it would be likely that there would be sufficient new shell growth that would be representative of the controlled conditions. Also, it is likely that juvenile *A. islandica* animals would grow substantially more shell material than adult quahogs.

4.3.2 Effects of Temperature and Salinity on Shell Carbonate ($\delta^{18}\text{O}_{\text{aragonite}}$)

The relationship between culture temperature and shell carbonate values (corrected for the isotopic composition of water; related to salinity) is shown in Figure 4.6. Further, these results are compared to the aragonite equation for mollusks derived by Grossman and Ku (1986) (Fig. 4.6). The Grossman and Ku (1986) aragonite equation is generally assumed to represent isotope equilibrium for biogenic aragonite (Weidman, et al., 1994). The isotopic variability ($\delta^{18}\text{O}_{\text{shell}} - \delta^{18}\text{O}_{\text{water}}$) at each temperature range is extremely large ($1 \sigma = 0.82 \text{‰}$ at 15 °C, 0.98 ‰ at 19 °C, 1.34 ‰ at 11 °C, and 1.42 ‰ at 7 °C) compared to similar studies where values ranged from 0.10 ‰ to ~ 0.30 ‰ at any one temperature (e.g., Epstein et al., 1953; Grossman and Ku, 1986; Owen et al., 2000a; Wanamaker et al., 2006). Further, the isotopic variability at any one temperature was consistently much larger than the combined analytical errors associated with measuring $\delta^{18}\text{O}_{\text{c}}$ and $\delta^{18}\text{O}_{\text{w}}$ of $\pm 0.22 \text{‰}$ (Miller and Miller, 1993). The mean isotopic value ($\delta^{18}\text{O}_{\text{shell}} - \delta^{18}\text{O}_{\text{water}}$) for each temperature is 1.89 ‰ at 19 °C, 1.81 ‰ at 15 °C, 2.35 ‰ at 11 °C, and 2.47 ‰ at 7 °C. There is no isotopic difference between 19 °C and 15 °C or between 11 °C and 7 °C. These results suggest that the carbonate material precipitated during culture does not reflect ambient temperature very accurately, or that the material sampled for analysis contained a mixture of new (this study) and old (previous to culture) aragonitic growth. Further, the isotopic composition of the water used in this study had

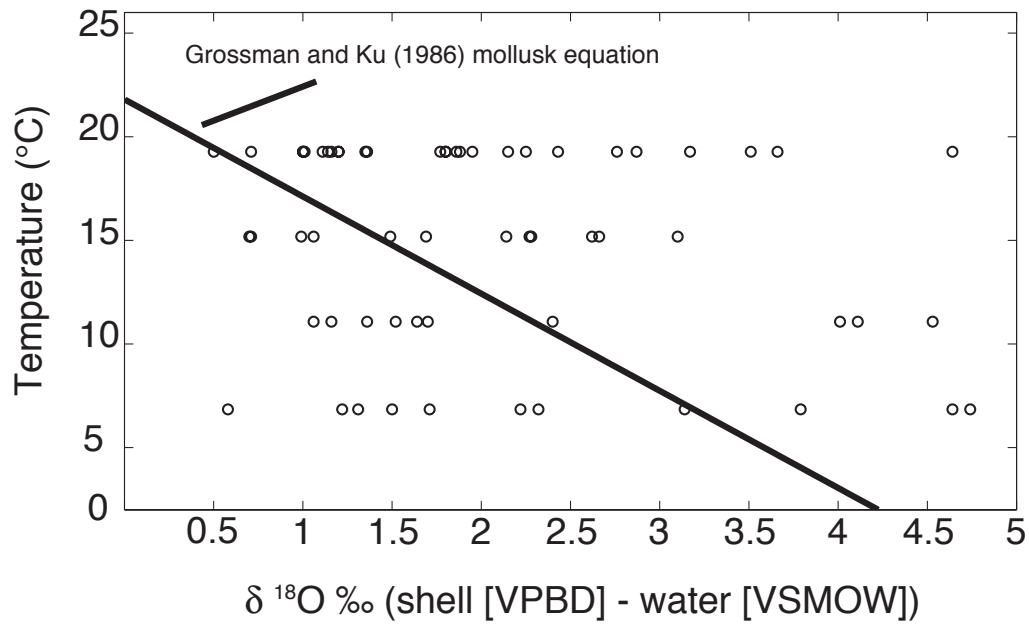


Figure 4.6. Oxygen isotope results for *A. islandica* (open circles) during culture compared to the mollusk equation of Grossman and Ku (1986) (solid black line). The combined analytical error associated with the measurements (carbonate and water) is ± 0.22 ‰ (VSMOW). The water temperature was measured with an error of ± 0.5 °C.

variations on the order of 0.22 ‰ to 0.43 ‰ (Fig. 4.3). These variations in $\delta^{18}\text{O}_{\text{water}}$ are three to six time greater than error associated with the measurement (± 0.07 ‰). Reservoir tanks were subjected to freezing in December 2003, which made the isotopic composition of the water heavier (Fig. 4.3). This may explain approximately 25% of the isotopic variability (0.82 – 1.42 ‰) noted here (Fig. 4.6).

4.3.3 Previous Work- An *In situ* Isotope Study Using *A. islandica*

Weidman et al. (1994) demonstrated that a 38-year-old *A. islandica* bivalve collected alive in 1991 near the Nantucket Shoals Lightship (Cape Cod, Massachusetts) in 60 m water depth grew its shell in isotope equilibrium with seawater. Daily water temperature and weekly salinity measurements were recorded during from 1956-1971. Oxygen isotope values using the Grossman and Ku (1986) mollusk temperature equation

during this interval (1956-1971) yielded reasonably accurate and precise (+ 0.38 °C and ± 1.1 °C) bottom water temperature estimates based on the measured temperature and salinity values (see Weidman et al., 1994 for details). Based on this result, and the lack of a successful calibration noted here, we assume that *A. islandica* deposits its shell in oxygen isotope equilibrium with seawater. However, the Weidman et al. (1994) study only consisted of one individual, and they were unable to assess potential vital effects based on size or age. We suggest that water temperature estimates derived (if salinity is known) from *A. islandica*, based on the Grossman and Ku (1986) mollusk equation, are scientifically valid, but considerable uncertainties still exist (e.g., magnitude of error and potential vital effects). Therefore, we believe that it is still an important goal to perform an isotope-based calibration of *A. islandica*.

4.4. Improvements and Future Work

4.4.1 Growth Estimation

Systematic errors may have been introduced during monthly shell measurements if the digital calipers were slightly offset along the maximum growth axis. This potential error can be introduced because the shell morphology of the valve is fairly variable (Fig. 4.1). All growth estimates were based on initial shell length measurements at the onset of culturing. Therefore, any errors associated with the initial size determination were propagated during the entire experiment. Further, introduced errors during growth determination may have inflated growth estimates, which may help explain why the isotopic variability of aragonitic material was so high. This would support the idea that shell samples were a mixture of new and old aragonite. This error can be minimized in the future by marking the outer shell with a line along the axis of maximum growth to ensure that measurements are taken from the same location consistently.

An additional technique to determine growth rates in the future will include bio-

marking (e.g., Kaehler and McQuaid, 1999; Day et al., 1995; Pirker and Schiel, 1993), which involves immersing the animal in a solution that will mark the shell (e.g., calcein, tetracycline, alizarin red). As the animals deposit new shell material, they incorporate the marking solution as a disturbance line in the shell. Most bio-marking solutions illuminate under ultra violet light, making it fairly easy to determine new growth during culture.

4.4.2 Aquaculture Design and Culture Duration

Many improvements need to be made to the aquaculture system in order to successfully grow *A. islandica*. Steps need to be taken to ensure that the reservoirs holding the water to be used for water changes (pre-mixed for a specific isotopic composition) are not subject to freezing and thawing cycles. Because the reservoirs are large (~ 2 m diameter) they occupy considerable floor space. However, arrangements were made based on this study to move reservoirs indoors for future work. This improvement will greatly decrease the isotopic variability of water used during culture.

The quality of food used during this experiment may also have affected growth rates, because it was a concentrated formula rather than live algae. A concentrated food (Shellfish Diet; Innovative Aquaculture Products, Ltd.) was used because it would not alter the isotopic composition of the water used during culture. However, it is possible to centrifuge fresh algae on site (Feindel, pers. com.). This would likely improve the quality of food and may improve growth.

The time of culture for *A. islandica* should be increased to 1-2 years at least, because they are among the slowest growing bivalves (Thompson et al., 1980; Ropes et al., 1984; Kennish et al., 1994). If growth of *A. islandica* in future experiments increased compared to this study so that sufficient new shell material (~ 2 mm) was deposited, then the experiment could be stopped early. Also, if new shell growth is too low, we would experiment (separately) with changing the environmental conditions (e.g., temperature) to stimulate growth. We would do this via a flowing seawater apparatus (e.g., Kraus

et al., 1992), where temperature and salinity vary seasonally. Annual values for water temperature, salinity, and shell oxygen isotope composition ($\delta^{18}\text{O}_{\text{shell}}$) would be used to determine if *A. islandica* deposits its shell in isotope equilibrium with seawater.

Further, it is likely that *A. islandica* would grow better (faster) in a larger container. Thus, the size of the buckets should be increased (at least doubled) to allow for a greater volume of water during growth. In addition, only ten animals should be used in each bucket, decreasing metabolic waste. This is not risky because of the low mortality rates reported in this study. If possible, small adults or juvenile specimens of *A. islandica* should be used in future experiments because juveniles tend to grow faster than adults (e.g., Kraus et al., 1992).

4.5. Conclusions

In this five-month aquaculture experiment we attempted to quantify temperature and salinity effects on the isotopic composition of shell material for the bivalve *A. islandica*. Results from this study are compared to the mollusk aragonite equation developed by Grossman and Ku (1986). Based on this comparison, either *A. islandica* does not deposit its shell in isotope equilibrium with ambient water, or the sampled shells contained a mixture of new (from this study) and old (prior to culture) carbonate material. However, based on limited growth during the culture period, experimental errors (growth estimation), and highly variable culture conditions (in $\delta^{18}\text{O}_{\text{water}}$), it is more likely that the shells sampled in this experiment contained a mixture of new and old aragonite material, and that a large portion (25 – 30 %) of the isotopic variability ($\delta^{18}\text{O}_{\text{shell}} - \delta^{18}\text{O}_{\text{water}}$) was a result of variable $\delta^{18}\text{O}_{\text{water}}$ conditions. A future effort to determine if *A. islandica* deposits its shell in isotope equilibrium is still needed, and improvements noted here will help make it possible.

5. A Late Holocene paleo-productivity record in the Western Gulf of Maine, USA inferred from growth histories of the long-lived ocean quahog (*Arctica islandica* L.)

To investigate environmental variability during the late Holocene in the Western Gulf of Maine, USA, we collected a 142-year old living bivalve (*Arctica islandica* Linné) in 2004, and three fossil *A. islandica* shells of the Medieval Warm Period (MWP) and late MWP / Little Ice Age (LIA) period (corrected $^{14}\text{C}_{\text{AMS}} = 1030 \pm 78 \text{ AD}$; $1320 \pm 45 \text{ AD}$; $1357 \pm 40 \text{ AD}$) in 1996. We compared the growth record of the modern shell with continuous plankton recorder (CPR) time-series (1961 - 2003) from the Gulf of Maine. A significant correlation ($r^2 = 0.55$; $p < 0.0001$) exists between the standardized annual growth index (SGI) of the modern shell and the relative abundance of zooplankton species *Calanus finmarchicus*. We therefore propose that SGI data from *A. islandica* is a valid proxy for paleo-productivity of at least one major zooplankton taxa. SGIs from these shells reveal significant periods of two to six years (NAO-like) based on wavelet analysis, multitaper method (MTM) analysis and singular spectrum analysis (SSA) during the late Holocene. Based on established physical oceanographic observation in the Gulf of Maine, we suggest that slopewater variability coupled with North Atlantic Oscillation (NAO) dynamics is primarily responsible for the observed SGI variability.

5.1. Introduction

The Gulf of Maine is a mid-latitude sea situated in the northwestern Atlantic Basin located along a hydrographic and faunal transition zone that is sensitive to minor climate shifts (Fig. 5.1) (e.g., Marine Ecosystem Response to Climate In the North Atlantic: MERCINA, 2001; 2003). The Gulf of Maine is an extremely productive ocean environment that supports a rich and dynamic ecosystem. Because of its geographic location, changes in the strength and/or position of slope water currents (e.g., Labrador Current, Gulf Stream) are thought to significantly affect the oceanography (temperature,

salinity, productivity, etc.) in the Gulf of Maine (Dickson et al., 1996; Keigwin and Pickart 1999; Pickart et al. 1999; MERCINA 2001; Greene and Pershing 2001; Conversi et al., 2001). Further, dominant modes of climate variability in the North Atlantic such as the North Atlantic Oscillation (NAO) have been linked to variability in ecosystem dynamics (e.g., Drinkwater and Mountain, 1997; Drinkwater et al., 2003). Understanding the mechanisms responsible for the observed interannual-to-decadal changes in zooplankton levels in the Gulf of Maine remains a fundamental research problem (e.g., Pershing et al., 2005). A better understanding of zooplankton dynamics would provide a framework for policy makers to protect and conserve the ecosystem (MERCINA, 2001; 2003; Greene and Pershing, 2003; Pershing et al., 2004; 2005). Knowledge of past productivity levels in the Gulf of Maine would substantially improve the ability of biological modelers to forecast changes in the Gulf of Maine's ecosystem. In addition, long, continuous environmental records would also allow investigations into the connections among climate, oceanography, and ecosystem dynamics in the Gulf of Maine.

The Continuous Plankton Recorder (CPR) survey is slightly longer than 40 years in the Gulf of Maine and is operated by the National Oceanic and Atmospheric Administration (NOAA). The CPR survey consists of continuous horizontal tows between Boston, Massachusetts and Cape Sable, Nova Scotia at 10 m depth approximately monthly, by ship-of-opportunity (e.g., Pershing et al., 2005). The CPR filters zooplankton via a silk gauze with a 270- μm mesh, collecting zooplankton and relatively large phytoplankton. The resulting CPR dataset contains spatially indexed zooplankton taxa abundances (e.g., Clark et al., 2001). Because the CPR survey is relatively short, it is necessary to use proxy records to reconstruct productivity prior to the 1960s. Shells of bivalve mollusks serve as important archives of paleoenvironmental conditions, and can provide high-resolution records of past and present ocean variability (e.g., temperature, salinity, productivity, dissolved inorganic carbon [DIC], pCO_2 ,

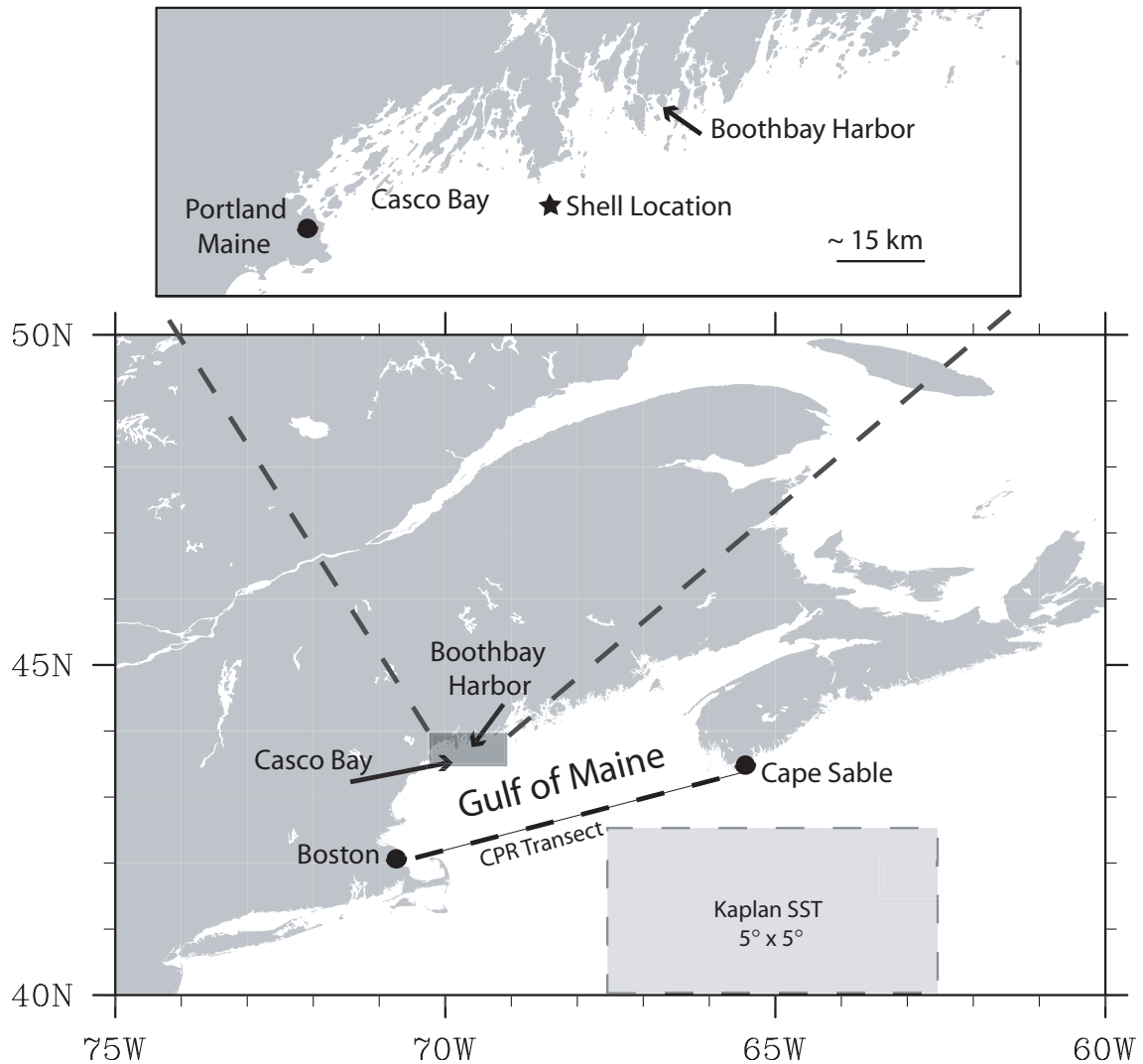


Figure 5.1. The general geographic map for the Gulf of Maine (bottom), noting Casco Bay, shell location, and Boothbay Harbor (SST record) (top panel) is shown. The CPR transect (dashed black line) from Boston, Massachusetts to Cape Sable, Nova Scotia, and the northernmost half of the Kaplan Extended SST V2 area are illustrated (bottom).

pollution) (e.g., Schöne et al., 2005a; Shanahan et al., 2005). Shells from the bivalve *Arctica islandica* (Linnaeus, 1767) (ocean quahog; tree of the sea) have been widely used in paleoceanography (Weidman and Jones, 1993a; 1993b; Weidman et al., 1994; Witbaard et al., 1994; Marsh et al., 1999; Marchitto et al., 2000; Schöne et al., 2003; 2004; 2005a; 2005b, Scourse et al., 2006). Growth of the ocean quahog appears to be primarily related

to food quality and availability (e.g., depth of the water column, horizontal advection, mixing, etc.) as well as water temperature (Beal and Kraus, 1989; Witbaard, 1996; Witbaard et al., 1999). Therefore, growth records from *A. islandica* may be used to reconstruct environmental conditions when instrumental data is sparse or non-existing.

In this paper, we investigate environmental variability in the Western Gulf of Maine for periods during the late Holocene using growth histories from *A. islandica*. We present an annualized marine-based record of paleo-productivity for intervals of the late Holocene that begins ca. 1000 AD and spans the climate transition between the Medieval Warm Period (MWP) and the Little Ice Age (LIA). Further, we investigate dominant modes of environmental variability and show how those modes vary through time.

5.2. Methods and Results

5.2.1 Animal Collection

One specimen of *A. islandica* was collected alive in the Western Gulf of Maine, USA (43° 39' 22.14" N, 69° 48' 6.01" W), in 30 meters water depth via the fishing vessel *FV Foxy Lady* on March 14, 2004 during a Maine Department of Marine Resources dredge survey (Fig. 5.1). Three well-preserved articulated fossils of *A. islandica* were collected 3 kilometers away (43° 41' 13.14" N, 69° 47' 56.34" W) in 38 meters water depth via a Rossfelder vibracore (SBVC-9609) on September 29, 1996 (Belknap and Kelley, pers. comm.) (Fig. 5.1). Because the animals were collected from the same oceanographic setting (location and water depth), comparisons among the shells to assess changes in ocean conditions through time is thought to be appropriate.

5.2.2 Sample Preparation

In preparation for sclerochronological analysis (see Schöne et al., 2005a for details), the left valve from each shell was mounted on a plexiglass block. A quick drying

metal epoxy resin (JB KWIK-Weld) was then applied to the surface (inside and out). A thick section (3mm) of shell was cut from the valve along the axis of maximum growth, and perpendicular to the annual growth lines with a Buehler Isomet low-speed saw using a 0.3 mm thick diamond wafering blade. Each section was mounted on a glass slide, ground with 800 and 1200 SiC grit, polished with 1 μm Al_2O_3 powder and cleaned with dehydrated ethyl alcohol.

5.2.3 Radiocarbon Dating

$^{14}\text{C}_{\text{AMS}}$ dating (analyzed at National Ocean Sciences Accelerator Mass Spectrometry Facility, Woods Hole Oceanographic Institution) was used to determine the approximate calendar age of the outermost shell portion (oldest). The periostracum was removed with a razor blade, and approximately 100 μg of shell carbonate was milled from the outer shell layer. Calibrated ^{14}C ages (cal yr AD) were calculated using Calib 5.01 (Stuiver and Reimer, 1993) using a regional Gulf of Maine marine reservoir effect of $\Delta\text{R} = 39 \pm 40$ by Tanaka et al. (1990), which included quahog shells (*Arctica islandica* and *Merceneria mercenaria*) from museum collections. The calendar age assigned to the entire shell resulted from counting the annual growth layers (Jones, 1980) from the ventral margin back to the umbo region.

5.2.4 Sclerochronological Analyses

We used methods outlined by Schöne et al. (2005a) to resolve annual growth patterns. Polished shell sections were immersed in Mutvei's solution for 20 minutes at ~ 38 $^{\circ}\text{C}$. The treated shell was immediately rinsed with demineralized water and air-dried. The growth patterns of the etched shell were viewed under a reflected light stereomicroscope (Leica Wild M3Z) and digitized using a Nikon Coolpix 995 camera. Annual growth widths were determined to the nearest 1 μm with Scion Image (version

1.63). Measurements were conducted on the outer shell surface. Determination of ontogenetic age was established by counting annual increment layers (Jones, 1980; Ropes et al., 1984).

Based on sclerochronological analyses, the modern *A. islandica* shell was 142 years old and lived from 1863-2004 cal yr AD (Fig. 5.2). The fossils recovered from vibracore SBVC-9609 in the Western Gulf of Maine were from 48 cm, 40 cm, and 30 cm core depths, and the sclerochronological ages based on $^{14}\text{C}_{\text{AMS}}$ analyses associated with the fossil shells were 1030 - 1078 \pm 78 AD (48 years old), 1320 - 1354 \pm 48 AD (34 years old), 1356 - 1470 \pm 45 AD (114 years old), respectively.

5.2.5 Detrending Age-Related Growth Patterns

The growth of *A. islandica* decreases with increasing ontogenetic age (Fig. 5.2a), thus long-term growth patterns were removed in order to evaluate environmental signals contained in the annual growth increment time-series. We used a power growth model to detrend the time-series (e.g., Cook and Kairiukstis, 1990) (Fig. 5.2b). The calculated growth indices (GI) were calculated by dividing measured by predicted growth (based on power growth model) values for each year. Indexing removes age-related growth trends from the time-series. Then, the GI data were standardized by subtracting the mean and dividing by the standard deviation of the GI time-series (Fig. 5.2b). The standardized growth index (SGI) is a dimensionless parameter of how growth deviates from the average growth trend (e.g., Schöne, 2003). SGI values were prewhitened with first-order autoregressive (AR-1) modeling (Box and Jenkins, 1976), which successfully removed lag-1 autocorrelation from each SGI time-series. Further, we used a low-pass filter (Savitzky-Goley; window length = 5) on SGI time-series to emphasize decadal-to-multi-decadal changes in ambient growing conditions.

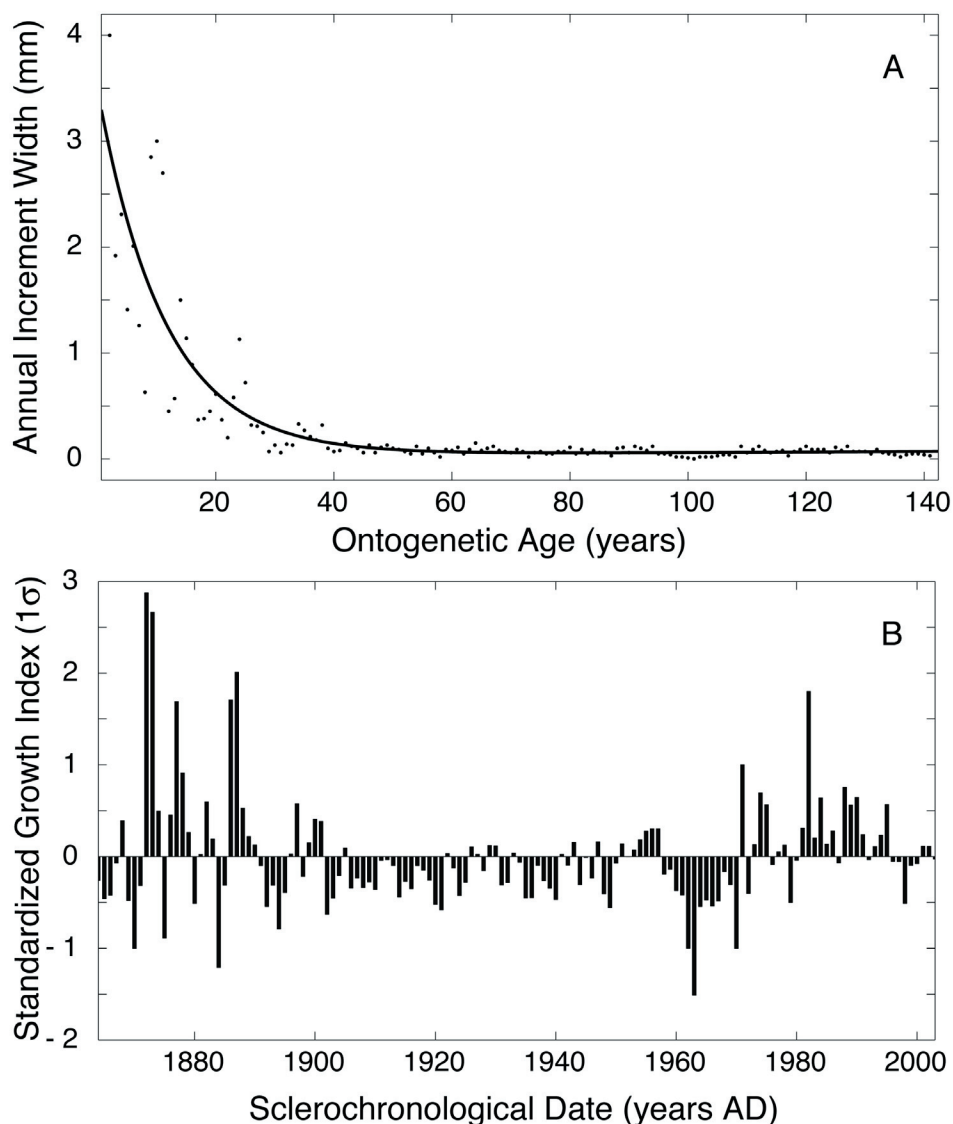


Figure 5.2. (A) Annual growth of shell SF1 and ontogenetic age (black dots). The age-related growth trend was removed with a power growth model (solid black line). (B) Standardized growth index (SGI) for shell SF1 (see text for details) and sclerochronological age.

5.2.6 Continuous Plankton Recorder (CPR) Data

The CPR program for the Gulf of Maine is operated by NOAA Fisheries, which began taking CPR transects in 1961 (see Jossi and Goulet, 1993 for details). These measurements consist of a single transect between Boston, Massachusetts and Cape Sable, Nova Scotia (Fig. 5.1) by ship-of-opportunity approximately monthly. Several taxa of zooplankton and relatively large phytoplankton are represented in the CPR data,

which are spatially indexed by relative abundance. We used CPR data that focused on the central Gulf of Maine region as outlined by Pershing et al. (2005). The modern shell SGI time-series (SF1) was compared with CPR data (1961-2003) to determine if there is a relationship between zooplankton levels and shell growth.

5.2.6.1 Relationship between CPR Data and Shell Growth

The comparison between the SGI for the modern shell and the relative abundance of zooplankton species *Calanus finmarchicus* is shown in Figure 5.3. A strong relationship between annual shell growth and *C. finmarchicus* abundance is evident ($r^2 = 0.55$; $p < 0.0001$), and *C. finmarchicus* abundance levels can explain approximately 55 % of SGI variability. This result demonstrates the utility of *A. islandica* as a proxy for paleo-productivity (*C. finmarchicus*) for the Western Gulf of Maine. Other zooplankton taxa that showed considerable interannual variability (*Oithona* spp., *Centropages typicus*) did not correlate significantly with the SGI time-series.

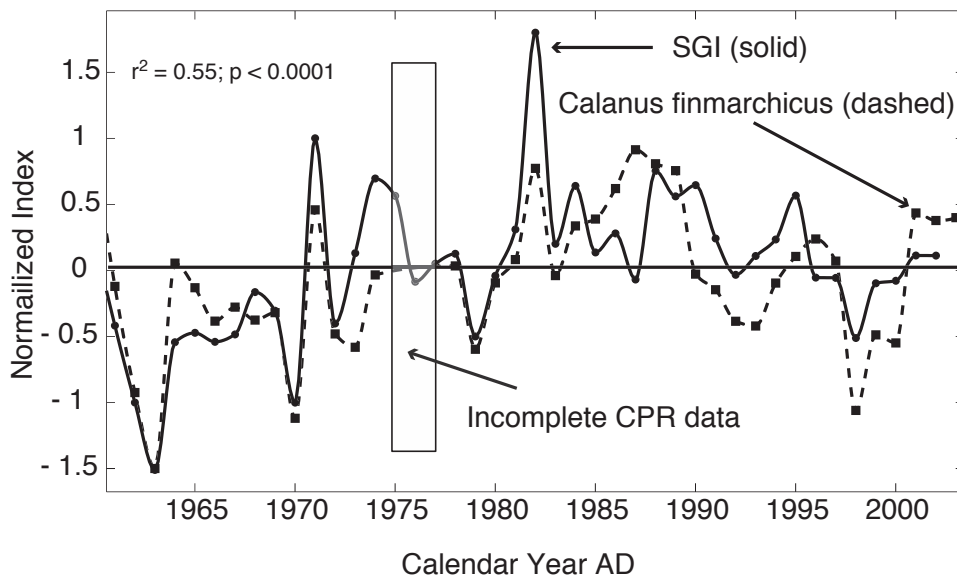


Figure 5.3. Time-series of shell SF1 SGI (solid black line) and zooplankton *Calanus finmarchicus* relative abundance (dashed black line) is shown. Continuous Plankton Recorder (CPR) data for the Gulf of Maine was incomplete during 1975, 1976, and 1977.

5.2.7 Relationship between SST and Shell Growth

The closest SST record to the shell collection site is in Boothbay Harbor (BBH) (Fig. 5.1), where the Maine Department of Marine Resources began measuring SST on a daily basis in 1905. This record is available to the public and contains monthly and annual SST averages (Lazzari, 2001). The modern shell (SF1) SGI time-series was compared with BBH SST record to assess influences of water temperature on shell growth. There is a weak but significant correlation between annual shell growth and annual SST ($r^2 = 0.04$; $p < 0.05$) from 1905-2003. The highest significant correlation between annual shell growth and seasonal SST values at BBH (1905-2003) was during the fall (SON) and winter (DJF) seasons ($r^2 = 0.11$; $p < 0.0009$). The fall and winter SSTs at BBH had an equal effect on annual shell growth.

We also compared the modern SGI record with $5^\circ \times 5^\circ$ SST data outside the Gulf of Maine (37.5 - 42.5 N; 62.5 - 67.5 W) (Kaplan et al., 1998; Kaplan SST V2) from 1960 – 1990 (Fig. 5.1). A significant relationship ($r^2 = 0.17$; $p < 0.009$) exists between annual SST data outside the Gulf of Maine and the SGI record from 1960-1990 with a 1 yr lag. This result supports previous findings that indicated water temperature significantly impacts *A. islandica* shell growth (Beal and Kraus, 1989; Witbaard, 1996; Witbaard et al., 1999). However, the relationship noted here between shell growth in the Western Gulf of Maine and SST outside the Gulf of Maine (Kaplan SST V2) suggests that slopewater entering the Gulf of Maine is more important to shell growth than temperature at BBH (Fig. 5.1).

5.2.8 Relationship with the NAO and Shell Growth

To test the connection between NAO activity and oceanographic variability in the Gulf of Maine (e.g., MERCINA 2001; Greene and Pershing 2001; Conversi et al., 2001; Drinkwater et al., 2003), we compared the winter (Dec-Mar) NAO index (e.g., Hurrell, 1995) with the modern shell SGI record with various lags. We found a statistically

significant relationship ($r^2 = 0.29$; $p < 0.002$) between our modern SGI record and the winter NAO index with a 1 yr lag from 1960 – 1990. This result supports a NAO-forcing on zooplankton dynamics in the Gulf of Maine previously discussed.

5.2.9 Calibrated Late Holocene SGI Time-Series

The master SGI record from the Western Gulf of Maine is shown in Figure 5.4. Although the record is not continuous, it offers insights into environmental variability during the late Holocene. There are distinct periods with either high or low shell growth. Five zones are highlighted (Fig. 5.4), each depicting periods that tend to be in one mode for greater than 10 years. Two periods of relatively low SGI values occur from ~ 1360 – 1400 AD and ~1910 – 1970 AD. Three periods of relatively high SGI values occur from ~1450 – 1470 AD, ~1864 – 1890, and ~1975 – 2003. The periods not highlighted exhibit substantial interannual variability in SGI values, but do not exhibit any decadal trends.

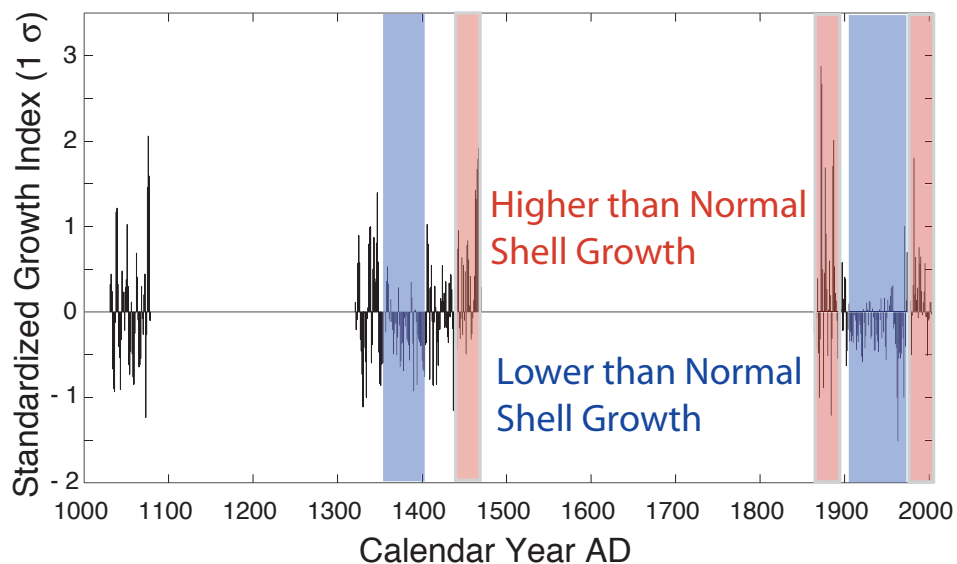


Figure 5.4. The late Holocene SGI time-series is illustrated. Red highlighted zones represent higher than normal shell growth, while blue highlighted zones represent lower than normal shell growth.

5.2.10 Spectral Analyses

To assess persistent patterns in shell growth (SGIs), we employed three independent techniques of spectral analyses; wavelet analysis (Torrence and Compo, 1998), multitaper method (MTM; Thompson 1982, Mann and Lees 1996) and singular spectrum analysis (SSA; Vautard and Ghil, 1989). Each of these methods offer distinct advantages over traditional Blackman-Tukey analysis, which is susceptible to aliasing and requires several window lengths to extract dominant frequencies, and Fourier transforms, which are ineffective on nonstationary time-series. Wavelet analysis decomposes a time-series into time-frequency space, which allows one to visualize dominant modes of variability and how those modes vary through time (Torrence and Compo, 1998). Further, wavelet transforms can be used to evaluate time-series that are nonstationary and contain a variety of frequencies (Daubechies, 1990). SSA enables a time-series decomposition into trend, oscillating, and noise components by analyzing its covariance matrix (Vautard and Ghil, 1989). MTM is a refined Fourier-based analysis that offers better resolution and decreased spectral leakage (Thompson, 1982).

We performed wavelet analyses (Morlet; $m = 6$) on the SGI time-series that were greater than 100 years long to determine dominant modes (periods) in both records, and how those modes varied through time (Torrence and Compo, 1998) (Fig. 5.5). Both records were normalized relative to a global wavelet spectrum in order to compare relative power of the signals temporally, and significance at the 95% confidence interval (CI) was determined against a red-noise (autoregressive lag1) background spectrum. The modern shell record (SF1) showed significant periodicities in the 2-16 year range from the 1860s – 1900. Also, from ~ 1970 – 1985 a shorter period (2-3 year) was significant (Fig. 5.5, top). The longest paleo-shell (SBVC 9609-30cm) showed significant periods of 2 to 4 years after 1400 AD (Fig. 5.5, bottom). Further, at the end of the record there is a shift to longer periods (8-16 year). Both SGI time-series exhibit non-stationary tendencies, which suggests that the forcing mechanism (s) may also be non-stationary.

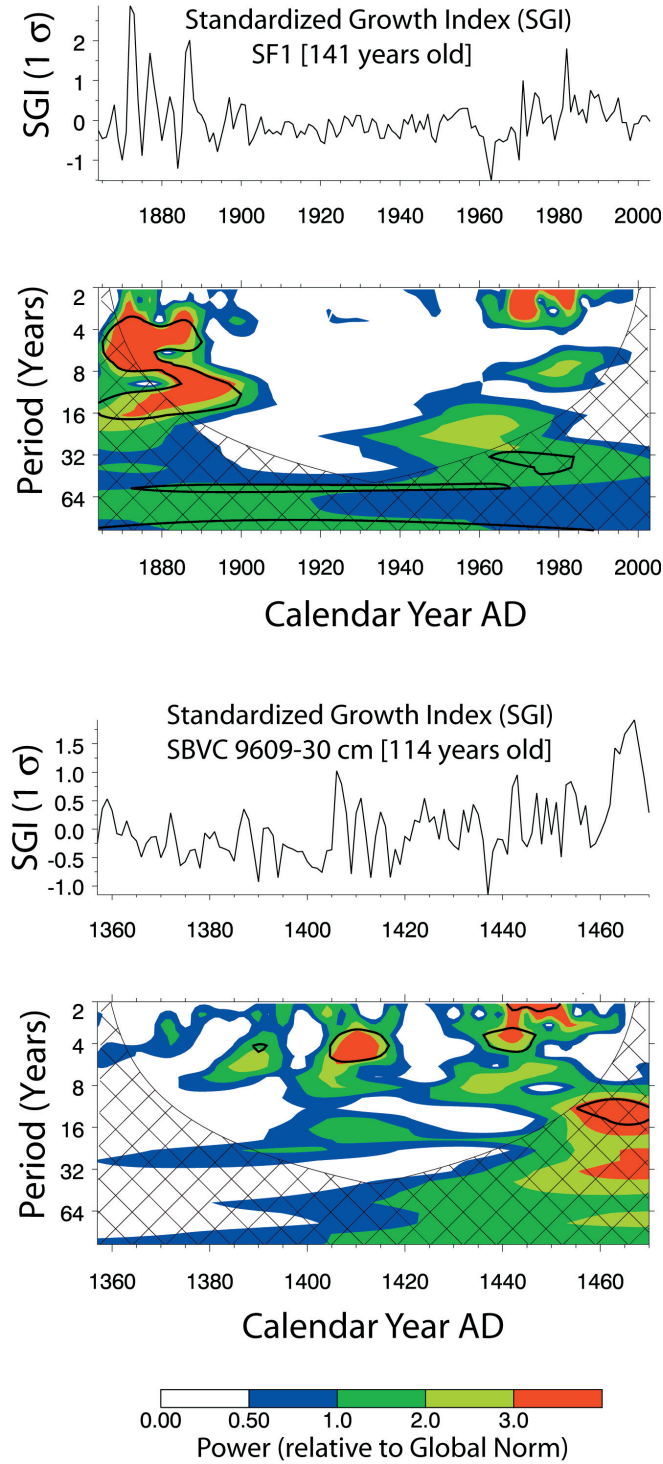


Figure 5.5. Wavelet spectra for shells SF1 (top) and SBVC9609-30cm (bottom) using the Morlet ($m = 6$) wavelet. The power has been scaled by the global wavelet spectrum. The cross-hatched region is the cone of influence, where zero padding has reduced the variance. Black contour is the 5% significance level, using a red-noise (autoregressive lag1) background spectrum (Torrence and Compo, 1998).

We used MTM and SSA to determine persistent patterns in SGI values. For both techniques, significance at the 95% C.I. was determined using a red-noise (autoregressive lag1) background spectrum using KSpectra (SpectraWorks, version 2.2). The spectral features for modern shell (SF1; 1864-2003 AD) are shown in Figure 5.6. MTM analysis

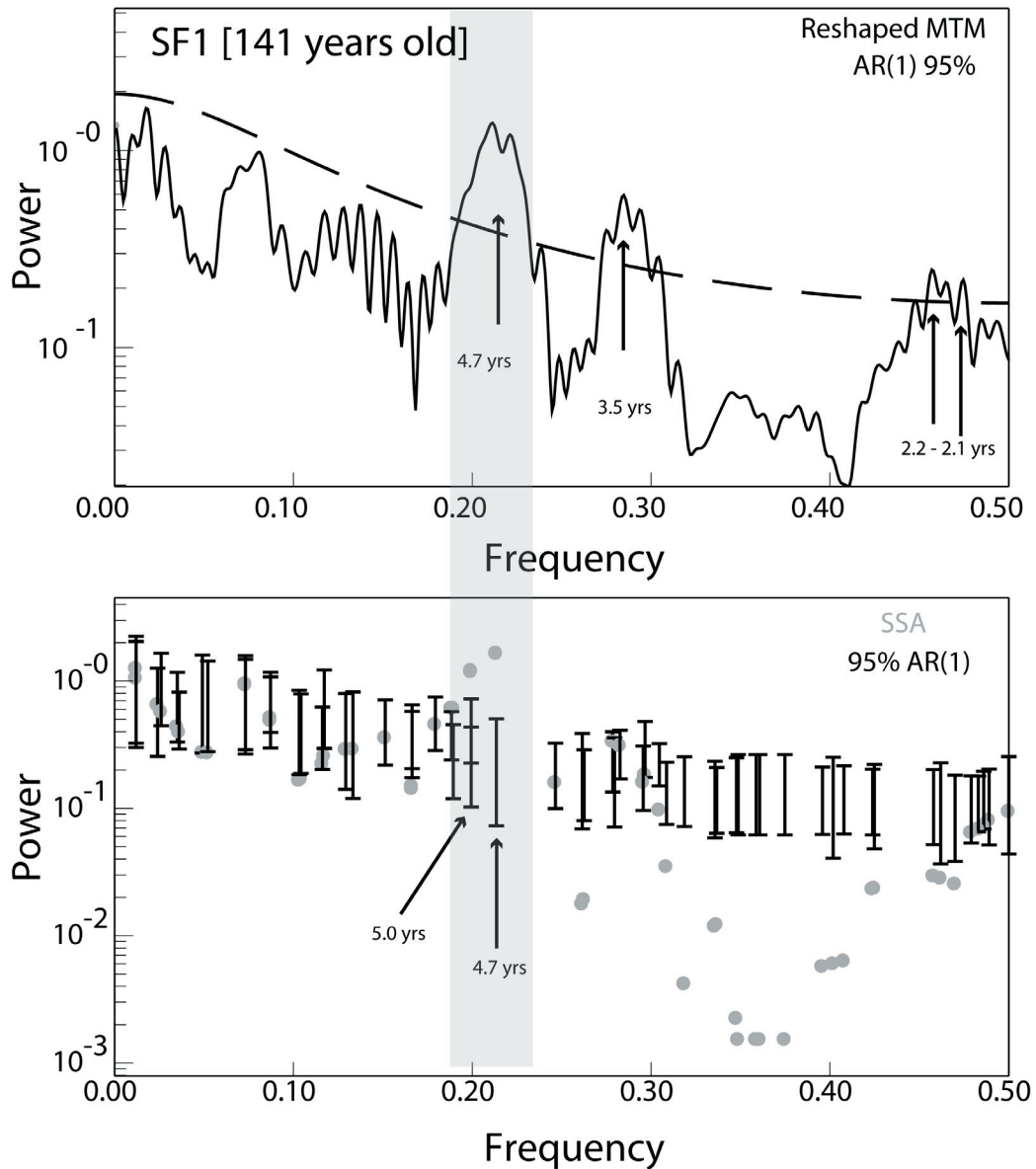


Figure 5.6. Spectral analysis for 142-year-old shell SF1 using MTM (top) and SSA (bottom) using KSpectra (version 2.2) is shown. The black dashed contour (top) and the black vertical bars (bottom) are the 5% significance levels, using a red-noise (autoregressive lag1) background spectrum.

produced significant periods of ~ 2.1 , 3.5, and 4.7 years (Fig. 5.6, top). SSA produced significant periods of 4.7 and 5.0 years (Fig. 5.6, bottom). The common signal between both techniques is 4.7 years (Fig. 5.6). The spectral features for paleo-shell (SBVC9609-30cm; 1357-1470 \pm 40 AD) are shown in Figure 5.7. MTM analysis produced significant

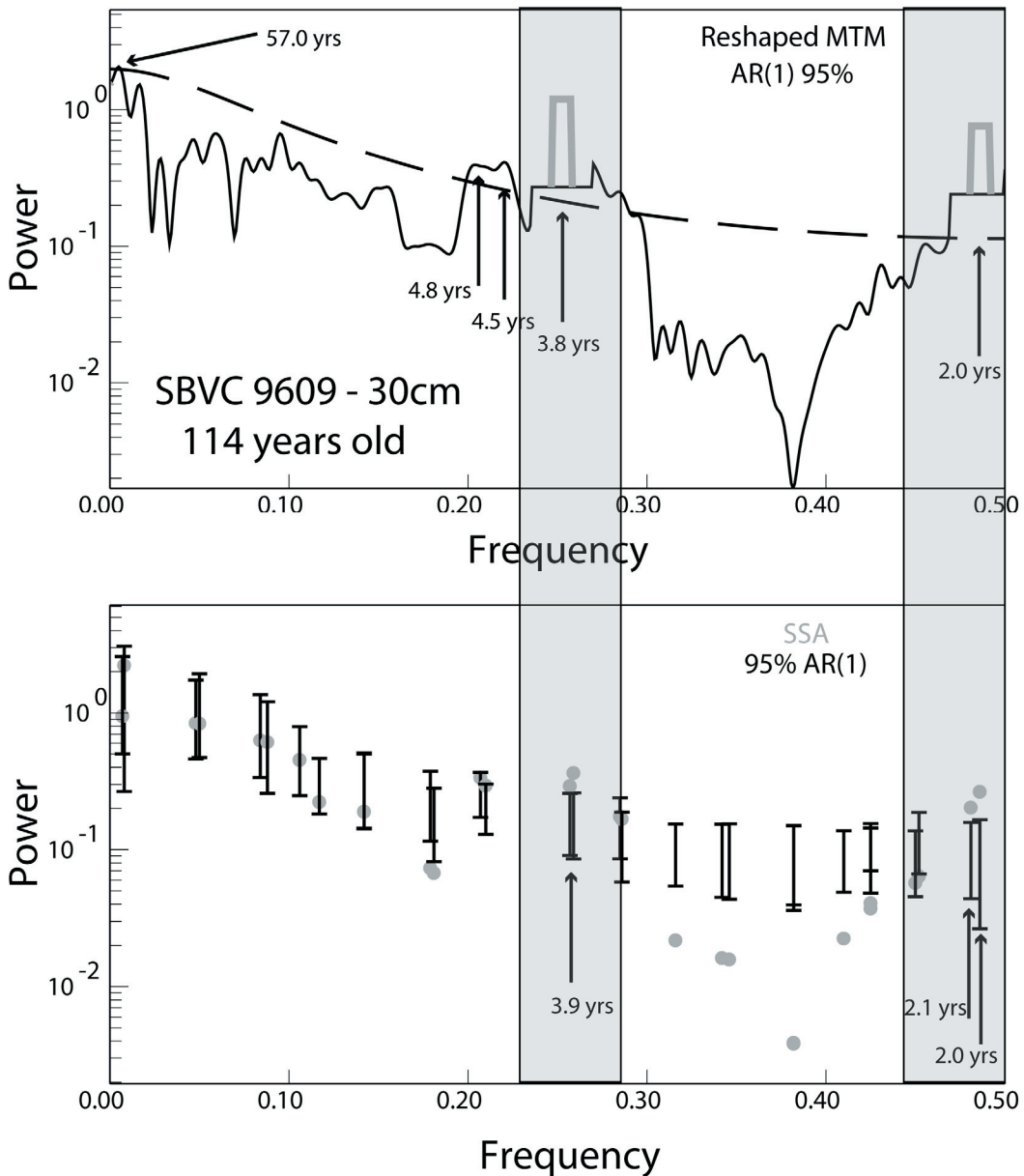


Figure 5.7. Spectral analysis for 114-year-old shell SBVC9609-30cm using MTM (top) and SSA (bottom) using KSpecra (version 2.2) is shown. The black dashed contour (top) and the black vertical bars (bottom) are the 5% significance levels, using a red-noise (autoregressive lag1) background spectrum.

periods of 2.0, 3.8, 4.5, 4.8, and 57.0 years (Fig. 5.7, top). SSA produced significant periods of ~ 2.1 and 3.9 years (Fig. 5.7, bottom). The common signals between both techniques are ~ 2.1 and 3.8-3.9 years (Fig. 5.7). The shorter shell records (SBVC-9609-48, 1030 ± 78 AD; SBVC-9609-40, 1320 ± 45) yielded signals of 6.6 years and 5.5 years respectively based on MTM analysis and SSA. All four SGI records have significant NAO-like periods in the 2 to 6 year range.

5.3. Discussion

5.3.1 A Paleo-productivity Proxy- SGI and *Calanus finmarchicus* Abundance Levels

It is assumed that growth histories from *A. islandica* reflect important changes in water column processes, including primary production and sedimentation rates (Witbaard et al., 1997), because *A. islandica* is an active suspension feeder in the benthic zone primarily relying on phytoplankton supply (Cargnelli et al., 1999). The strong positive relationship between the relative abundance of zooplankton *C. finmarchicus* and shell growth ($r^2 = 0.55$; $p < 0.0001$) suggests that it is appropriate to use SGIs from *A. islandica* to reconstruct at least one major component of productivity in the Western Gulf of Maine. However, the connection between *C. finmarchicus* and *A. islandica* growth is still poorly understood (e.g., Planque and Fromentin, 1996; Witbaard et al., 2003). Planque and Fromentin (1996) proposed a food-web-competition model to explain the significant negative relationship between *C. finmarchicus* abundance and *A. islandica* growth in the northern North Sea. In the Planque and Fromentin (1996) model high *C. finmarchicus* levels (related to local ocean conditions) would lead to low phytoplankton levels due to predation by *C. finmarchicus*, which would result in less export of phytoplankton into the benthic zone, and less *A. islandica* shell growth. However, we propose a hydrographic-based model to link *C. finmarchicus* levels and *A. islandica* growth in the Gulf of Maine.

Greene and Pershing (2001) suggested that *C. finmarchicus* is a deepwater zooplankton species derived from a North Atlantic source that is subject to advective transport processes. We suggest that *C. finmarchicus* is a tracer of slopewater input from the North Atlantic, and the hydrographic properties (temperature, salinity, nutrients, etc.) are significantly affecting primary productivity (e.g., phytoplankton) in the Gulf of Maine. Therefore, increased phytoplankton abundance would lead to greater *A. islandica* growth. Further, this idea is supported by a significant relationship ($r^2 = 0.17$; $p < 0.009$) between annual SST data outside the Gulf of Maine (Kaplan Extended SST V2) and the SGI record from 1960-1990 with a 1 yr lag, indicating a slopewater connection. Therefore, we believe that *C. finmarchicus* levels are associated with slopewater properties and are a proxy of primary production in the Western Gulf of Maine.

C. finmarchicus dynamics and SST outside the Gulf of Maine explain most of the SGI variability from the modern shell record. Fall and winter SST at BBH explains ~ 11% of SGI variability from 1905-2003. Other local mechanisms that may be responsible for part of the SGI variability include river discharge (nutrients), coastal currents changes (e.g., Eastern Maine Coastal Current, Western Maine Coastal Current), stratification during the summer months, and winter mixing.

5.3.2 North Atlantic Climate Variability and Ecosystem Dynamics in the Gulf of Maine

A strong relationship is documented between NAO variability and changes in various trophic levels of the North Atlantic marine ecosystem (Drinkwater et al., 2003). Drinkwater et al. (2003) reported that NAO variability affected abundance, biomass, distribution, species assemblages, growth rates, and survival rates for phytoplankton, zooplankton, benthos, fish, marine diseases, whales and seabirds. However, the relationships among climate variability, NAO variability and the oceanographic response in the Gulf of Maine are still unresolved. The oceanography of the region is, in part,

influenced by fluctuations in the cold polar waters from the northeast, and the warm temperate waters from the south, and freshwater input via rivers (Loder et al., 1998; Pettigrew et al., 1998). To the northeast, the Labrador Current (LC), which is primarily a buoyancy-driven coastal current formed in the Labrador Sea, flows southeastward over the continental shelves and slopes of Labrador and Newfoundland and mixes along the Scotian Shelf (Lazier and Wright, 1993; Loder et al., 1998). The sources for the LC are from the Nordic Sea and Canadian Archipelago (Loder et al., 1998). The LC-derived current brings cold (4°- 8 °C), relatively fresh and nutrient poor (Petrie and Yeats, 1993; Drinkwater et al., 2003; Thomas et al., 2003; Townsend et al., 2006) water to the GOM region (Loder et al., 1998). To the south, the warm (8°-12 °C), relatively saline and nutrient rich (Townsend et al., 2006) Atlantic Temperate Slope Water moves northward along the continental slope toward the GOM region (Drinkwater et al., 1999), and is thought to vary in accordance with the location of the Gulf Stream (Taylor and Stephens, 1998; Loder et al., 2001).

The MERCINA working group (2001) reported that fluctuations in the ocean-climate system are reflected in the changes in composition and relative distributions of phytoplankton. Low concentrations of phytoplankton in 1998 were coincident with negative anomalies in sea surface temperatures (SST) and follow the intrusion of the nutrient poor LC possibly induced by the sudden negative shift in the NAO in 1996 (Thomas et al., 2003). Greene and Pershing (2001; 2003) showed that the NAO is positively correlated with changes in zooplankton (*C. finmarchicus*) abundance at lags of 2-4 years. Conversi et al. (2001) also reported significant positive correlations between the NAO index and *C. finmarchicus* abundance ($r^2 = 0.25$) with a 4 yr lag, and winter SST (derived from the Comprehensive Ocean-Atmosphere Data Set [COADS]) ($r^2 = 0.22$) with a 2 yr lag over a 30 yr period (1961 – 1991) in the Gulf of Maine. Because phytoplankton and zooplankton are at the base of the food chain, and *C. finmarchicus* alone represents more than 70% of the region's springtime zooplankton biomass, it is

crucial to understand the possible causes in their fluctuations. Zooplankton changes in marine ecosystems offer an essential connection between primary producers and higher trophic levels. Many marine animals, such as planktivorous fish, marine mammals, and seabirds depend upon *C. finmarchicus* as their primary nutrition (Greene and Pershing, 2003). Drinkwater et al. (2003) suggested the abundance of herbivorous zooplankton, such as *C. finmarchicus*, usually follows local phytoplankton patterns, but with a slight lag. The NAO phase and distribution of zooplankton relationship is opposite in the Northeast Atlantic than in the Northwest Atlantic (Conversi et al., 2001). This out-of-phase relationship between the northwestern and northeastern Atlantic and the NAO high phase was described by Drinkwater et al. (2003) as a result of colder conditions in the eastern Atlantic Basin, causing zooplankton levels to decrease, whereas they increased in the western Atlantic due to warmer conditions. Recently, Pershing et al. (2004; 2005) reported that *C. finmarchicus* dynamics in the Gulf of Maine are coincident with the NAO index at times, but substantial zooplankton community shifts have occurred independent of NAO activity. Further, Pershing et al. (2005) suggested that slopewater variability (i.e., advective transport processes) is a viable mechanism that links North Atlantic climate and *C. finmarchicus* levels in the Gulf of Maine.

5.3.2.1 Relationship between the NAO and Shell Growth

There is a statistically significant relationship ($r^2 = 0.29$; $p < 0.002$) between our modern SGI record and the winter (Dec-Mar) NAO index (e.g., Hurrell, 1995) with a 1 yr lag from 1960 – 1990. It appears that NAO activity is in part controlling shell growth via advective processes between the North Atlantic and the Western Gulf of Maine. In addition, Greene and Pershing (2001) suggested that a substantial part of the stock is derived from inputs from populations off the continental shelf, because *C. finmarchicus* prefers deepwater during autumn and winter. Therefore, it is possible that *C. finmarchicus* levels are subject to climate forcing mechanisms (NAO) outside the Gulf of Maine. If advection processes into the Gulf of Maine are more important in controlling *C.*

finmarchicus levels than local processes such as mixing, stratification, or salinity, then a relationship between the NAO and *C. finmarchicus* levels would be expected (e.g., Drinkwater et al., 2003). We suggest that the relationship noted here between SST outside the Gulf of Maine (Kaplan Extended SST V2) and shell growth are linked to NAO dynamics as reported by Drinkwater et al. (2003), and that the SGI record is composed of mixed signal, with origins in the North Atlantic and locally within the Gulf of Maine. In addition, we propose that positive SGI values represent relatively more input of Atlantic Temperate Slope Water, while negative SGI values represent relatively more input of LC-derived water into the Gulf of Maine. This conclusion corroborates previous findings of nutrient pathways into the Gulf of Maine (e.g., Petrie and Yeats, 1993; Drinkwater et al., 2003; Thomas et al., 2003; Townsend et al., 2006).

5.3.3 Interannual-to-Decadal SGI Variations

The modern (SF1) and paleo-shell (SBVC9609-30cm) SGI records are dominated by significant (above 95% C.I.) high frequency oscillations in the 2-5 year periods (NAO-like). This result is based on robust spectral techniques, including wavelet analysis, MTM, and SSA. This suggests the mechanism responsible for the 2-5 yr period noted in the SGI records (productivity) has not changed since ~ 1350 AD. Evident patterns in SGI variability exist throughout much of the record, and the SGI record tends toward long periods of either relatively fast (more productive) or slow (less productive) growing conditions (Fig. 5.4). These decadal patterns in shell growth exist from ~ 1350 – 1470 AD and during the modern period (~ 1864 – 2003 AD), but they are not evident in the shorter SGI record. The SGI records during the MWP (SBVC-9609-48, 1030 ± 78 AD) and late MWP (SBVC-9609-40, 1320 ± 45) are dominated by 6.6 and 5.5 year periods, respectively. Neither of these paleo-SGI records produced the higher frequency period of 2 years noted in the longer shell records. The absence of the higher frequency signal may be attributed to milder and less variable ocean conditions during the MWP.

5.4. Conclusions and Future Work

We present a calibrated proxy for at least one major component of paleo-productivity (*Calanus finmarchicus* abundance) in the Western Gulf of Maine based on growth records (SGIs) from *A. islandica*. The late Holocene SGI record has substantial interannual-to-decadal variability. We propose that slopewater variability coupled with North Atlantic Oscillation (NAO) dynamics is primarily responsible for the observed SGI variability. SGIs from these shells reveal significant periods (95 % C.I.) of 2-6 years (NAO-like) based on wavelet analysis, MTM analysis and SSA during the late Holocene. Spectral analyses on SGI records indicate a shift in periodicity from 5-6 years to 2-5 years after ~ 1350 AD, possibly related to the MWP/LIA transition. Further, decadal trends in SGI variability are clearly noted, and likely related to long-term changes in slopewater properties in the northwestern Atlantic basin. This record should improve the understanding of past environmental variability in the Gulf of Maine beyond the CPR instrumental record. The development of a new paleo-productivity proxy is promising for this region. A major goal is to complete a 1,000-year continuous SGI record using multiple overlapping shells (similar to tree ring master chronologies) from the region to assess multi-decadal-to-centennial components of the coupled ocean-biology-climate system. Paleoenvironmental information derived from the shells of *A. islandica* provides a framework for both climate and marine biological modelers to improve their understanding of past environmental conditions. The longevity and geographic distribution of the bivalve *A. islandica*, and its utility as an ocean proxy offers significant advances in paleoceanography, especially in mid-to-high latitudes.

6. Coupled North Atlantic Slope Water Forcing on Gulf of Maine Temperatures over the Past Millennium

To investigate ocean variability during the last millennium in the Western Gulf of Maine (GOM), we collected a 142-year old living bivalve (*Arctica islandica* L.) in 2004, and three fossil *A. islandica* shells (calibrated $^{14}\text{C}_{\text{AMS}} = 1030 \pm 78 \text{ AD}$; $1320 \pm 45 \text{ AD}$; $1357 \pm 40 \text{ AD}$) for stable isotope and growth increment analysis. A statistically significant relationship exists between modern GOM temperature records (shell isotope-derived [30m] [$r = -0.79$; $p < 0.007$], Prince 5 [50m] [$r = -0.72$; $p < 0.019$], Boothbay Harbor SST [$r = -0.76$; $p < 0.011$]), and Labrador Current (LC) transport data from the Eastern Newfoundland Slope during 1993 – 2003. In all cases, as LC transport increased, GOM water temperatures decreased the following year. Decadal trends in the North Atlantic Oscillation (NAO) and the Atlantic Multi-decadal Oscillation (AMO) influence GOM water temperatures in the most recent period, with water temperatures decreasing during NAO and AMO negative modes most likely linked to LC transport and Gulf Stream interaction. Mean shell-derived isotopic changes ($\delta^{18}\text{O}_\text{c}$) during the last 1000 years were $+0.47 \text{ ‰}$ and likely reflect a $2 \text{ }^\circ\text{C}$ cooling from 1000 AD to present. Based on these results, we suggest that the LC transport increased by $\sim 0.7 \text{ Sv}$ ($1 \text{ Sv} = 10^6 \text{ m}^3 \text{ s}^{-1}$) over the past millennium, possibly due to a persistent NAO negative mode and decreased Gulf Stream influence on the GOM.

6.1. Introduction

The oceanography along the slope of the Eastern Canadian coast and the deep Gulf of Maine (GOM) is strongly influenced by the position, strength, and properties of the Labrador Current (LC) (Fig. 6.1). The LC has two distinct branches of flow: the principal branch that flows generally southward along the continental slope, and an inner branch that flows over the Labrador and Newfoundland continental shelf regions (Lazier

and Wright, 1993). At times, water of LC origin extends from the western Labrador Sea to the Middle Atlantic Bight (e.g., Petrie and Drinkwater, 1993; Loder et al., 2001), and has a net cooling effect on both air and coastal water temperatures along the Canadian Atlantic provinces (e.g., Drinkwater et al., 1999). Han and Li (2004) estimated an annually averaged flow of ~ 6 Sv for the LC along the Eastern Newfoundland Slope (200 m – 3000 m) using TOPEX/Poseidon satellite altimeter data (Figs. 6.1, 6.2). Gatién (1976) identified two types of slope waters outside the GOM and along the Scotian Shelf, Labrador Slope Water (LSW) and Warm Slope Water (WSW). From the Labrador Sea, the cold, relatively fresh and nutrient-poor water masses of the southward flowing LSW mix with the warm, relatively saline and nutrient-rich waters of the WSW (Gulf Stream-derived) moving northward (Lazier and Wright, 1993; Drinkwater et al., 1999; Petrie and Yeats, 2000). Further, Gatién (1976) suggested that the slope water properties for the region depend upon whether the LSW or WSW component is dominant. Petrie and Drinkwater (1993) postulated that oceanographic conditions in the GOM and along the Scotian Shelf partly reflect the penetration of slope waters onto the shelf in the deep layers through gullies and channels, related to meteorological events, Gulf Stream activity (rings), or gravitational flows generated by differences in the density of the water on and off the shelf. In addition to several large rivers (St. John, Penobscot, Kennebec, and Androscoggin), the freshwater budget for the GOM is significantly controlled by the inflow of Scotian Shelf Water (SSW) (Smith, 1983; Brown and Irish, 1993), a water mass that is characterized as relatively cold and with low salinity (e.g., Pettigrew et al., 1998). SSW is a mixture of water from the Labrador and Newfoundland shelf regions, as well as water from the Gulf of St. Lawrence (e.g., Houghton and Fairbanks, 2001). SSW flows southward along the continental shelf of Nova Scotia and into the GOM.

Dominant modes of atmospheric and oceanic variability such as the North Atlantic Oscillation (NAO) and the Atlantic Multi-Decadal Oscillation (AMO) have been linked to environmental change in the North Atlantic and surrounding regions (e.g.,

Enfield et al., 2001; Drinkwater et al., 2003; Sutton and Hodson, 2003; 2005; Knight et al., 2005, 2006). NAO forcing has been linked to LC transport variability (e.g., Myers et al., 1989; Dickson et al., 1996; Marsh et al., 1999), the position of the northern Gulf Stream wall (Taylor and Stephens, 1998), and certain zooplankton levels in the Gulf of Maine (e.g., Conversi et al., 2001; MERCINA, 2001; Greene and Pershing, 2003). In an NAO low mode (weaker atmospheric flow over the Labrador Sea and North Atlantic) there is decreased winter heat loss, decreased winter storminess, and suppressed ocean convection. These conditions are thought to lead to an increased buildup of fresh surface water in the Labrador Sea, and increased buoyancy-driven LC transport (e.g., Dickson et al., 1996). A persistent NAO low pattern may cause GOM water temperatures to decrease for two reasons: 1) increased LSW water would likely enter the GOM (e.g., MERCINA, 2001), and 2) a southward displacement of the northern wall of the Gulf Stream would allow decreased transport of WSW to enter the GOM.

The AMO is a measure of SST temperature anomalies in the North Atlantic possibly related to thermohaline circulation (THC) (e.g., Delworth and Mann, 2000; Sutton and Hodson, 2005). The AMO has been associated with precipitation patterns in the United States and Western Europe (e.g., Enfield et al., 2001), winter air temperatures in Europe (Folland et al., 1986), and Atlantic hurricane formation (Goldenberg et al., 2001). Although the relationship between Gulf Stream transport and the AMO is still poorly understood, it is plausible that lower frequency changes (decadal-to-multidecadal) in the THC would cause SST anomalies in the North Atlantic (e.g., Delworth and Mann, 2000). Because water temperatures in the GOM are partly influenced by the relative input of WSW (Gulf Stream-derived) (e.g., Loder et al., 2001), a relationship likely exists among Gulf Stream transport, the AMO, and GOM water temperatures. We suggest that as Gulf Stream transport increases (positive phase of the AMO), the northernmost wall of the Gulf Stream moves northward, and a greater portion of the slope water entering the GOM is WSW-derived (e.g., Gatién, 1976). Further, because deep inflow is

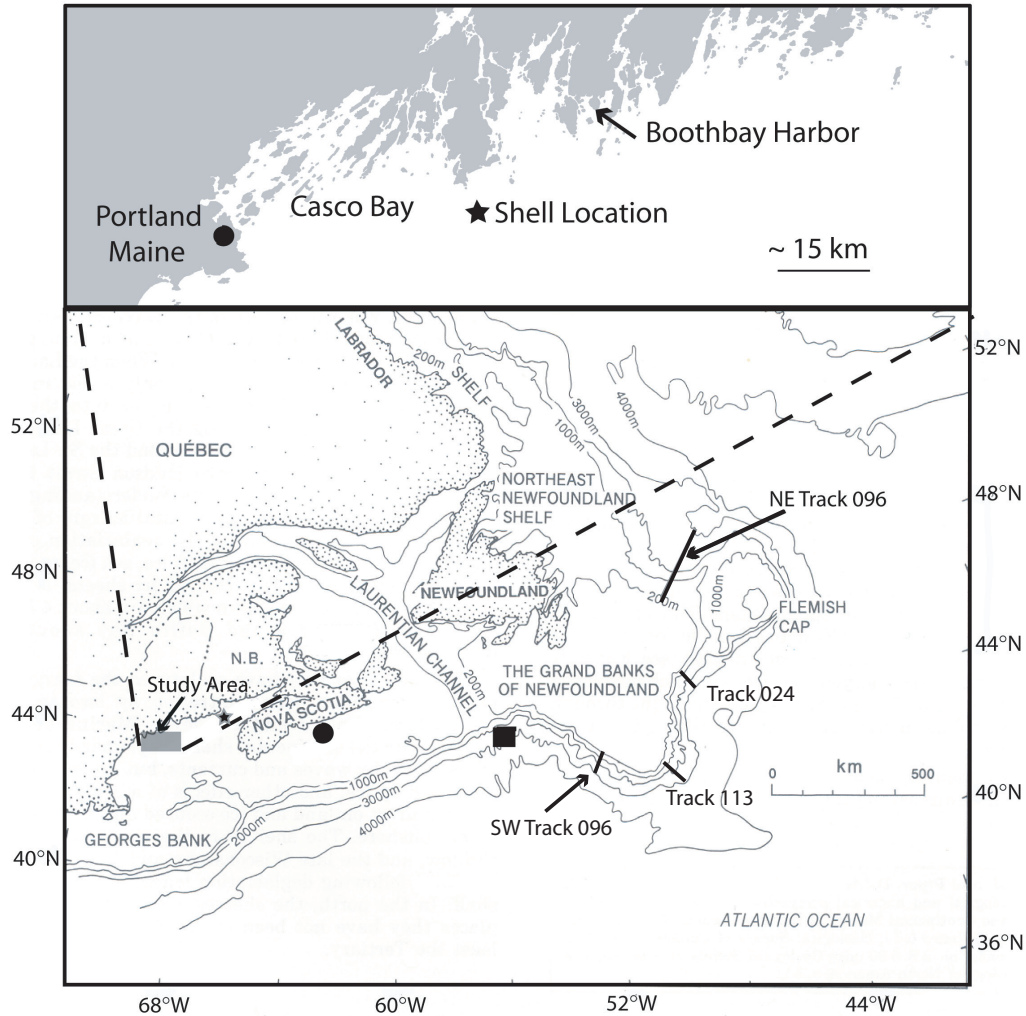


Figure 6.1. The general bathymetric map for the Gulf of Maine region and Eastern Canada, noting long-term climate stations (Portland [air temperature]; Boothbay Harbor [SST]) and the shell collection location in the Western Gulf of Maine (top) are shown (modified from Keen and Piper, 1990). Within the Gulf of Maine (bottom) is the Prince 5 station (50 m water temperature and salinity) (filled star). The approximate Labrador Current transects (NE Track 096; Track 024; Track 113; SW Track 096) located along the Newfoundland Slope of Han and Li (2004) are illustrated. The locations for the studies of Keigwin et al. (2003) (Emerald Basin, off Nova Scotia; filled circle) and Marchitto and deMenocal (2003) (located south of Newfoundland and the Grand Banks; filled square) are shown.

primarily driven by density contrasts between the GOM and the adjacent slope waters, we speculate that inflow may be increased when WSW is prevalent rather than LSW based on Temperature-Salinity (T-S) envelopes for both water masses as proposed by Gatiien (1976). Modern water temperatures in the GOM appear to be significantly influenced

by coupled slope water dynamics between the LSW and WSW (MERCINA, 2001). In fact, water temperatures in the GOM have been increasing since approximately the 1920s, which corresponds to increased Gulf Stream transport (Lund et al., 2006), and is consistent with warmer sea surface temperatures (SST) from Emerald Basin along the Scotian Shelf (e.g., Keigwin et al., 2003) during the early to mid 1900s. The Gulf Stream transports ~ 31 Sv of water in the Straits of Florida and exports $\sim 1.3 \times 10^{15}$ W of heat into the North Atlantic (Larsen, 1992; Leaman et al., 1995; Baringer and Larsen, 2001), and variability in Gulf Stream strength may be linked to abrupt climate change in the North Atlantic (e.g., Lund et al., 2006, Lund and Curry, 2006). Lund et al. (2006) concluded that the Gulf Stream transport in the Straits of Florida decreased during the Little Ice Age (LIA), and may in part be responsible for cooling in Europe, consistent with previous work by Keigwin (1996). In addition, recent studies (Keigwin et al., 2003; Marchitto and deMenocal, 2003; Keigwin et al., 2005; Sachs, 1997) have suggested that the slope and shelf waters in the Northwestern Atlantic have been cooling during the late Holocene. However, the relationships among dominant climate modes (NAO and AMO), slope water currents, and water temperatures in the GOM are poorly understood over the past millennium.

Oxygen isotopes ($\delta^{18}\text{O}_\text{o}$) from the shells of the bivalve *Arctica islandica* (Linnaeus, 1767) (ocean quahog) have been used extensively in paleoceanography (Weidman and Jones, 1993a; Weidman et al., 1994; Marsh et al., 1999; Schöne et al., 2004; 2005a; 2005b). Weidman et al. (1994) concluded that *A. islandica* precipitates its aragonitic shell ($\delta^{18}\text{O}_\text{o}$) in isotope equilibrium with ambient seawater, thus water temperature estimates can be made when the isotopic composition of the water ($\delta^{18}\text{O}_\text{w}$) is known or can be estimated ($\delta^{18}\text{O}_\text{w}$ – related to salinity). The ocean quahog is a slow-growing bivalve that commonly lives more than 100 years (e.g., Ropes and Murawski, 1983; Forsythe et al., 2003; Schöne et al., 2005a) with a sub-arctic to mid-latitude distribution in the North Atlantic (Cargnelli et al., 1999). Because *A. islandica* deposits

distinct annual lines in its shell, it is possible to reconstruct past ocean environments at sub-annual-to-annual resolution (Thompson et al., 1980; Jones, 1983; Ropes, et al., 1984) (Appendix C), and if the collection date is known, paleoenvironmental reconstructions with an absolute chronology can be created (e.g., Jones, 1983). Our goals in this paper are to 1) use both modern and $^{14}\text{C}_{\text{AMS}}$ dated fossil *A. islandica* shells to document ocean variability during the late Holocene in the Western Gulf of Maine, 2) identify possible local and regional-scale mechanisms responsible for the shell-derived isotope time-series based on comparisons with instrumental data from the GOM and the North Atlantic, and 3) estimate the influence of North Atlantic atmospheric and oceanic variability on GOM oceanography over the past millennium.

6.2. Experimental Methods

6.2.1. Sample Collection

One specimen of *A. islandica* was collected alive in the Western Gulf of Maine, USA (43° 39' 22.14" N, 69° 48' 6.01" W), in 30 m water depth via the fishing vessel *FV Foxy Lady* on March 14, 2004 during a Maine Department of Marine Resources dredge survey (Fig. 6.1). Three well-preserved articulated fossils of *A. islandica* were collected 3 kilometers away (43° 41' 13.14" N, 69° 47' 56.34" W) in 38 m water depth at depths of 30, 40, and 48 cm in a Rossfelder vibracore (SBVC-9609) on September 29, 1996 (Fig. 6.1).

6.2.2. Sclerochronological and Isotope Analyses

In preparation for sclerochronological and isotope analyses, we used methods outlined by Schöne et al. (2005a). Annual oxygen isotope values ($\delta^{18}\text{O}_c$) (autumn to autumn) were calculated by averaging sub-annual $\delta^{18}\text{O}_c$ samples for each year. Based on approximately 3000 $\delta^{18}\text{O}_c$ analyses on the four shells, the average number of sub-

annual $\delta^{18}\text{O}_c$ samples per year was ~ 8 (range 1-54). A complete description of isotopic measurements of shell material is previously described in earlier sections.

6.2.3. Calculation of Sea Water Temperatures and Shell $^{14}\text{C}_{\text{AMS}}$ Dating

We used the modified Grossman and Ku (1986) aragonite equation (Eq. 6.1) with the Houghton and Fairbanks (2001) GOM isotope/salinity mixing line from the Northeast Channel (Eq. 6.2) to calculate annual water temperatures, which are shown below ($\delta^{18}\text{O}_c$ ‰ [VPBD]; $\delta^{18}\text{O}_w$ ‰ [VSMOW]):

$$T (\text{°C}) = 20.60 - 4.34 * (\delta^{18}\text{O}_c - (\delta^{18}\text{O}_w - 0.20)), \text{ and} \quad (6.1)$$

$$\delta^{18}\text{O}_w \text{ ‰ (VSMOW)} = (0.57 * \text{Salinity}) - 19.5. \quad (6.2)$$

Salinity values were available (see below) from 1928 to present. Prior to 1928, salinity (practical salinity units; PSU) was estimated based on the long-term mean at the Canadian Prince 5 station (32.1 ± 0.22 PSU) to calculate annual water temperatures.

$^{14}\text{C}_{\text{AMS}}$ dating was used to determine the approximate calendar age of the outermost shell portion (youngest with respect to ^{14}C). Calibrated ^{14}C ages (cal yr AD) were calculated using Calib 5.01 (Stuiver and Reimer, 1993) using a regional GOM marine reservoir effect of $\Delta R = 39 \pm 40$ (Tanaka et al., 1990), which included quahog shells (*Arctica islandica* and *Merceneria mercenaria*) from museum collections. The calendar age assigned to the entire shell resulted from counting the annual growth layers (Jones, 1980) from the ventral margin back to the umbo region.

6.2.4. Instrumental Data

Instrumental data used in this paper includes air temperatures from Portland, Maine (1895- present), SST from Boothbay Harbor (Lazzari, 2001) (1905- present), and 50m water temperature and salinity values from Prince 5 station (1928- present) (Fig. 6.1). We used a winter (DJFM) NAO index (NOAA, Climate Prediction Center), an AMO index (Enfield et al., 2001), and Labrador Current (LC) volume transport data (1992-2003) (Han and Li, 2004) to assess the influences of NAO, AMO and LC variability on instrumental and shell-derived water temperatures in the GOM.

6.3. Results and Discussion

6.3.1. Relationships Between Air Temperatures and Sea Water Temperatures

There is a significant relationship ($r = 0.59$; $p < 0.0001$) between annual air temperatures from Portland, Maine and the annual SST record at Boothbay Harbor from 1905-2003. Further, there is a relatively weak but statistically significant ($r = 0.33$; $p < 0.0003$) relationship between local air temperatures (Portland) and the shell-derived water temperature in the Western GOM during the same time interval. The strongest relationship ($r = 0.71$; $p < 0.0001$) is between annual SST at Boothbay Harbor and the annual shell-derived water temperature in the Western GOM at 30 m water depth during 1905-2003 (Fig. 6.2). On average the SST at Boothbay Harbor is 2.2 °C warmer than water temperatures at 30 m. Based on a comparison with SST at Boothbay Harbor, the shell-derived water temperature record (Fig. 6.2) illustrates the capability of *A. islandica* to accurately incorporate environmental variability on interannual-to-decadal timescales. These results suggest that local air temperature in the GOM region strongly impacts SST at Boothbay Harbor, and local air temperatures weakly impact water temperatures at 30 m in the Western GOM. The strong relationship between SST and the water temperature

where the shell grew indicates that the surface waters are strongly coupled with water at 30 m in the Western GOM.

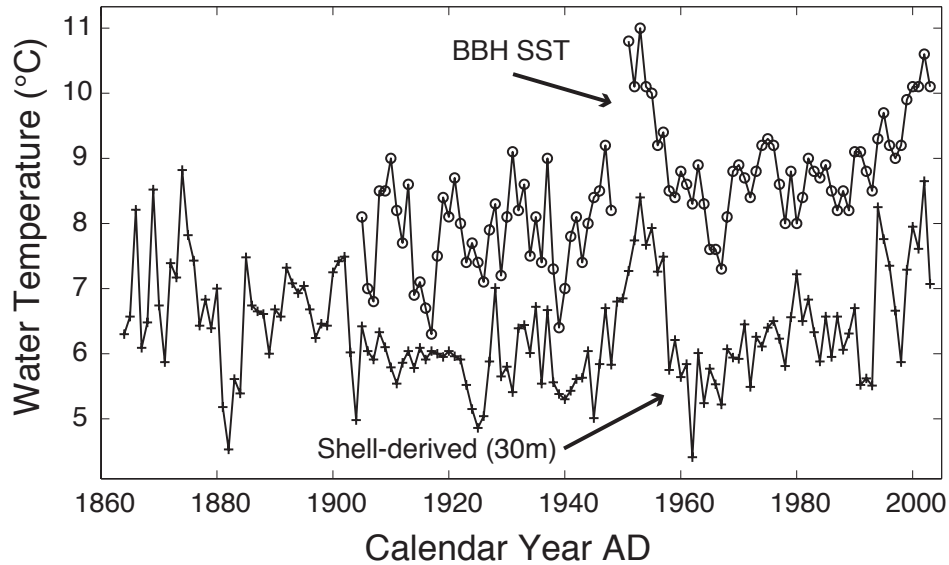


Figure 6.2. Shell isotope-derived 30 m water temperature (plus sign) and BBH SST record (open circles) (Lazzari, 2001) are illustrated. Annual linear correlation (r) from 1905-2003 is $r = 0.71$ ($p < 0.0001$).

6.3.2. Labrador Current Influence on GOM Water Temperatures

The relationship between annually averaged LC transport (NE Track 096 [transect length = 243.6 km], Eastern Newfoundland Slope) (Fig. 6.1) and the shell-derived temperature with a one-year lag is shown in Figure 6.3 (top). LC transport variability at this location explains most ($r = -0.79$; $p < 0.007$) of the temperature variability at 30 m in the Western GOM from 1993-2003. In addition, LC transport variability explains ~ 51% ($r = -0.72$; $p < 0.019$; [1993-2003]) of the Prince 5 (50 m) water temperature record, and ~ 58 % ($r = -0.76$; $p < 0.011$; [1994-2004]) of SST variability at Boothbay Harbor with a one-year lag (Fig. 6.3; top). The strength of the correlations, and the slopes between LC transport and GOM water temperatures are very similar for all three site locations, suggesting that LC transport modifies water temperatures in the entire GOM

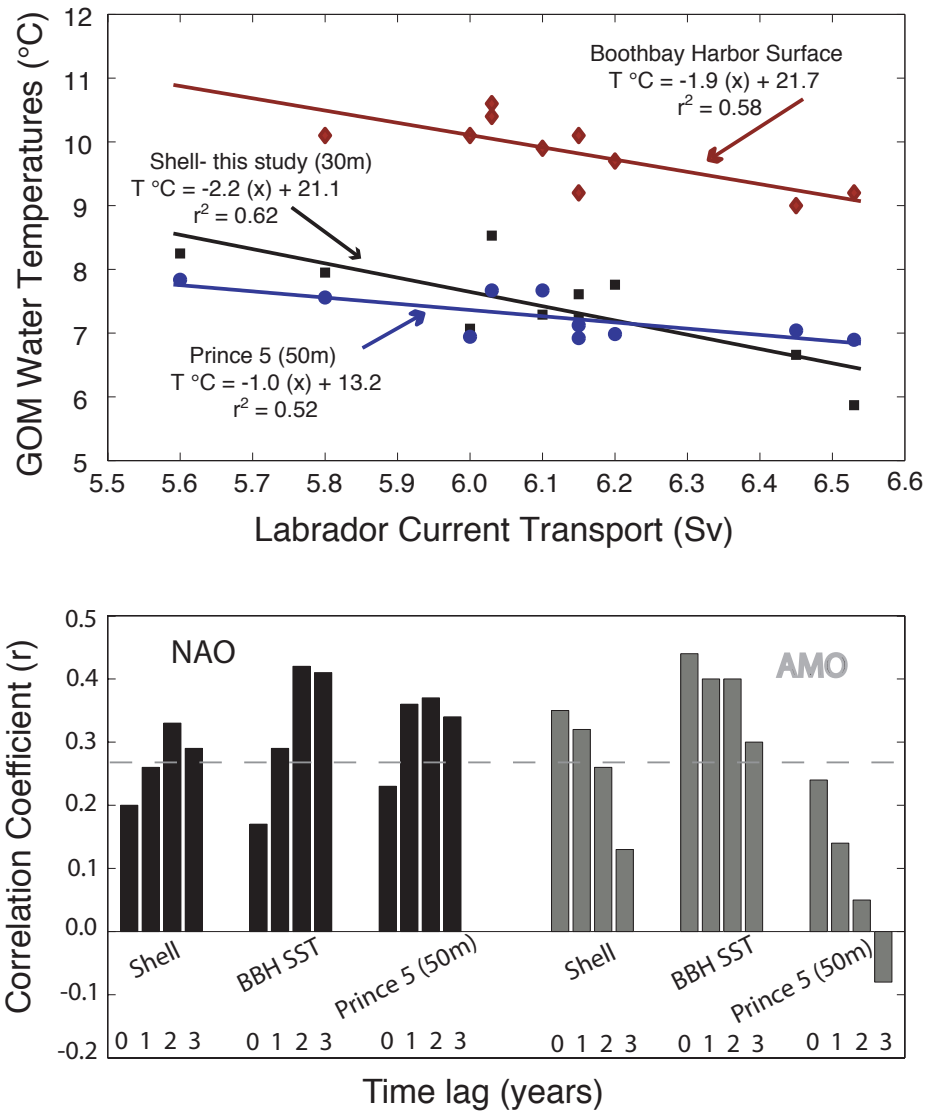


Figure 6.3. (top) The relationship between Labrador Current (LC) transport (Han and Li, 2004) from the Eastern Newfoundland Slope (NE Track 096) (Fig. 1) and water temperatures in the Gulf of Maine (GOM) with a 1-year lag are shown. Shell isotope-derived temperatures (30 m) (black squares and black line; 1993-2003); Boothbay Harbor Surface (red diamonds and red line; 1994-2004); Prince 5 (50 m) (blue circles and blue line; 1993-2003). (bottom) Linear correlations between annual Gulf of Maine temperature records (Shell; BBH = Boothbay Harbor; Prince 5 [50 m]) and dominant modes of North Atlantic climate (NAO [black] and AMO [gray]) with various lags from 1950-2003. Gray dashed line represents significance at the 95 % confidence interval ($r > 0.26$).

basin through deep water mixing processes. This result highlights the importance of LC variability on the modern oceanography in the GOM, and appears to be consistent with previously proposed mechanisms (e.g., Petrie and Drinkwater, 1993; Drinkwater et al., 1999; MERCINA, 2001; Loder et al., 2001). However, estimated LC transport data from locations along the Southern Newfoundland Slope (tracks 024 [transect length = 75.4 km], 113 [transect length = 98.6 km], and SW 096 [transect length = 69.6 km]) (Fig. 6.1), have substantially lower correlations ($r = -0.19$ [track 024], $r = -0.25$ [track 113], $r = -0.44$ [SW track 096]) with the GOM shell-derived water temperature record (with a one-year lag) that are not statistically significant (e.g., $r > 0.63$; $p < 0.05$). The correlations are weak, because a substantial portion of the LC flows across the Grand Banks south of NE track 096 (see Han and Li, 2004), thus these southerly transects do not fully capture LC variability.

6.3.3. NAO and AMO Forcing of GOM Water Temperatures

The relationships between water temperatures in the GOM and the winter NAO and AMO are illustrated (Fig. 6.3; bottom). We used unsmoothed values for the winter NAO to assess the role of this climate mode on GOM water temperatures. The unsmoothed NAO correlations with GOM water temperatures were statistically significant with the highest correlations occurring with a two-year lag (Fig. 6.3; bottom). Further, to assess decadal influences of North Atlantic SSTs on GOM water temperatures we used the AMO index of Enfield et al. (2001). Using this method, the AMO accounts for about 6 - 19 % (0 yr lag) of water temperature variability in the GOM from 1950-2003, and the NAO accounts for approximately 11 - 18 % (2 yr lag) of water temperature variability during the same time interval (Fig. 6.3; bottom). Each of these climate modes separately influences water temperatures in the GOM, as the AMO and NAO are not correlated at a statistically significant level ($r = -0.18$ [no lag], $r = 0.05$ [1 yr lag, AMO lags the NAO], $r = -0.09$ [2 yr lag], $r = 0.01$ [3 yr lag]). Because the AMO index is a

homogenized (0°-70°N) North Atlantic SST anomaly pattern the best correlation at each site location is without any temporal lag. However, the highest correlations between the NAO and GOM water temperatures occur with a 2-year lag. Changes in LC transport associated with the NAO take approximately 1.5 to 2 years to reach the GOM (see Drinkwater et al. (1999) for a detailed description). These results suggest that decadal patterns of the AMO and the NAO significantly impact water temperatures in the GOM. We suggest that the NAO modulates LC transport, and speculate that the AMO pattern broadly represents Gulf Stream transport. The combined effects of the NAO and AMO primarily control GOM water temperatures on decadal-to-multidecadal timescales by modifying the relative amounts of each water mass (LSW and WSW) that enters the GOM. Persistent negative (positive) modes of the NAO and AMO would lead to colder (warmer) GOM water temperatures, thus changes in either of these climate modes during the late Holocene should be reflected by concurrent changes in the GOM.

6.3.4. Shell-Derived Isotope Record and Reconstructed GOM Water Temperatures During the Last Millennium

The reconstructed water temperatures (using a fixed salinity) for intervals during the late Holocene from the Western GOM in 30-38 m of water are illustrated in Figure 6.4A. The rationale for fixing salinity to reconstruct temperature prior to 1928 is based on the modern 75-year salinity mean (32.1 ± 0.22 PSU) at the Prince 5 (50m) station, which shows no significant long-term trend. Because shell $\delta^{18}\text{O}_c$ is a function of water temperature and the isotopic composition of the water ($\delta^{18}\text{O}_w$; related to salinity) (e.g., Epstein et al., 1953), we considered the possible effects of changing salinity assuming a constant water temperature. The reconstructed water salinities for intervals during the late Holocene from the Western GOM in 30-38 m of water are illustrated in Figure 6.4B. Salinity values were calculated using the $\delta^{18}\text{O}_c$ long-term means for each of the intervals and fixing mean water temperatures. The salinity change during the record was modeled

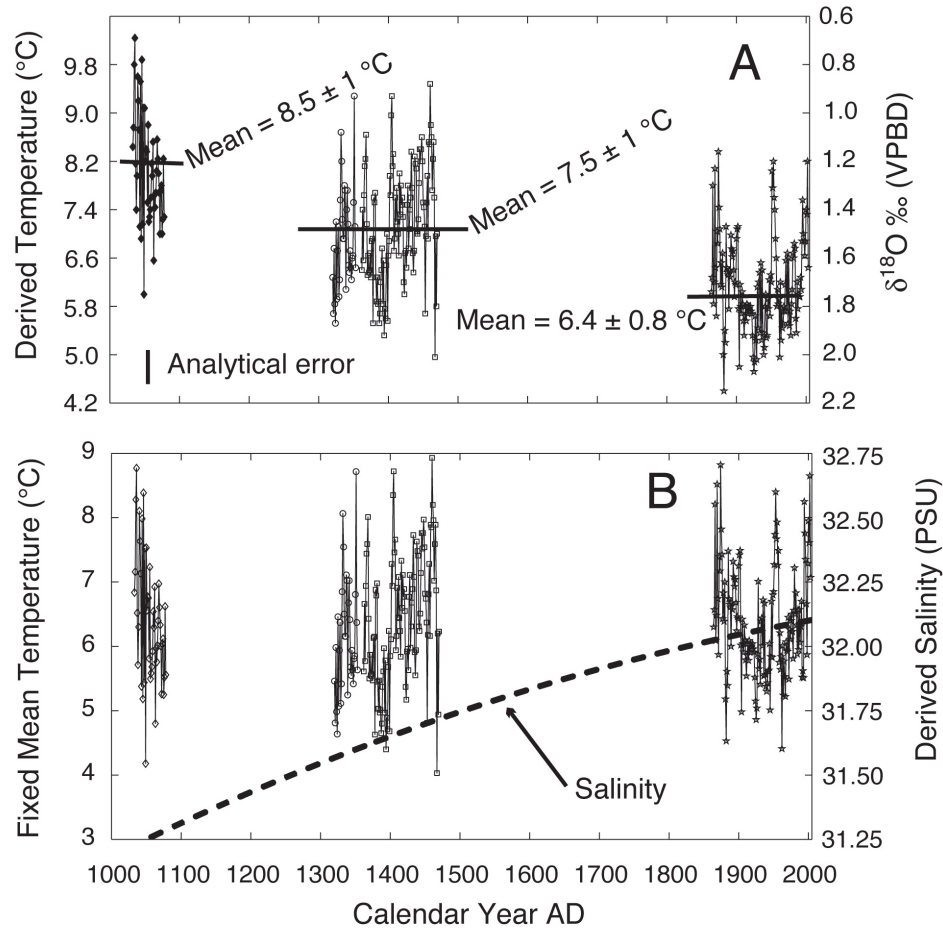


Figure 6.4. (A) Late Holocene shell-derived water temperatures with a fixed salinity and $\delta^{18}\text{O}_c$ record, (B) and late Holocene shell-derived salinity values with fixed mean water temperatures are shown (see text for details).

by a second-order polynomial ($\text{salinity} = [-4 \times 10^{-7} * x^2 + 0.0022 * x + 29.44]$) to estimate a gradual change in salinity. Alternatively the salinity change could have happened in a step-like function. Although we currently do not have a mechanism to explain an increased salinity regime in the GOM during the late Holocene, it is an end-member condition that can explain shell $\delta^{18}\text{O}_c$ variability. However, because the strength of the relatively warm and salty Gulf Stream weakened during this time period (Lund et al., 2006) an excursion of more saline water into the GOM is unlikely, except for the most recent period (after the 1800s). The magnitude of a mean salinity increase of ~ 0.85 PSU during the past 1000 years is relatively large and unlikely.

Using a fixed salinity model, mean annual water temperatures from 1030 -1078 \pm 78 AD (Medieval Warm Period) were 8.5 °C (1 σ = 1 °C) based on the 46-year mean of shell $\delta^{18}\text{O}_c = 1.24$ ‰ (1 σ = 0.23 ‰). From 1321 – 1470 \pm 45 AD (Little Ice Age) mean annual water temperatures were 7.5 °C (1 σ = 1 °C) based on the 143-year mean of shell $\delta^{18}\text{O}_c = 1.47$ ‰ (1 σ = 0.23 ‰), while modern (1864-2003 AD) mean annual water temperatures were 6.4 °C (1 σ = 0.8 °C) based on the 140-year mean shell $\delta^{18}\text{O}_c = 1.71$ (1 σ = 0.19 ‰) (Figs. 6.4A, 6.5A). Interannual variability of shell $\delta^{18}\text{O}_c$ from 1030 -1078 \pm 78 AD and 1321 – 1470 \pm 45 AD was equal (1 σ = 0.23 ‰), and only slightly less during the modern record (1 σ = 0.19 ‰). This suggests that the forcing mechanisms controlling interannual oceanographic conditions for the GOM region have been relatively similar and persistent at least during these intervals. Using the relationship between LC transport variability and the shell-derived and instrumental water temperatures in the GOM (Fig. 6.2), we propose that LC transport increased during the late Holocene by approximately 0.7 Sv, resulting in an overall decrease in GOM water temperatures of 2 °C.

6.3.5. Independent Evidence for late Holocene Cooling in the Northwestern Atlantic based on Multiple Marine and Terrestrial Records

Marchitto and deMenocal (2003) showed a cooling of ~ 1 °C of deep bottom water (1854 m) from the Laurentian Slope, south of Newfoundland using Mg/Ca ratios derived from benthic foraminifera from ~ 900 AD – 1800 AD (Fig. 6.5B). Because the Mg/Ca ratio temperature estimations of Marchitto and deMenocal (2003) are independent of salinity values, they provide a relatively pure temperature signal. The alkenone-based SST reconstruction of Keigwin et al. (2003) for Emerald Basin along the Scotian Shelf showed a similar magnitude cooling of ~ 0.8 °C from ~ 400 AD – 1900 AD (Fig. 6.5C), which is likely a reflection of St. Lawrence outflow and possibly a minor contribution from the inshore branch of the LC. The data of Keigwin et al. (2003) provide an independent measure of SST along the Scotian Shelf, which is consistent with other

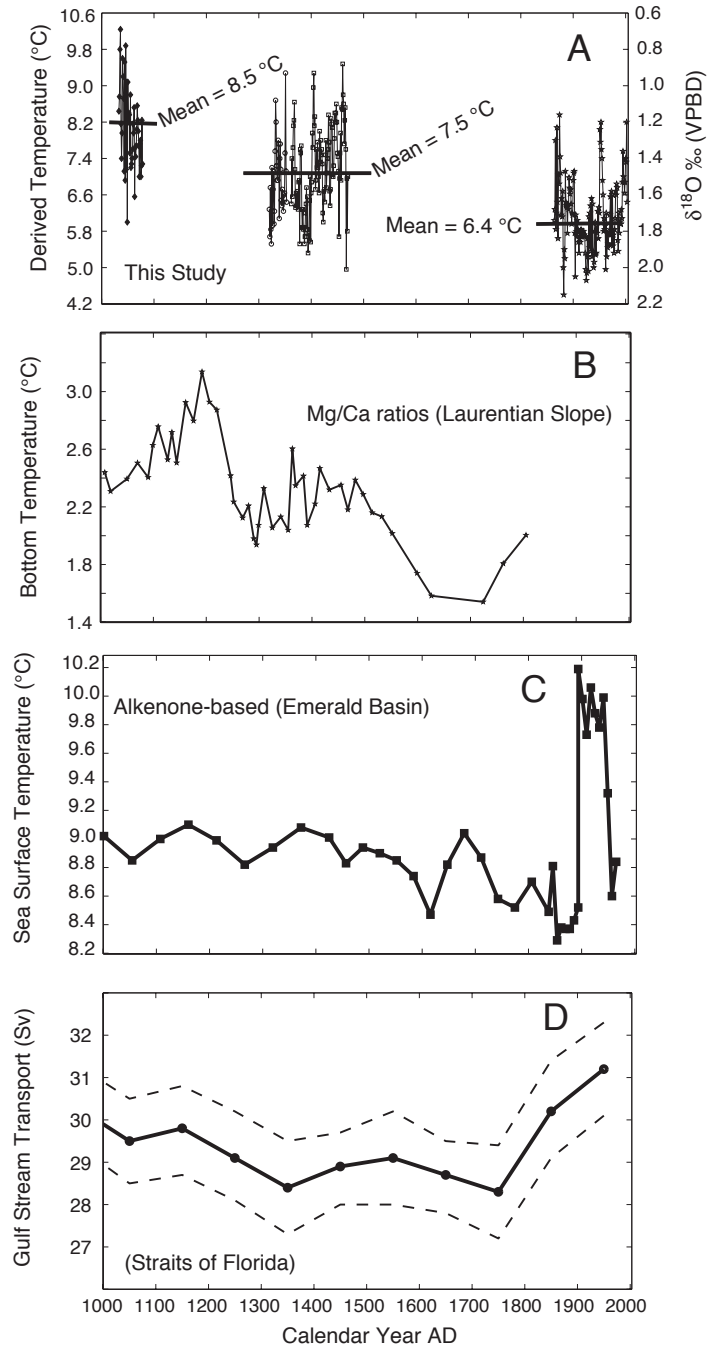


Figure 6.5. (A) Late Holocene shell-derived water temperatures with a fixed salinity and $\delta^{18}\text{O}_c$ record (this study), (B) part of the Mg/Ca ratio derived bottom water temperatures from the Laurentian Slope (1854 m) (Marchitto and deMenocal, 2003), (C) part of the alkenone-based SST record (Keigwin et al., 2003) from Emerald Basin (Scotian Shelf), and (D) estimated Gulf Stream Transport in the Straits of Florida with 95 % confidence intervals (dashed lines) (Lund et al., 2006) are shown for comparison.

marine-based studies (e.g., Keigwin et al., 2005; Sachs, 2007). Further, proxy data by Lund et al. (2006) suggested that the transport of the relatively warm Gulf Stream water decreased by 2-3 Sv (6 – 10 %) from ~ 1000 AD – 1800 AD. Thus a coupled increase of LC transport and a corresponding decrease in Gulf Stream-derived water (WSW) entering the GOM is a likely explanation of the shell-derived water temperature record from 1000 AD to the early 1900s. During the last 100 years, water temperatures in the GOM have been increasing (Fig. 6.2), which corresponds to increased Gulf Stream transport and is consistent with warmer SSTs from Emerald Basin during the early to mid 1900s (Fig. 6.5). Because we do not have any shell-derived temperature data ca. 1700 AD - 1850 AD (Little Ice Age) in the GOM, we are unable to determine if GOM water temperatures were lower toward the end of the Little Ice Age compared to the modern shell-derived water temperature record (Fig. 6.2).

Evidence from terrestrial sites in Northeastern United States indicates cooler and wetter conditions during the late Holocene, consistent with changes in LC and Gulf Stream forcing on GOM. Fossil pollen data from Gajewski (1988) demonstrate that summer air temperatures in Maine (Conroy Lake and Basin Pond) cooled by 1-2 °C during the past 1000 - 1500 years. In addition, Gajewski (1988) and Dieffenbacher-Krall and Nurse (2005) show that the climate in Northern Maine (e.g., Whited Lake) became progressively wetter in the late Holocene. Schauffler and Jacobson (2002) demonstrated that spruce (*Picea* spp.) pollen increased dramatically during the last 1000 years in Northern Maine, also indicating colder and wetter conditions. If wetter conditions prevailed to the north, then the LC transport would strengthen from the increased run-off, because the LC is primarily a buoyancy-driven current. There is a significant negative correlation between the NAO mode and precipitation rates in the Labrador Sea from 1950 –2003 (Fig. 6.6). A persistently low NAO pattern for periods in the late Holocene could have caused wetter conditions in northern Maine and the Labrador Sea region. Further, Shindell et al. (2001) reported that decreased solar forcing can lead to a negative shift

in the NAO, which apparently occurred in the late Holocene during the LIA. Keigwin et al. (2005) and Sachs (2007) concluded that slope waters in the Northwestern Atlantic have cooled dramatically (4 - 10 °C) from Virginia to Nova Scotia during the Holocene possibly related to decreased solar insolation or THC variability, specifically a southward migration of the Gulf Stream. Based on the marine (Fig. 6.5) and terrestrial proxy records, we suggest that increased LC transport and decreased Gulf Stream influence during the late Holocene were the primary controls on GOM temperatures, with shell-derived water temperatures in 30-38 m of water in the Western GOM decreasing by ~ 2 °C during the last millennium.

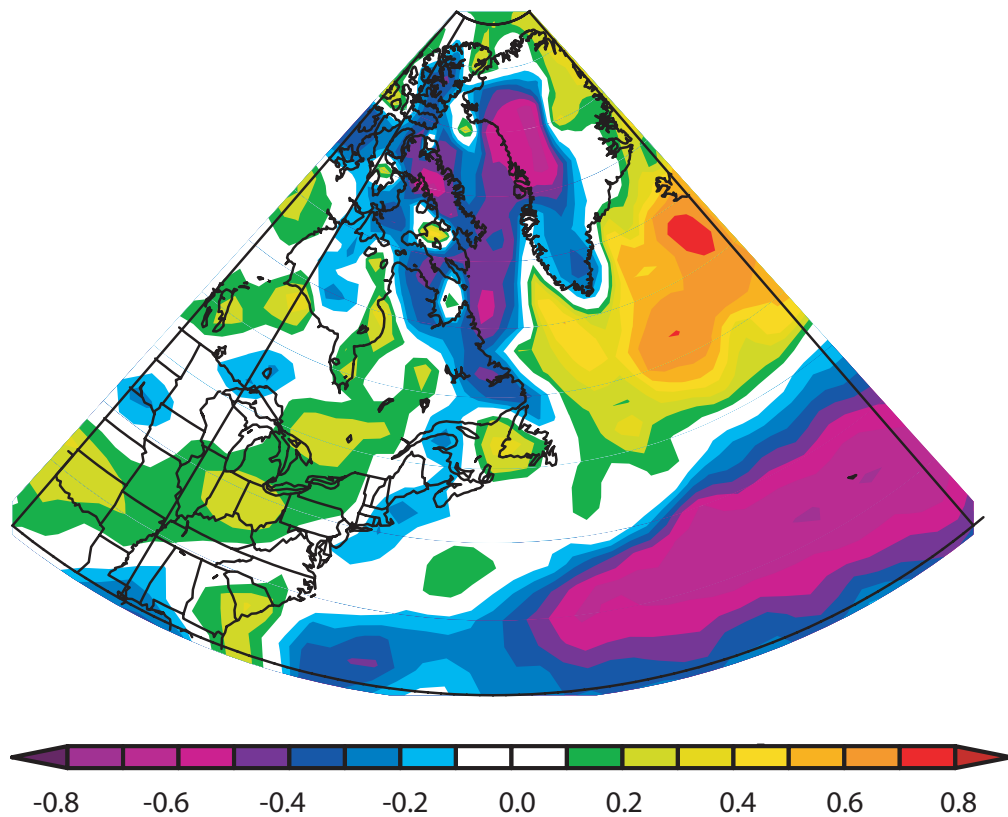


Figure 6.6. Correlation (r) between winter (DJFM) NAO index and NCEP reanalysis precipitation rates during the same season from 1950-2003.

6.4. Conclusions and Future Work

In this paper we present an annualized shell-derived $\delta^{18}\text{O}_c$ record in the Western GOM for intervals of the past 1000 years that demonstrates major shifts in mean isotopic values likely related to slope water circulation. In either end-member configuration, the oceanic conditions in the Western GOM have changed considerably ($\sim 2^\circ\text{C}$ or 0.82 PSU at 30m) during the late Holocene. A substantial portion (51-62 %) of modern temperatures (with a 1-year lag) in the GOM are explained by LC transport variability along the Eastern Newfoundland Slope. Although the $\delta^{18}\text{O}_c$ record can be explained by changes in water temperature, salinity, or both, we believe that the majority of the $\delta^{18}\text{O}_c$ record is best explained by temperature changes caused by coupled slope water dynamics related to the NAO and the AMO. An increased transport of ~ 0.7 Sv in the LC and a corresponding decrease in Gulf Stream-derived water during the past millennium could explain a 2°C cooling in the Western GOM.

During the last century, local air temperatures in the GOM region strongly influenced the SST record at Boothbay Harbor, and weakly impacted water temperatures at 30m in the Western GOM. Over the last millennium, on decadal to centennial timescales water temperatures in the GOM primarily appear to reflect conditions in the North Atlantic. Future work will include independently constraining temperature or salinity conditions (e.g., alkenones, Sr/Ca ratios) in the Western GOM and developing a continuous shell-derived $\delta^{18}\text{O}_c$ record during the late Holocene to assess interannual-to-millennial scale oceanographic changes.

Additional data associated with this study can be found in Appendix C, including subannual plots of oxygen isotope profiles from each of the shells used from the Gulf of Maine.

7. Concluding Remarks

The research and results presented in this dissertation greatly improve the techniques used in paleoceanography to develop accurate and precise estimations of seawater temperature (using bivalve carbonate geochemistry), and productivity. Calibrated bivalve proxy records offer significant advantages over non-calibrated records, because the error of the paleotemperature estimation is clearly known. Further, species-specific calibrations have fewer uncertainties associated with them, because potential vital effects and/or isotope disequilibrium are clearly determined. The results presented in section III is based on the first experiment in the field of paleoceanography that investigated possible genetic/physiological isotope effects for bivalves collected from two distinct climate regimes (sub-polar and temperate). These data indicate that species-specific paleotemperature relationships can be used confidently over large geographic ranges (at least for *M. edulis*), including different climate zones (e.g., Greenland and Maine), because there are no discernable differences in shell isotope geochemistry. These findings clearly will improve estimations of seawater temperatures using methods outlined in sections II and III. Further, because bivalves are widely distributed both temporally and spatially throughout geologic time, future work has the potential to document ocean variability in the mid-to-high latitude marine environments, where relatively few records exist.

The work presented in sections V and VI is the first high-resolution (annualized) marine record from the Gulf of Maine for intervals during the late Holocene. In all, approximately 1/3 of the last 1,000 years is represented by shell growth histories and oxygen isotope profiles. These data indicate that the Gulf of Maine has undergone considerable changes during the last millennium, and specifically the shell-derived temperature record suggests that the Gulf of Maine has cooled by ~ 2 °C. It appears that the small changes in the relative input of Labrador Slope Water (LSW) and Warm Slope

Water (WSW) (Gulf Stream-derived) greatly impacts water temperatures in the Gulf of Maine. Moreover, on decadal-to-centennial timescales the Gulf of Maine follows the general conditions in the Northwestern Atlantic. This contribution corroborates that the climate in the region during the late Holocene has cooled, and perhaps the Gulf of Maine and Northwestern Atlantic are still in a transient state from the early Holocene (see Keigwin et al., 2005; Sachs, 2007). These changes in water temperature are attributed to decreased Gulf Stream influence and possibly a simultaneous increase in the strength of the Labrador Current.

In section VI, the longest water temperature record for the Gulf of Maine is presented. The modern shell-derived record spans from 1864 - 2003, extending our knowledge of oceanic conditions back some 40 years with direct overlap from the longest instrumental record; ultimately expanding water temperatures back 1000 years. The Boothbay Harbor sea surface temperature record began in 1905, and the comparison between the shell-derived water temperature record and the Boothbay record is exceptional. This record is absolutely dated (similar to tree rings) and illustrates relatively warmer (~ 1 °C) water temperatures during the mid 19th century compared to the early 20th century, with a warming trend since the 1920s. It is unclear if the recent warming in the shell-derived record and instrumental records is part of a natural climate cycle, or if the region is responding to increased warming of the atmosphere in the Northern Hemisphere. Clearly, more work needs to be conducted in this region, and a 1000-year continuous shell-derived oxygen isotope record would substantially address this concern.

The development of a paleo-productivity proxy in the Western Gulf of Maine (section V) is a significant advance for addressing pertinent biological questions. This research demonstrates the concept that shell growth histories reflect basic hydrographic conditions in which they grew. Particularly, results in this section indicate that *A. islandica* growth records correspond to certain zooplankton dynamics (*C. finmarchicus*). Although the mechanisms responsible for the correspondence are not completely

understood (clams do not eat zooplankton), results from this section indicate that slope-water dynamics may be forcing the primary productivity levels in the Gulf of Maine. In general, when the relative input of the cold, nutrient-poor Labrador Current-derived (LSW) water is greatest, water temperatures and shell growth is decreased, while a greater relative input of the warm, nutrient-rich Gulf Stream-derived water (WSW) leads to increased water temperatures and shell growth. This result is promising and should be further tested with many more shell-growth records from different locations within the Gulf of Maine.

Results presented in sections V and VI corroborate that the North Atlantic Oscillation (NAO) remotely forces oceanographic conditions in the Gulf of Maine, including water temperature and productivity levels. Further, it appears that the NAO affects the entire basin with a 1 - 2 year lag. Also, temperature records (shell and instrumental) correlate significantly with the Atlantic Multi-decadal Oscillation (AMO). To my knowledge, this is the first suggestion that oceanographic conditions in the Gulf of Maine are linked to the AMO pattern. The AMO is likely a result in thermohaline circulation (THC) variability, and there is a strong probability that Gulf Stream activity and the AMO result from the same variability in THC. Thus, the interpretation presented here is that the ~ 2 °C cooling in the Gulf of Maine during the last millennium resulted from decreased WSW influence (Gulf Stream-derived) (corroborated by other researchers [e.g., Lund et al., 2006]), and increased LSW (Labrador Current-derived) input.

Although more work is needed to establish the relative importance of each forcing mechanism on the Gulf of Maine's oceanography, results presented here greatly improve and extend the understanding of late Holocene ocean variability for the region. It appears that the majority of ocean variability in the Gulf of Maine on decadal or longer timescales originates from the North Atlantic, while regional conditions (storms, winds, water stratification, freshwater input, air temperature, etc.) tend to impact the Gulf of Maine on shorter timescales (intra-to-inter annual). As expected, there is a relatively

strong relationship between local air temperatures and sea surface temperatures in the Gulf of Maine. However, it is unclear how they are coupled. Is air temperature driving water temperature? Or, is water temperature driving local air temperature? In summary, water temperatures from the Gulf of Maine reflect a relatively complex, mixed signal of slope water input (LSW and WSW) and local forcing mechanisms related to regional climate patterns.

The results presented here contribute significantly to the current understanding of late Holocene climate in the Northwestern Atlantic. In particular, the shell-derived reconstructed late Holocene water temperature record from the Western Gulf of Maine illustrates the importance of including marine-based climate archives in the context of Holocene climate change. This record demonstrates a substantial cooling from 1000 AD to the 1920s, with a warming into the 21st century. Even with the recent warming in the marine record, it is still cooler now than during the LIA and MWP. Thus, the Gulf of Maine does not show a typical climate signal when compared to the Northern Hemisphere air temperature record for the last 1000 years (i.e., see Mann et al., 1999), nor does it show the classic Euro-centric MWP and LIA climate patterns. This noted difference demonstrates the need to include climate records from a variety of sources (terrestrial and marine) that are spatially diverse to better capture and understand global climate change. Although the Gulf of Maine water temperature record does not reflect Northern Hemisphere air temperatures, it does reflect changes in the Northwestern Atlantic, such as the documented weakening of the Gulf Stream (e.g., Lund et al., 2006), and possible strengthening of the Labrador Current. Thus, the climate record derived from this study may be more appropriately compared to other marine-based climate records that reflect the broad properties of THC (e.g., Lund and Curry, 2006; Keigwin et al., 2005; Sachs, 2007). Although it is unclear what has caused the observed cooling along the Northwestern Atlantic during the last millennium, it is plausible that the cooling may be linked to substantial shifts in THC (e.g., Sachs, 2007). Further, these

results re-enforce that the climate system is complex and results from many feedbacks that are poorly understood. Additional work is still warranted and necessary to unravel the complex relationships among local, regional, and North Atlantic climate forcing mechanisms and the oceanography in the Gulf of Maine.

REFERENCES CITED

- Adkins, J. F., Boyle, E. A., Curry, W. B., and Lutringer, A., 2003, Stable isotopes in deep-sea corals and a new mechanism for “vital effects”: *Geochimica et Cosmochimica Acta*, v. 67, no. 6, p. 1129-1143.
- Al-Horani, F. A., Al-Moghrabi, S.M., and de Beer, D., 2003, Microsensor study of photosynthesis and calcification in the scleractinian coral, *Galaxea fascicularis*: active internal carbon cycle: *Journal of Experimental Marine Biology and Ecology*, v. 288, p. 1-15.
- Arthur, M. A., Williams, D. F., and Jones, D. S., 1983, Seasonal temperature-salinity changes and thermocline development in the mid-Atlantic Bight as recorded by the isotopic composition of bivalves: *Geology*, v. 11, p. 655-659.
- Baringer, M. O., and Larsen, J. C., 2001, Sixteen years of Florida Current transport at 27°N: *Geophysical Research Letters*, v. 28, p. 3179-3182.
- Bayne, B. L., Thompson, R. J., and Widdows, J., 1973, Some effects of temperature and food on the rate of oxygen consumption by *Mytilus edulus* L., in Wieser, W., ed., *Effects of temperature on ectothermic organisms*: Heidelberg, Springer-Verlag, p. 181-193.
- Beal, B. F., and Kraus, M. G., 1989, Effects of intraspecific density on the growth of *Arctica islandica* Linné inside field enclosures located in eastern Maine, USA: *Journal of Shellfish Research*, v. 8, p. 462.
- Bemis, B. E., Spero, H. J., and Lea, D. W., 1998, Reevaluation of the oxygen isotopic composition of planktonic foraminifera: experimental results and revised paleotemperature equations: *Palaeoceanography*, v. 13, p. 150-160.
- Bijma, J., Hemleben, C., Huber, B. T., Erlenkeuser, H., and Kroon, D., 1998, Experimental determination of the ontogenetic stable isotope variability in two morphotypes of *Globigerinella siphonifera* (d'Orbigny): *Marine Micropaleontology*, v. 35, no. 2, p. 141-160.

- Borns, H. W., Jr., Doner, L., Dorion, C., Jacobson, G., Kaplan, M., Kreutz, K., Lowell, T., Thompson, W., and Weddle, T., 2004, The deglaciation of Maine, U.S.A., in Ehlers, J., and Gibbard, P.L., ed., Quaternary Glaciations-Extent and Chronology, Part II, Elsevier, p. 89-109.
- Box, G., and Jenkins, G. M., 1976, Time Series Analysis: San Francisco, Holden-Day, 553 p.
- Bradley, R. S., Hughes, M. K., and Diaz, H. F., 2003, Climate in Medieval Time: Science, v. 302, p. 404-405.
- Bradley, R. S., and Jones, P. D., 1993, "Little Ice Age" summer temperature variations: their nature and relevance to recent global warming trends: The Holocene, v. 3, p. 367-376.
- Brown, W. S., and Irish, J. D., 1993, The annual variation of water mass structure in the Gulf of Maine: 1986-1987: Journal of Marine Research, v. 51, p. 53-107.
- Cargnelli, L. M., Griesbach, S. J., Packer, D. B., and Weissberger, E., 1999, Ocean quahog, *Arctica islandica*, life history and habitat characteristics: National Marine Fisheries Service-National Oceanic and Atmospheric Administration.
- Carre, M., Bentaleb, I., Blamart, D., Ogle, N., Cardenas, F., Zevallos, S., Kalin, R. M., Ortlieb, L., and Fontugne, M., 2005, Stable isotopes and sclerochronology of the bivalve *Mesodesma donacium*: Potential application to Peruvian paleoceanographic reconstructions: Palaeogeography, Palaeoclimatology, Palaeoecology, v. 228, p. 4-25.
- Chauvaud, L., Lorrain, A., Dunbar, R. B., Paulet, Y.-M., Thouzeau, G., Jean, F., Guarini, J.-M., and Mucciarone, D., 2005, Shell of the Great Scallop *Pecten maximus* as a high-frequency archive of paleoenvironmental changes: Geochemistry, Geophysics, Geosystems, v. 6, Q08001, doi:10.1029/2004GC000890.
- Chen, J. L., Wilson, C. R., and Tapley, B. D., 2006, Satellite gravity measurements confirm accelerated melting of Greenland ice sheet: Science, v. 10.1126/science.1129007.

- Clark, R. A., Frid, C. L. J., and Batten, S. D., 2001, A critical comparison of two long-term zooplankton time-series from the central-west North Sea: *Journal of Plankton Research*, v. 23, p. 27-39.
- Cohen, A. L., and McConnaughey, T. A., 2003, Geochemical perspectives on coral mineralization: *Biom mineralization*, v. 54, no. 1, p. 151-187.
- Cole, J. E., Fairbanks, R. G., and Shen, G. T., 1993, Recent variability in the Southern Oscillation: Isotopic results from a Tarawa Atoll Coral: *Science*, v. 260, p. 1790-1793.
- Conversi, A., Piontkovski, S., and Hameed, S., 2001, Seasonal and interannual dynamics of *Calanus finmarchicus* in the Gulf of Maine (Northeastern US shelf) with reference to the North Atlantic Oscillation: *Deep-Sea Research II*, v. 48, p. 519-530.
- Cook, E. R., and Kairiukstis, L. A., 1990, *Methods of Dendrochronology: Applications in the environmental sciences*: Dordrecht, Kluwer Academic Publishers, 394 p.
- Craig, H., 1965, Measurement of oxygen isotope paleotemperatures, in Tongiorni, E., ed., *Stable Isotopes in Oceanographic Studies and Paleotemperatures*: Spoleto, Italy, Cons. Naz. Delle Ric., p. 161-182.
- Curry, R., and Mauritzen, C., 2005, Dilution of the northern North Atlantic Ocean in recent decades: *Science*, v. 308, p. 1772-1774.
- Daubechies, I., 1990, The wavelet transform time-frequency localization and signal analysis: *Institute of Electrical and Electronics Engineers Transactions, Information Theory*, v. 36, p. 961-1004.
- Day, R. W., Williams, M. C., and Hawkes, G. P., 1995, A comparison of fluorochromes for marking abalone shells: *Marine Freshwater Resources*, v. 46, p. 599-605.

- De Ridder, F. R., Pintelon, R., Schoukens, J., Gillikin, D. P., Andre, L., Baeyens, W., de Brauwere, A., and Dehairs, F., 2004, Decoding nonlinear growth rates in biogenic environmental archives: *Geochemistry, Geophysics, Geosystems*, v. 5, Q12015, doi:10.1029/2004GC000771, no. 12.
- Delworth, T. L., and Mann, M. E., 2000, Observed and simulated multidecadal variability in the Northern Hemisphere: *Climate Dynamics*, v. 16, no. 9, p. 661-676.
- DeNiro, M. J., and Epstein, S., 1978, Influence of diet on the distribution of carbon isotopes in animals: *Geochimica et Cosmochimica Acta*, v. 42, p. 495-506.
- Dettman, D., Reische, A., and Lohmann, K. C., 1999, Controls on the stable composition of seasonal growth bands in aragonitic fresh-water bivalves (*unionidae*): *Geochimica et Cosmochimica Acta*, v. 63, no. 7/8, p. 1049-1057.
- Dickson, B., Yashayaev, I., Melncke, J., Turrell, B., Dye, S., and Holfort, J., 2002, Rapid freshening of the deep North Atlantic Ocean over the past four decades: *Nature*, v. 416, p. 832-837.
- Dickson, R., Lazier, J., Meincke, J., Rhines, P., and Swift, J., 1996, Long-term coordinated changes in the convective activity of the North Atlantic: *Progress in Oceanography*, v. 38, p. 241-295.
- Dieffenbacher-Krall, A. C., and Nurse, A. M., 2005, Late-glacial and Holocene record of lake levels of Mathews Pond and Whitehead Lake, northern Maine, USA: *Journal of Paleolimnology*, v. 34, p. 283-310.
- Donner, J., and Nord, A. G., 1986, Carbon and oxygen stable isotope values in shells of *Mytilus edulis* and *Modiolus modiolus* from Holocene raised beaches at the outer coast of the Varanger Peninsula, North Norway: *Paleogeography, Paleoclimatology, Paleoecology*, v. 56, p. 35-50.
- Drinkwater, K. F., Belgrano, A., Borja, A., Conversi, A., Edwards, M., Greene, C. H., Ottersen, G., Pershing, A. J., and Walker, H., 2003, The Response of Marine Ecosystems to Climate Variability Associated With the North Atlantic Oscillation,

in Hurrell, J., Kushnir, Y., Ottersen, G., and Visbeck, M, ed., The North Atlantic Oscillation: Climate Significance and Environmental Impact: Washington, D.C., American Geophysical Union, p. 211-234.

Drinkwater, K. F., and Mountain, D. B., 1997, Climate and Oceanography in Northwest Atlantic Groundfish, Perspectives on a Fishery Collapse: Bethesda, MD, American fisheries Society, 3-25 p.

Drinkwater, K. F., Mountain, D. B., and Herman, A., 1999, Variability in the slope water properties off eastern North America and their effects on adjacent shelves: International Council for the Exploration of the Sea - Journal of Marine Science 1999/O:08, p. 26.

Emiliani, C., 1966, Isotopic Paleotemperatures: Science, v. 154, no. 3751, p. 851-857.

Enfield, D. B., Mestas-Nunez, A. M., and Trimble, P. J., 2001, The Atlantic multidecadal oscillation and its relation to rainfall and river flows in the continental U.S.: Geophysical Research Letters, v. 28, no. 10, p. 2077-2080.

Epstein, S., Buchsbaum, R., Lowenstam, H. A., and Urey, H. C., 1953, Revised carbonate-water isotopic temperature scale: Bulletin of the Geological Society of America, v. 64, p. 1315-1326.

Erez, J., 1978, Vital effect on stable-isotope composition seen in foraminifera and coral skeletons: Science, v. 273, p. 199-202.

Erez, J., and Luz, B., 1983, Experimental paleotemperature equation for planktonic foraminifera: Geochimica et Cosmochimica Acta, v. 47, p. 1025-1031.

Fagan, B., 2000, The Little Ice Age: How climate made history 1300-1850: New York City, Basic Books, 246 p.

Feindel, S., Schick, D., and Porter, K., 2003, Gulf of Maine Ocean Quahog (*Arctica islandica*) Assessment: Maine Department of Marine Resources.

- Feyling-Hanssen, R. W., 1955, Stratigraphy of the marine Late-Pleistocene of Billefjorden, Vestspitsbergen, Norsk Polarinstitut Skrifter, 186 p.
- Folland, C. K., Palmer, T. N., and Parker, D. E., 1986, Sahel rainfall and worldwide sea temperatures: *Nature*, v. 320, p. 602-606.
- Forsythe, G. T. W., Scourse, J. D., Harris, I., Richardson, C. A., Jones, P., Briffa, K., and Heinemeier, J., 2003, Towards an absolute chronology for the marine environment: the development of a 1000-year record from *Arctica islandica*: *Geophysical Research Abstracts*, European Geophysical Society, v. 5.
- Freitas, P., Clark, L. J., Kennedy, H., Richardson, C., and Abrantes, F., 2005, Mg/Ca, Sr/Ca, and stable-isotope (d18O and d13C) ratio profiles from fan mussel *Pinna nobilis*: Seasonal records and temperature relationships: *Geochemistry, Geophysics, Geosystems*, v. 6, Q04D14, doi:10.1029/2004GC000872, no. 4, p. 1-16.
- Friedman, I., and O'Neil, J. R., 1977, Compilation of stable isotope fractionation factors of geochemical interest, *in* Fleisher, M., ed., *Data of Geochemistry*, 6th edition. U.S. Geology Survey Professional Paper 776, p. 1-37.
- Furla, P., Galgani, I., Durand, I., and Allemand, D., 2000, Sources and mechanisms of inorganic carbon transport for coral calcification and photosynthesis: *Journal of Experimental Biology*, v. 203, p. 3445-3457.
- Gajewski, K., 1988, Late Holocene climate changes in eastern North America estimated from pollen data: *Quaternary Research*, v. 29, p. 255-262.
- Gatien, M. G., 1976, A study in the slope water region south of Halifax: *Journal of Fisheries Research Board of Canada*, v. 33, p. 2213-2217.
- Geist, J., Auerswald, K., and Boom, A., 2005, Stable carbon isotopes in freshwater mussel shells: Environmental record or marker for metabolic activity?: *Geochimica et Cosmochimica Acta*, v. 69, no. 14, p. 3545-3554.

- Gillikin, D. P., Dehairs, F., Lorrain, A., Steenmans, D., Baeyens, W., and Andre, L., 2006a, Barium uptake into the shells of common mussel (*Mytilus edulis*) and the potential for estuarine paleo-chemistry reconstruction: *Geochimica et Cosmochimica Acta*, 70, 395-407.
- Gillikin, D. P., Lorrain, A., Bouillon, S., Willenz, P., and Dehairs, F., 2006b, Stable carbon isotopic composition of *Mytilus edulis* shells: relation to metabolism, salinity, $\delta^{13}\text{C}_{\text{DIC}}$ and phytoplankton: *Organic Geochemistry*, 37, 1371-1382.
- Goldenberg, S. B., Lansea, C. W., Mestas-Nunez, A. M., and Gray, W. M., 2001, The recent increase in Atlantic hurricane activity: Causes and implications: *Science*, v. 293, p. 474-479.
- Gonzalez, L. A., and Lohmann, K. C., 1985, Carbon and oxygen isotopic composition of Holocene reef carbonates: *Geology*, v. 13, p. 811-814.
- Goodwin, D. H., Flessa, K. W., Schone, B. R., and Dettman, D. L., 2001, Cross-calibration of daily growth increments, stable isotope variation, and temperature in the Gulf of California bivalve mollusk *Chione cortezi*: Implications for paleoenvironmental analysis: *Palaios*, v. 16, p. 387-398.
- Goodwin, D. H., Flessa, K. W., Tellez-Duarte, M. A., Dettman, D. L., Schöne, B. R., and Avila-Serrano, G. A., 2004, Detecting time-averaging and spatial mixing using oxygen isotope variation: a case study: *Palaeogeography, Palaeoclimatology, Palaeoecology*, v. 205, p. 1-21.
- Greene, C. H., and Pershing, A. J., 2001, The response of *Calanus finmarchicus* populations to climate variability in the Northwest Atlantic: Basin-scale forcing associated with the North Atlantic Oscillation (NAO): *International Council for the Exploration of the Sea - Journal of Marine Science*, v. 57, p. 1536-1544.
- , 2003, The Flip-side of the North Atlantic Oscillation and modal shifts in slope-water circulation patterns: *Limnology and Oceanography*, v. 48, no. 1, p. 319-322.
- Griffies, S. M., and Bryan, K., 1997, Predictability of North Atlantic multidecadal climate variability: *Science*, v. 275, p. 181-184.

- Grossman, E. L., and Ku, T. L., 1986, Oxygen and carbon isotope fractionation in biogenic aragonite: Temperature effects: *Chemical Geology*, v. 59, p. 59-74.
- Grossman, E. L., Mii, H.-S., and Yancey, T. E., 1993, Stable isotopes in Late Pennsylvanian brachiopods from the United States: Implications for Carboniferous paleoceanography: *Geological Society of America Bulletin*, v. 105, p. 1284-1296.
- Häkkinen, S., and Rhines, P. B., 2004, Decline of subpolar North Atlantic circulation during the 1990s: *Science*, v. 304, p. 555.
- Han, G., and Li, J., 2004, Sea Surface Height and Current Variability on the Newfoundland Slope from TOPEX/Poseidon Altimetry: Canadian Technical Report, Hydrography and Ocean Sciences, 234 viii.
- Harrington, R. J., 1989, Aspects of growth deceleration in bivalves: Clues to understanding the seasonal $\delta^{18}\text{O}$ and $\delta^{13}\text{C}$ record- a comment on Krantz et al. (1987): *Paleogeography, Paleoclimatology, Paleocology*, v. 70, p. 399-403.
- Heath, D. D., Rawson, P. D., and Hilbish, T. J., 1995, PCR-based nuclear markers identify alien blue mussel (*Mytilus spp.*) genotypes on the west coast of Canada: *Canadian Journal of Fisheries and Aquatic Sciences*, v. 52, p. 2621-2627.
- Hjort, C., and Funder, S., 1974, The subfossil occurrence of *Mytilus edulis L.* in central Greenland: *Boreas*, v. 3, p. 22-33.
- Horibe, Y., and Oba, T., 1972, Temperature scales of aragonite-water systems: *Paleontological Society of Japan*, v. 23-24, p. 69-79.
- Houghton, R. W., and Fairbanks, R. G., 2001, Water sources for Georges Bank: Deep-Sea Research II, v. 48, p. 95-114.
- Hurrell, J. W., 1995, Decadal trends in the North Atlantic Oscillation: Regional temperatures and precipitation: *Science*, v. 269, p. 676-679.

- Incze, L. S., R.A., L., and Watling, L., 1980, Relationships between effects of environmental temperature and seston on growth and mortality of *Mytilus edulis* in a temperate northern estuary: *Marine Biology*, v. 57, p. 147-156.
- IPCC, 2007, *Climate Change 2007: The Physical Science Basis- Summary for Policy Makers*: Intergovernmental Panel on Climate Change.
- Ivany, L. C., Wilkinson, B. H., and Jones, D. S., 2003, Using stable isotopic data to resolve rate and duration of growth throughout ontogeny: an example from the surf clam, *Spisula solidissima*: *Palaios*, v. 18, p. 126-137.
- Johannessen, O. M., Shalina, E. V., and Miles, M. W., 1999, Satellite evidence for an Arctic sea ice cover in transformation: *Science*, v. 286, p. 1937-1939.
- Jones, D. S., 1980, Annual cycle of shell growth increment formation in two continental shelf bivalves and its paleoecologic significance: *Paleobiology*, v. 6, p. 331-340.
- , 1981, Repeating layers in the molluscan shell are not always periodic: *Journal of Paleontology*, v. 55, p. 1076-1082.
- , 1983, Sclerochronology: Reading the record of the molluscan shell: *American Scientist*, v. 71, p. 384-391.
- Jones, D. S., Arthur, M.A., and Allard, D.J., 1989, Sclerochronological records of temperature and growth from shells of *Mercenaria mercenaria* from Narragansett Bay, Rhode Island: *Marine Biology*, v. 102, p. 225-234.
- Jossi, J. W., and Goulet, J., 1993, Zooplankton trends: US north-east shelf ecosystems and adjacent regions differ from north-east Atlantic and North Sea: *International Council for the Exploration of the Sea - Journal of Marine Science*, v. 50, p. 303-313.
- Kaehler, S., and McQuaid, C. D., 1999, Use of the fluorochrome calcein as *in situ* growth marker in the brown mussel *Perna perna*: *Marine Biology*, v. 133, p. 455-460.

- Kaplan, A., Cane, M. A., Kushnir, Y., Clement, A. C., Blumenthal, M. B., and Rajagopalan, B., 1998, Analyses of global sea surface temperature 1856-1991: *Journal of Geophysical Research*, v. 103, no. C9, p. 18,567-18,589.
- Keen, M. J., and Piper, D. J. W., 1990, Geological and historical perspective, in Keen, M. J., and Williams, G. L., eds., *Geology of the continental margin of eastern Canada*: Ottawa, Canadian Government Publishing Centre, p. 5-30.
- Keigwin, L. D., 1996, The Little Ice Age and Medieval Warm Period in the Sargasso Sea: *Science*, v. 274, no. 5292, p. 1503-1508.
- Keigwin, L. D., and Pickart, R. S., 1999, Slope water current over the Laurentian Fan on interannual to millennial timescales: *Science*, v. 286, p. 520-523.
- Keigwin, L. D., Sachs, J. P., and Rosenthal, Y., 2003, A 1600-year history of the Labrador Current off Nova Scotia: *Climate Dynamics*, v. 21, p. 53-62.
- Keigwin, L. D., Sachs, J. P., Rosenthal, Y., and Boyle, E. A., 2005, The 8200 year B.P. event in the slope water system, western subpolar North Atlantic: *Paleoceanography*, v. 20, p. doi: 10.1029/2004PA001074.
- Kennish, M. J., Lutz, R. A., Dobarro, J. A., and Fritz, L. W., 1994, In situ growth rates of the ocean quahog, *Arctica islandica* (Linnaeus, 1767), in the Middle Atlantic Bight: *Journal of Shellfish Research*, v. 13, no. 2, p. 473-478.
- Killingley, J. S., and Berger, W. H., 1979, Stable isotopes in a mollusc shell: Detection of upwelling events: *Science*, v. 205, p. 186-188.
- Kim, S. T., and O'Neil, J. R., 1997, Equilibrium and nonequilibrium oxygen isotope effects in synthetic carbonates: *Geochimica et Cosmochimica Acta*, v. 61, p. 3461-3475.
- Klein, R. T., Lohmann, K. C., and Thayer, C. W., 1996, Sr/Ca and $^{13}\text{C}/^{12}\text{C}$ ratios in skeletal calcite of *Mytilus trossulus*: Covariation with metabolic rate, salinity, and carbon isotopic composition of seawater: *Geochimica et Cosmochimica Acta*, v. 60, no. 21, p. 4207-4221.

- Knight, J. R., Allan, R. J., Folland, C. K., Vellinga, M., and Mann, M. E., 2005, A signature of persistent natural thermohaline circulation cycles in observed climate: *Geophysical Research Letters*, v. 32, p. doi: 10.1029/2005GL024233.
- Knight, J. R., Folland, C. K., and Scaife, A., 2006, Climate impacts of the multidecadal oscillation: *Geophysical Research Letters*, v. 33, L17706, doi:1029/2006GL026242.
- Krabill, W., Hanna, E., Huybrechts, P., Abdalati, W., Cappelen, J., Csatho, B., Frederick, E., Manizade, S., Martin, C., Sonntag, J., Swift, R., Thomas, R., and Yungel, J., 2004, Greenland Ice Sheet: Increased coastal thinning: *Geophysical Research Letters*, v. 31, L24402, doi:10.1029/2004GL021533.
- Krantz, D. E., Jones, D. S., and Williams, D. F., 1989, Reply to “Aspects of growth deceleration in bivalves: clues to understanding the seasonal $\delta^{18}\text{O}$ and $\delta^{13}\text{C}$ record”: *Palaeogeography, Palaeoclimatology, Palaeoecology*, v. 70, p. 403-407.
- Krantz, D. E., Williams, D. F., and Jones, D. S., 1987, Ecological and paleoenvironmental information using stable isotope profiles from living and fossil molluscs: *Palaeoceanography, Paleoclimatology, Paleoecology*, v. 58, p. 249-266.
- Kraus, M. G., Beal, S. R., Chapman, S. R., and McMartin, L., 1992, A comparison of growth rates in *Arctica islandica* (Linnaeus, 1767) between field and laboratory populations: *Journal of Shellfish Research*, v. 11, no. 2, p. 289-294.
- Kreutz, K. J., Mayewski, P. A., Meeker, L. D., Twickler, M. S., Whitlow, S. I., and Pittalwala, I. P., 1997, Bipolar changes in atmospheric circulation during the Little Ice Age: *Science*, v. 277, p. 1294-1296.
- Lamb, H. H., 1965, The early Medieval warm epoch and its sequel: *Palaeogeography, Palaeoclimatology, Palaeoecology*, v. 1, p. 13-37.
- Larsen, J. C., 1992, Transport and heat flux of the Florida Current at 27°N derived from cross-stream voltages and profiling data: theory and observations: *Philosophical Transactions of the Royal Society A*, v. 338, p. 169-236.

- Lazier, J. R. N., and Wright, D. G., 1993, Annual velocity variations in the Labrador Current: *Journal of Physical Oceanography*, v. 23, p. 659-678.
- Lazzari, M., 2001, Monthly and annual means of sea surface temperature: Boothbay Harbor, Maine 1905-2004.
- Leaman, K. D., Vertes, P. S., Atkinson, L. P., Lee, T. N., Hamilton, P., and Waddell, E., 1995, Transport, potential vorticity, and current/temperature structure across Northwest Providence and Santaren Channels and the Florida Current off Cay Sal Bank: *Journal of Geophysical Research*, v. 100, no. C5, p. 8561-8569.
- Loder, J. W., Petrie, B., and Gawarkiewicz, G., 1998, The coastal ocean off northeastern North America: a large-scale view: *The Sea*, v. 11, p. 105-133.
- Loder, J. W., Shore, J. A., Hannah, C. G., and Petrie, B. D., 2001, Decadal-scale hydrographic and circulation variability in the Scotia-Maine region: *Deep-Sea Research II*, v. 48, p. 3-35.
- Lorrain, A., Paulet, Y.-M., Chauvaud, L., Dunbar, R., Mucciarone, D., and Fontugne, M., 2004, $\delta^{13}\text{C}$ variation in scallop shells: Increasing metabolic carbon contribution with body size?: *Geochimica et Cosmochimica Acta*, v. 68, no. 17, p. 3509-3519.
- Lund, D. C., and Curry, W., 2006, Florida Current surface temperature and salinity variability during the last millennium: *Paleoceanography*, v. 21, p. doi: 10.1029/2005PA001218.
- Lund, D. C., Lynch-Stieglitz, J., and Curry, W. B., 2006, Gulf Stream density structure and transport during the past millennium: *Nature*, v. 444, p. 601-604.
- Lutz, R. A., 1976, Annual growth patterns in the inner shell layer of *Mytilus edulis L.*: *Journal of Marine Biological Association of the United Kingdom*, v. 56, p. 723-731.

- Lutz, R. A., Goodsell, J. G., Castagna, M., and Stickney, A. P., 1983, Growth of experimentally cultured ocean quahogs (*Arctica islandica* L.) in north temperate embayments: *Journal of World Mariculture Society*, v. 14, p. 185-190.
- Maasch, K. A., Mayewski, P. A., Rohling, E. J., Stager, J. C., Karlen, W., Meeker, L. D., and Meyerson, E. A., 2005, A 2000-year context for modern climate change: *Geografiska Annaler*, v. 87, p. 7-15.
- Mann, M. E., Bradley, R. S., and Hughes, M. K., 1999, Northern Hemisphere temperatures during the past millennium: inferences, uncertainties, and limitations: *Geophysical Research Letters*, v. 26, no. 6, p. 759-762.
- Mann, M. E., and Lees, J., 1996, Robust estimation of background noise and signal detection in climatic time series: *Climate Change*, v. 33, p. 409-445.
- Mann, R., 1982, The Seasonal Cycle of Gonadal Development in *Arctica-Islandica* from the Southern New-England Shelf: *Fishery Bulletin*, v. 80, no. 2, p. 315-326.
- Marchitto, T. M., and deMenocal, P., 2003, Late Holocene variability of upper North Atlantic Deep Water temperature and salinity: *Geochemistry, Geophysics, Geosystems*, v. 4(12), 1100, doi:10.1029/2003GC000598.
- Marchitto, T. M., Jones, G. A., Goodfriend, G. A., and Weidman, C. R., 2000, Precise temporal correlation of Holocene mollusk shells using sclerochronology: *Quaternary Research*, v. 53, p. 236-246.
- Marsh, R., Petrie, B., Weidman, C. R., Dickson, R. R., Loder, J. W., Hannah, C. G., Frank, K., and Drinkwater, K., 1999, The 1882 tilefish kill- a cold event in shelf waters off the north-eastern United States?: *Fisheries Oceanography*, v. 8, no. 1, p. 39-49.
- Marshall, J. M., Kushnir, Y., Battisti, D., Chang, P., Czaja, A., Dickson, R., Hurrell, J., McCartney, M., Saravanan, R., and Visbeck, M., 2001, North Atlantic Climate Variability: Phenomena, Impacts and Mechanisms: *International Journal of Climatology*, v. 21, p. 1863-1898.

- McConnaughey, T., 1989a, ^{13}C and ^{18}O isotopic disequilibrium in biological carbonates: I. Patterns: *Geochimica et Cosmochimica Acta*, v. 53, p. 151-162.
- , 1989b, ^{13}C and ^{18}O isotopic disequilibrium in biological carbonates: II. In Vitro simulation of kinetic isotope effects: *Geochimica et Cosmochimica Acta*, v. 53, p. 163-171.
- McConnaughey, T. A., Burdett, J., Whelan, J. F., and Paull, C. K., 1997, Carbon isotopes in biological carbonates: respiration and photosynthesis: *Geochimica et Cosmochimica Acta*, v. 61, p. 611-622.
- McCrea, J. M., 1950, On the isotopic chemistry of carbonates and a paleotemperature scale: *Journal of Chemical Physics*, v. 18, p. 849-857.
- MERCINA, 2001, Oceanographic responses to climate in the Northwest Atlantic: *Oceanography*, v. 14, p. 76-82.
- , 2003, Trans-Atlantic responses of *Calanus finmarchicus* populations to basin-scale forcing associated with the North Atlantic Oscillation: *Progress in Oceanography*, v. 58, p. 301-312.
- Miller, J. C., and Miller, J. N., 1993, *Statistics for Analytical Chemistry*: New York, Prentice Hall, 233 p.
- Mook, W. G., 1971, Paleotemperatures and chlorinities from stable carbon and oxygen isotopes in shell carbonate: *Paleogeography, Paleoclimatology, Paleoecology*, v. 9, p. 245-263.
- Mook, W. G., and Vogel, J. C., 1968, Isotopic equilibrium between shells and their environment: *Science*, v. 159, p. 874-875.
- Myers, R. A., Helbig, J., and Holland, D., 1989, Seasonal and interannual variability of the Labrador Current and West Greenland Current: *International Council for the Exploration of the Sea - Journal of Marine Science*, v. 16, p. 18pp.

- O'Neil, J. R., Clayton, R. N., and Mayeda, T. K., 1969, Oxygen isotope fractionation in divalent metal carbonates: *Journal of Chemical Physics*, v. 51, no. 12, p. 5547-5557.
- Owen, R., Kennedy, H., and Richardson, C., 2002a, Experimental investigation into partitioning of stable isotopes between scallop (*Pecten maximus*) shell calcite and sea water: *Paleogeography, Paleoclimatology, Paleoecology*, v. 185, no. 1, p. 163-174.
- , 2002b, Isotopic partitioning between scallop shell calcite and seawater: Effect of shell growth rate: *Geochimica et Cosmochimica Acta*, v. 66, no. 10, p. 1727-1737.
- Paneth, P., and O'Leary, M. H., 1985, Carbon isotope effect on dehydration of bicarbonate ion catalyzed by carbonic-anhydrase: *Biochemistry*, v. 24, p. 5143-5147.
- Pershing, A. J., Greene, C. H., Jossi, J. W., O'Brien, L., Brodziak, J. K. T., and Bailet, B. A., 2005, Interdecadal variability in the Gulf of Maine zooplankton community, with potential impacts on fish recruitment: *International Council for the Exploration of the Sea - Journal of Marine Science*, v. 62, p. 1511-1523.
- Pershing, A. J., Greene, C. H., Planque, B., and Fromentin, J.-M., 2004, The influences of climate variability on North Atlantic zooplankton populations, *in* Stenseth, N. C., Ottersen, G., Hurrell, J., and Belgrano, A., ed., *Ecological effects of climatic variations in the North Atlantic*, Oxford University Press, p. 56-69.
- Petit, J. R., Jouzel, J., Raynaud, D., Barkov, N. I., Barnola, J. M., Basile, I., Bender, M., Chappellaz, J., Davis, M., Delaygue, G., Delmotte, M., Kotlyakov, V. M., Legrand, M., Lipenkov, V. Y., Lorius, C., Pepin, L., Ritz, C., Saltzman, E., and Stievenard, M., 1999, Climate and atmospheric history of the past 420,000 years from the Vostok ice core, Antarctica: *Nature*, v. 399, p. 429-436.
- Petrie, B., and Drinkwater, K., 1993, Temperature and salinity variability on the Scotian Shelf and in the Gulf of Maine: *Journal of Geophysical Research*, v. 98, no. C11, p. 20,079-20,090.

- Petrie, B., and Yeats, P., 2000, Annual and interannual variability of nutrients and their estimated fluxes in the Scotian Shelf- Gulf of Maine region: *Canadian Journal of Fisheries and Aquatic Sciences*, v. 57, no. 12, p. 2536-2546.
- Pettigrew, N. R., Townsend, D. W., Xue, H., Wallinga, J. P., Brickley, P. J., and Hetland, R. D., 1998, Observations of the Eastern Maine Coastal Current and its offshore extensions in 1994: *Journal of Geophysical Research*, v. 103, no. C13, p. (30), 623-639.
- Pickart, R. S., McKee, D. J., and Harrington, S. A., 1999, Mean structure and interannual variability of the slope water south of Newfoundland: *Journal of Physical Oceanography*, v. 29, p. 2541-2558.
- Pirker, J. G., and Schiel, D. R., 1993, Tetracycline as a fluorescent shell-marker in the abalone *Haliotis iris*: *Marine Biology*, v. 116, p. 81-86.
- Planque, B., and Fromentin, J., 1996, *Calanus* and the environment in eastern North Atlantic. II. Influence of the North Atlantic Oscillation on *C. finmarchicus* and *C. helgolandicus*: *Marine Ecology Progress Series*, v. 134, p. 111-118.
- Pocker, Y., and Tanaka, N., 1978, Inhibition of carbonic-anhydrase by anions in carbon dioxide-bicarbonate system: *Science*, v. 199, p. 907-909.
- Purton, L., and Brasier, M., 1999, Giant protist Nummulites and its Eocene environment: Life span and habitat insights from d18O and d13C data from Nummulites and Venericardia, Hampshire basin, UK: *Geology*, v. 27, no. 8, p. 711-714.
- Rawson, P. D., Hayhurst, S., and Vanscoyoc, B., 2001, Species composition of the blue mussel populations in the northeastern Gulf of Maine: *Journal of Shellfish Research*, v. 20, p. 31-38.
- Rawson, P. D., Joyner, K., and Hilbish, T. J., 1996, Evidence for intragenetic recombination within a novel genetic marker that distinguishes mussels in the *Mytilus edulis* species complex: *Heredity*, v. 77, p. 599-607.

- Raymo, M. E., 1994, The initiation of Northern Hemisphere glaciation: Earth and Planetary Science Letters, v. 22, p. 353-383.
- Read, K. R., and Cumming, K. B., 1967, Thermal tolerance of bivalve molluscs *modiolus* (L.), *Mytilus edulis* L., and *Brachidontes demissus*: Biochemistry Physiology, v. 22, p. 149 - 155.
- Richardson, C. A., 1989, An analysis of the microgrowth bands in the shell of the common mussel *Mytilus edulis*: Journal of Marine Biological Association of the United Kingdom, v. 69, no. 2, p. 477-491.
- Romanek, C. S., Grossman, E.L., and Morse, J.W., 1992, Carbon isotopic fractionation in synthetic aragonite and calcite: Effects of temperature and precipitation rate: Geochimica et Cosmochimica Acta, v. 56, p. 419-430.
- Ropes, J. W., Jones, D. S., Murawski, S. A., Serchuck, F. M., and Jearld, A., 1984, Documentation of annual growth lines in ocean quahogs, *Arctica islandica* Linne: Fisheries Bulletin, v. 82, no. 1, p. 1-19.
- Ropes, J. W., and Muraski, S. A., 1983, Maximum shell length and longevity in ocean Quahogs, *A. islandica* Linné: International Council for the Exploration of the Sea - Journal of Marine Science, v. K:32, p. 1-8.
- Rowell, T. W., Chaisson, D. R., and McLane, J. T., 1990, Size and age of sexual maturity and annual gametogenic cycle in the ocean quahog, *Arctica islandica* (Linnaeus, 1767), from coastal waters in Nova Scotia, Canada: Journal of Shellfish Research, v. 9, p. 195-203.
- Rye, D. M., and Sommer, M. A., II, 1980, Reconstructing paleotemperature and paleosalinity regimes with oxygen isotopes, in Rhodes, D. C., and Lutz, R. A., eds., Skeletal Growth of Aquatic Organisms: Biological Record of Environmental Change, Plenum Press, p. 169-201.
- Sachs, J. P., 2007, Cooling of Northwest Atlantic slope waters during the Holocene: Geophysical Research Letters, v. 34, p. L03609; doi: 10.1029/2006GL028495.

- Salvigsen, O., Forman, S., and Miller, G., 1992, Thermophilous molluscs on Svalbard during the Holocene and their paleoclimatic implications: *Polar Research*, v. 11, no. 1, p. 1-10.
- Schauffler, M., and Jacobson, G. L., 2002, Persistence of coastal spruce refugia during the Holocene in northern New England, USA, detected by stand-scale pollen stratigraphies: *Journal of Ecology*, v. 90, p. 235-250.
- Schnitker, D., 1975, Late glacial to recent paleoceanography of the Gulf of Maine: First Int. Symp. on Continental Margin Benthonic Foraminifera Part B: *Paleoecology and Biostratigraphy, Maritime Sediments, Special Pub. 1*, p. 385-392.
- Schöne, B. R., 2003, A 'clam-ring' master-chronology constructed from a short-lived bivalve mollusc from the northern Gulf of California: *The Holocene*, v. 13, p. 39-49.
- Schöne, B. R., Dunca, E., Fiebig, J., and Pfeiffer, M., 2005c, Mutvei's solution: an ideal agent for resolving microgrowth structures of biogenic carbonates: *Palaeogeography, Palaeoclimatology, Palaeoecology*, v. 228, p. 149-166.
- Schöne, B. R., Fiebig, J., Pfeiffer, M., Gleß, R., Hickson, J., Johnson, A., Dreyer, W., and Oschmann, W., 2005a, Climate records from a bivalve *Methuselah (Arctica islandica)*, Mollusca; Iceland): *Palaeogeography, Palaeoclimatology, Palaeoecology*, v. 228, p. 130-148.
- Schöne, B. R., Freyre Castro, A. D., Fiebig, J., Houk, S. D., Oschmann, W., and Kroncke, I., 2004, Sea surface water temperatures over the period 1884-1983 reconstructed from oxygen isotope ratios of a bivalve mollusk shell (*Arctica islandica*, southern North Sea): *Palaeogeography, Palaeoclimatology, Palaeoecology*, v. 212, p. 215-232.
- Schöne, B. R., Houk, S., Freyre Castro, A. D., Fiebig, J., Oschmann, W., Kroncke, I., Dreyer, W., and Gosselck, F., 2005b, Daily growth rates in shells of *Arctica islandica*: assessing sub-seasonal environmental controls on a long-lived bivalve mollusk: *Palaios*, v. 20, p. 78-92.

- Schöne, B. R., Oschmann, W., Rössler, J., Freyre Castro, A. D., Houk, S. D., Kröncke, I., Dreyer, W., Janssen, R., Rumohr, H., and Dunca, E., 2003, North Atlantic oscillation dynamics recorded in shells of a long-lived bivalve mollusk: *Geology*, v. 31, p. 1237-1240.
- Schöne, B. R., Tanabe, K., Dettman, D.L., and Sato, S., 2003b, Environmental controls on shell growth rates and $\delta^{18}\text{O}$ of the shallow marine bivalve mollusk *Phacosoma japonicum* in Japan: *Marine Biology*, v. 142, p. 473-485.
- Scourse, J., Richardson, C., A., Forsythe, G., Harris, I., Heinemeier, J., Fraser, N., Briffa, K., and Jones, P., 2006, First cross-matched floating chronology from the marine fossil record: data from growth lines of the long-lived bivalve mollusc *Arctica islandica*: *The Holocene*, v. 16, no. 7, p. 967-974.
- Seed, R., and Suchanek, T. H., 1992, Population and community ecology of *Mytilus*, in Gossling, E. D., ed., *The mussel Mytilus: Ecology, Physiology, Genetics and Culture: Developments in Aquaculture and Fisheries Science*, Elsevier, p. 87-170.
- Shackleton, N., 1967, Oxygen isotope analyses and Pleistocene temperatures re-assessed: *Nature*, v. 215, p. 15-17.
- Shackleton, N. J., 1974, Attainment of isotopic equilibrium between ocean water and the benthonic foraminifera genus *Uvigerina*: isotopic changes in the ocean during the last glacial: *Colloques Internationaux du Centre National du Recherche Scientifique*, v. 219, p. 203-210.
- Shackleton, N. J., Wiseman, J. D. H., and Buckley, H. A., 1973, Non-equilibrium isotopic fractionation between seawater and planktonic foraminiferal tests: *Nature*, v. 242, p. 177-179.
- Shanahan, T. M., Pigati, J. S., Dettman, D. L., and Quade, J., 2005, Isotopic variability in the aragonite shells of freshwater gastropods living in springs with nearly constant temperature and isotopic composition: *Geochimica et Cosmochimica Acta*, v. 69, no. 16, p. 3946-3966.

- Shindell, D. T., Schmidt, G. A., Mann, M. E., Rind, D., and Waple, A., 2001, Solar forcing of regional climate change during the maunder minimum: *Science*, v. 294, p. 2149-2152.
- Smith, L. C., Sheng, Y., MacDonald, G. M., and Hinzman, L. D., 2005, Disappearing Arctic lakes: *Science*, v. 308, p. 1429.
- Smith, P. C., 1983, The mean and seasonal circulation off southwest Nova Scotia: *Journal of Physical Oceanography*, v. 13, p. 1034-1054.
- Spero, H. J., Bijma, J., D.W., L., and Bemis, B. E., 1997, Effect of sea water carbonate concentration on foraminiferal carbon and oxygen isotopes: *Nature*, v. 390, p. 497-500.
- Spero, H. J., and Lea, D. W., 1993, Intraspecific stable isotope variability in the planktic foraminifera *Globigerinoides sacculifer*: Results from laboratory experiments: *Marine Micropaleontology*, v. 22, p. 221-234.
- , 1996, Experimental determination of stable isotope variability in *Globigerina bulloides*: Implications for paleoceanographic reconstructions: *Marine Micropaleontology*, v. 28, p. 231-246.
- Stuiver, M., and Reimer, P. J., 1993, Extended ^{14}C data base and revised CALIB 3.0 ^{14}C Age calibration program: *Radiocarbon*, v. 35, p. 215-230.
- Sutton, R. T., and Hodson, D. L. R., 2003, Influence of the ocean on North Atlantic climate variability 1871-1999: *Journal of Climate*, v. 16, no. 20, p. 3296-3313.
- , 2005, Atlantic Ocean Forcing of North American and European Summer Climate: *Science*, v. 309, p. 115-118.
- Swart, P. K., 1983, Carbon and oxygen isotope fractionation in scleractinian corals: a review: *Earth Science Reviews*, v. 19, p. 51-80.

- Tanaka, N., Monaghan, M. C., and Rye, D. M., 1986, Contribution of metabolic carbon to mollusc and barnacle shell carbonate: *Nature*, v. 320, p. 520-523.
- Tanaka, N., Monaghan, M. C., and Turekian, K. W., 1990, $\Delta^{14}\text{C}$ balance for the Gulf of Maine, Long Island Sound and the northern Middle Atlantic Bight: Evidence for the extent of Antarctic Intermediate Water contribution: *Journal of Marine Research*, v. 48, p. 75-87.
- Tarutani, T., Clayton, R. N., and Mayeda, T. K., 1969, The effect of polymorphism and magnesium substitution on oxygen isotope fractionation between calcium carbonate and water: *Geochimica et Cosmochimica Acta*, v. 33, p. 987-996.
- Taylor, A. H., and Stephens, J. A., 1998, The North Atlantic Oscillation and the latitude of the Gulf Stream: *Tellus*, v. 50, no. A, p. 134-142.
- Taylor, J. D., Kennedy, W. J., and Hall, A., 1969, The shell structure and mineralogy of the Bivalvia: *Bulletin of the British Museum*, v. 3, p. 1-125.
- Tebble, N., 1966, *British bivalve seashells*: London, Trustees of the British National Museum (Natural History), 212 p.
- Thiesen, B. F., 1973, The growth of *Mytilus edulis* L. (Bivalvia) from Disko and Thule district, Greenland: *Ophelia*, v. 12, p. 59-77.
- Thomas, T. C., Townsend, D. W., and Weatherbee, R., 2003, Satellite-measured phytoplankton variability in the Gulf of Maine: *Continental Shelf Research*, v. 23, p. 971-989.
- Thompson, D. J., 1982, Spectrum estimation and harmonic analysis: *Institute of Electrical and Electronics Engineers Transactions, Information Theory*, v. 70, p. 1055-1096.
- Thompson, D. J. W., and Wallace, J. M., 1998, The Arctic Oscillation signature in the wintertime geopotential height and temperature fields: *Geophysical Research Letters*, v. 25, p. 1297-1300.

- Thompson, I., Jones, D. S., and Dreibelbis, D., 1980, Annual internal growth banding and life history of the ocean quahog *Arctica islandica* (Mollusca: Bivalvia): *Marine Biology*, v. 57, p. 25-34.
- Torrence, C., and Compo, G. P., 1998, A practical guide to wavelet analysis: *Bulletin of the American Meteorological Society*, v. 79, no. 1, p. 61-78.
- Tourre, Y. M., Rajagopalan, B., and Kushnir, Y., 1999, Dominant patterns of climate variability in the Atlantic Ocean during the past 136 years: *Journal of Climate*, v. 12, p. 2285-2299.
- Townsend, D. W., Thomas, A. C., Mayer, L. M., Thomas, M., and Quinlan, J., 2006, Oceanography of the Northwestern Atlantic Continental Shelf, *in* Robin, A. R., and Brink, K.H., ed., *The Sea*, Harvard University Press, p. 119-168.
- Urey, H. C., 1947, The thermodynamic properties of isotopic substances: *Journal of the Chemical Society*, v. 1947, p. 562-581.
- Usdowski, E., and Hoefs, J., 1993, Oxygen isotope exchange between carbonic acid, bicarbonate, carbonate, and water: A re-explanation of the data of McCrea (1950) and an expression for the overall partitioning of oxygen isotopes between the carbonate species and water: *Geochimica et Cosmochimica Acta*, v. 57, p. 3815-3818.
- Vander Putten, E., Dehairs, F., Keppens, E., and Baeyens, W., 2000, High resolution distribution of trace elements in the calcite shell layer of modern *Mytilus edulis*: Environmental and biological controls: *Geochimica et Cosmochimica Acta*, v. 64, no. 6, p. 997-1011.
- Vautard, R., and Ghil, M., 1989, Singular-Spectrum analysis: A toolkit for short, noisy chaotic signals: *Physica D*, v. 35, p. 395-424.
- Wanamaker, A. D., Jr., Kreutz, K. J., Borns, H. W., Jr., Introne, D. S., Feindel, S., and Barber, B. J., 2006, An aquaculture-based method for calibrated bivalve isotope paleothermometry: *Geochemistry, Geophysics, Geosystems*, v. 7, Q09011, doi:10.1029/2005GC001189, no. 9.

- Wefer, G., and Berger, W. H., 1991, Isotope paleontology: Growth and composition of extant calcareous species: *Marine Geology*, v. 100, p. 207-248.
- Weidman, C., and Jones, G., 1993a, Development of the mollusc *Arctica islandica* as a paleoceanographic tool for reconstructing annual and seasonal records of D14C and d18O in the mid-to high-latitude North Atlantic Ocean, *Isotope Techniques in the Study of Past and Current Environmental Changes in the Hydrosphere and the Atmosphere*: Vienna, International Atomic Agency, p. 461-470.
- Weidman, C., Jones, G. A., and Lohmann, K. C., 1994, The long-lived mollusk *Arctica islandica*: A new paleoceanographic tool for the reconstruction of bottom temperatures for the continental shelves of northern Atlantic Ocean: *Journal of Geophysical Research*, v. 99, p. 18,305-18,314.
- Weidman, C. R., and Jones, G. A., 1993b, A shell-derived time history of bomb 14C on Georges Bank and its Labrador Sea implications: *Journal of Geophysical Research*, v. 98, no. C8, p. 14,577-14,588.
- Weinberg, J., 1993, Ocean quahog populations from the Middle Atlantic to the Gulf of Maine in 1992: National Marine Fisheries Service-National Oceanic and Atmospheric Administration, Woods Hole.
- Wells, H. W., and Gray, I. E., 1960, The seasonal occurrence of *Mytilus edulis* on the Carolina coast as a result of transport around Cape Hatteras: *Biology Bulletin*, v. 119, p. 550-559.
- Williams, D. F., Arthur, M. A., Jones, D. S., and Healy-Williams, N., 1982, Seasonality and mean annual sea surface temperatures from isotopic and sclerochronological records: *Nature*, v. 296, p. 432-434.
- Witbaard, R., 1996, Growth variations in *Arctica islandica* L. (Mollusca): a reflection of hydrography-related food supply: International Council for the Exploration of the Sea - *Journal of Marine Science*, v. 53, p. 981-987.

- Witbaard, R., Duinveld, G. C. A., and de Wild, P. A. W. J., 1997, A long-term growth record derived from *Arctica islandica* (Mollusca, Bivalvia) from the Fladen Ground (Northern North Sea): Journal of the Marine Biological Association of the United Kingdom, v. 77, p. 801-816.
- , 1999, Geographical differences in growth rates of *Arctica islandica* (Mollusca: Bivalvia) from the North Sea and adjacent waters: Journal of the Marine Biological Association of the United Kingdom, v. 79, p. 907-915.
- Witbaard, R., Jansma, E., and Klaassen, U. S., 2003, Copepods link quahog growth to climate: Journal of Sea Research, v. 50, no. 1, p. 77-83.
- Witbaard, R., Jenness, M. I., Borg, K., and van der & Ganssen, G., 1994, Verification of annual growth increments in *Arctica islandica* L. from the North Sea by means of oxygen and carbon isotopes: Netherlands Journal of Sea Research, v. 33, p. 91-101.
- Zeebe, R. E., Wolf-Gladrow, D. A., Bijma, J., and Honisch, B., 2003, Vital effects in planktonic foraminifera do not compromise the use of ^{11}B as a paleo-pH indicator: Evidence from modeling: Paleoceanography, v. 18, no. 2, p. 1043.
- Zhou, G. T., and Zheng, Y. F., 2003, An experimental study of oxygen isotope fractionation between inorganically precipitated aragonite and water at low temperatures: Geochimica et Cosmochimica Acta, v. 67, no. 3, p. 387-399.
- Zimov, S. A., Schuur, E. A. G., and Chapin, F. S., III, 2006, Carbon budget: Science, v. 312, p. 1612-1613.

APPENDICES

Appendix A:

SUPPLEMENTARY DATA FOR CHAPTER 2

Table A.1. Information for each column [1-13] is shown here: sample identification [1], shell oxygen isotopic values ‰ (VPDB) [2], shell carbon isotopic values ‰ (VPDB) [3], salinity (ppt) [4], shell length (mm) [5], water isotopic composition ‰ (VSMOW) [6], calcite - water (VPDB - VSMOW) [7], measured temperature (°C) [8], predicted temperature (°C) [9], temperature deviation (°C) [10], months grown [11], estimated growth rates (mm/month) [12], and estimated new linear growth (mm) [13].

1	2	3	4	5	6	7	8	9	10	11	12	13
8-33A-3/29	0.7512	-0.4244	32	12.47	-1.30	2.05	7.10	7.32	-0.22	8.5	0.10	0.85
8-33A-3/29	0.6513	-0.9404	32	10.87	-1.30	1.95	7.10	7.71	-0.61	8.5	0.10	0.85
8-33A-3/29	0.6929	-0.2974	32	19.06	-1.30	1.99	7.10	7.55	-0.45	8.5	0.10	0.85
8-33A-3/29	0.7382	-0.3144	32	15.57	-1.30	2.04	7.10	7.37	-0.27	8.5	0.10	0.85
8-33A-3/29	0.7132	-0.6304	32	14.21	-1.30	2.01	7.10	7.47	-0.37	8.5	0.10	0.85
8-33A-3/29	0.9392	-0.9854	32	21.93	-1.30	2.24	7.10	6.60	0.50	8.5	0.10	0.85
8-33A-3/29	0.9022	-0.7584	32	21.14	-1.30	2.20	7.10	6.74	0.36	8.5	0.10	0.85
8-33A-3/29	0.8692	-0.8074	32	21.10	-1.30	2.17	7.10	6.87	0.23	8.5	0.10	0.85
8-33A-3/29	0.7732	-1.0334	32	20.73	-1.30	2.07	7.10	7.24	-0.14	8.5	0.10	0.85
8-33A-3/29	0.7262	-0.7174	32	20.86	-1.30	2.03	7.10	7.42	-0.32	8.5	0.10	0.85
8-33A-3/29	0.5692	-0.7894	32	21.99	-1.30	1.87	7.10	8.03	-0.93	8.5	0.10	0.85
8-33A-3/29	0.6572	-0.5314	32	15.99	-1.30	1.96	7.10	7.69	-0.59	8.5	0.10	0.85
8-33A-3/29	0.7232	-0.3384	32	20.81	-1.30	2.02	7.10	7.43	-0.33	8.5	0.10	0.85
8-33A-3/29	0.7782	-0.6664	32	17.38	-1.30	2.08	7.10	7.22	-0.12	8.5	0.10	0.85
8-33A-3/29	0.7712	-0.8464	32	19.30	-1.30	2.07	7.10	7.24	-0.14	8.5	0.10	0.85
11-12-8-33B	0.3850	-0.8083	32	20.35	-1.64	2.03	7.39	7.42	-0.03	4.0	0.10	0.40
8-33-A	0.5450	-0.3730	32	21.41	-1.62	2.17	7.39	6.88	0.51	5.0	0.10	0.50
8-33-A	0.4340	-0.6540	32	16.53	-1.62	2.05	7.39	7.31	0.08	5.0	0.10	0.50
8-28-A	-0.8160	-2.0780	28	18.47	-2.82	2.00	7.39	7.50	-0.11	5.0	0.10	0.50
8-28-A	-0.7630	-2.1500	28	17.09	-2.82	2.06	7.39	7.30	0.09	5.0	0.10	0.50
8-28-B	-0.8550	-1.6770	28	19.86	-2.80	1.95	7.39	7.74	-0.35	5.0	0.10	0.50
8-28-B	-0.6050	-1.1550	28	18.66	-2.80	2.20	7.39	6.77	0.62	5.0	0.10	0.50
8-28-B	-0.6230	-1.4860	28	17.04	-2.80	2.18	7.39	6.84	0.55	5.0	0.10	0.50
8-23-A	-1.6300	-2.3710	23	19.88	-3.70	2.07	7.39	7.25	0.14	5.0	0.10	0.50
11-12-12-33A	-0.7110	-1.4423	32	16.77	-1.64	0.93	10.93	11.92	-0.99	4.0	0.08	0.32
11-12-12-33A	-0.5510	-1.4453	32	17.29	-1.64	1.09	10.93	11.23	-0.30	4.0	0.08	0.32
11-12-12-33A	-0.5490	-1.5183	32	15.77	-1.64	1.09	10.93	11.22	-0.29	4.0	0.08	0.32
11-12-12-33B	-0.5370	-1.7950	32	19.83	-1.56	1.02	10.93	11.51	-0.58	4.0	0.08	0.32
11-12-12-33B	-0.4220	-1.7980	32	19.54	-1.56	1.14	10.93	11.02	-0.09	4.0	0.08	0.32
11-12-12-33A	-0.4190	-1.4413	32	16.22	-1.64	1.22	10.93	10.67	0.26	4.0	0.08	0.32
11-12-12-28A	-1.7880	-2.1310	28	19.50	-2.76	0.97	10.93	11.73	-0.80	4.0	0.08	0.32
11-12-12-28A	-1.7030	-2.1660	28	19.15	-2.76	1.06	10.93	11.37	-0.44	4.0	0.08	0.32
11-12-12-28B	-1.5890	-2.4893	28	15.96	-2.79	1.20	10.93	10.76	0.17	4.0	0.08	0.32

Table A.1. (cont.) Information for each column [1-13] is shown here: sample identification [1], shell oxygen isotopic values ‰ (VPDB) [2], shell carbon isotopic values ‰ (VPDB) [3], salinity (ppt) [4], shell length (mm) [5], water isotopic composition ‰ (VSMOW) [6], calcite - water (VPDB - VSMOW) [7], measured temperature (°C) [8], predicted temperature (°C) [9], temperature deviation (°C) [10], months grown [11], estimated growth rates (mm/month) [12], and estimated new linear growth (mm) [13].

1	2	3	4	5	6	7	8	9	10	11	12	13
11-12-12-28B	-1.5740	-2.2553	28	17.65	-2.79	1.22	10.93	10.69	0.24	4.0	0.08	0.32
11-12-12-23B	-2.6750	-2.4513	23	18.44	-3.92	1.25	10.93	10.57	0.36	4.0	0.08	0.32
11-12-12-23A	-2.5880	-3.4520	23	17.75	-3.93	1.34	10.93	10.17	0.76	4.0	0.08	0.32
11-12-12-23B	-2.5700	-2.9613	23	21.04	-3.92	1.35	10.93	10.14	0.79	4.0	0.08	0.32
11-12-12-23A	-2.5170	-3.4920	23	19.32	-3.93	1.41	10.93	9.87	1.06	4.0	0.08	0.32
12-28A	-1.2160	-1.9425	28	18.04	-2.32	1.10	11.09	11.17	-0.08	5.0	0.08	0.40
12-28A	-1.0580	-1.5245	28	18.53	-2.32	1.26	11.09	10.50	0.59	5.0	0.08	0.40
12-28A	-1.1670	-1.6345	28	15.01	-2.32	1.15	11.09	10.96	0.13	5.0	0.08	0.40
12-28A	-1.1740	-1.8715	28	12.76	-2.32	1.15	11.09	10.99	0.10	5.0	0.08	0.40
12-28A	-1.1980	-1.4085	28	20.02	-2.32	1.12	11.09	11.09	0.00	5.0	0.08	0.40
12-28A	-1.2980	-2.3275	28	21.58	-2.32	1.02	11.09	11.52	-0.43	5.0	0.08	0.40
12-28A	-1.2050	-2.0245	28	22.22	-2.32	1.12	11.09	11.12	-0.03	5.0	0.08	0.40
12-28A	-1.1710	-1.7605	28	18.62	-2.32	1.15	11.09	10.98	0.11	5.0	0.08	0.40
12-28A	-1.1578	-1.5245	28	19.52	-2.32	1.16	11.09	10.92	0.17	5.0	0.08	0.40
12-28A	-1.1560	-1.6345	28	19.51	-2.32	1.16	11.09	10.91	0.18	5.0	0.08	0.40
12-28A	-1.3830	-2.1595	28	20.88	-2.32	0.94	11.09	11.88	-0.79	5.0	0.08	0.40
12-28A	-1.0000	-1.5355	28	18.34	-2.32	1.32	11.09	10.26	0.83	5.0	0.08	0.40
12-28A	-1.2650	-1.7855	28	18.61	-2.32	1.06	11.09	11.38	-0.29	5.0	0.08	0.40
12-28A	-1.1890	-1.8435	28	18.09	-2.32	1.13	11.09	11.05	0.04	5.0	0.08	0.40
11-12-16-33B	-1.4970	-2.4523	32	20.68	-1.49	-0.01	15.18	16.12	-0.94	4.0	0.09	0.36
11-12-16-33A	-1.3070	-1.8060	32	25.46	-1.61	0.30	15.18	14.69	0.49	4.0	0.09	0.36
11-12-16-33B	-1.2550	-1.8273	32	15.47	-1.49	0.24	15.18	15.00	0.18	4.0	0.09	0.36
11-12-16-33A	-1.1900	-1.8910	32	28.49	-1.61	0.42	15.18	14.16	1.02	4.0	0.09	0.36
16-33A	-1.2610	-1.9840	32	21.90	-1.35	0.09	15.18	15.68	-0.50	5.0	0.09	0.45
16-33A	-1.0550	-1.4100	32	14.67	-1.35	0.30	15.18	14.73	0.45	5.0	0.09	0.45
16-33A	-0.9840	-1.7510	32	29.53	-1.35	0.37	15.18	14.41	0.77	5.0	0.09	0.45
16-33A	-1.1750	-1.8280	32	15.71	-1.35	0.18	15.18	15.28	-0.10	5.0	0.09	0.45
16-33A	-1.1710	-1.8470	32	26.25	-1.35	0.18	15.18	15.26	-0.08	5.0	0.09	0.45
16-33A	-1.0300	-1.7540	32	27.19	-1.35	0.32	15.18	14.62	0.56	5.0	0.09	0.45
16-33A	-1.1460	-1.7870	32	18.64	-1.35	0.20	15.18	15.15	0.03	5.0	0.09	0.45
16-33A	-1.2380	-1.8190	32	17.91	-1.35	0.11	15.18	15.57	-0.39	5.0	0.09	0.45
16-33A	-1.2200	-1.8700	32	12.99	-1.35	0.13	15.18	15.49	-0.31	5.0	0.09	0.45
16-33A	-1.1280	-1.8640	32	24.04	-1.35	0.22	15.18	15.06	0.12	5.0	0.09	0.45
16-33A	-1.1880	-1.7500	32	25.79	-1.35	0.16	15.18	15.34	-0.16	5.0	0.09	0.45
16-33A	-1.2440	-2.1370	32	28.59	-1.35	0.11	15.18	15.60	-0.42	5.0	0.09	0.45
16-33A	-1.1380	-2.1340	32	19.06	-1.35	0.21	15.18	15.11	0.07	5.0	0.09	0.45
16-33A	-1.3100	-1.9090	32	22.38	-1.35	0.04	15.18	15.91	-0.73	5.0	0.09	0.45
16-33A	-1.1970	-1.7190	32	23.32	-1.35	0.15	15.18	15.38	-0.20	5.0	0.09	0.45
11-12-16-28B	-2.6870	-2.8530	28	20.74	-2.75	0.06	15.18	15.80	-0.62	4.0	0.09	0.36

Table A.1.(cont.) Information for each column [1-13] is shown here: sample identification [1], shell oxygen isotopic values ‰ (VPDB) [2], shell carbon isotopic values ‰ (VPDB) [3], salinity (ppt) [4], shell length (mm) [5], water isotopic composition ‰ (VSMOW) [6], calcite - water (VPDB - VSMOW) [7], measured temperature (°C) [8], predicted temperature (°C) [9], temperature deviation (°C) [10], months grown [11], estimated growth rates (mm/month) [12], and estimated new linear growth (mm) [13].

1	2	3	4	5	6	7	8	9	10	11	12	13
11-12-16-28B	-2.6890	-3.5800	28	21.12	-2.75	0.06	15.18	15.81	-0.63	4.0	0.09	0.36
11-12-16-28A	-2.6690	-2.9303	28	27.73	-2.73	0.06	15.18	15.81	-0.63	4.0	0.09	0.36
11-12-16-28A	-2.4880	-3.3393	28	19.88	-2.73	0.24	15.18	14.97	0.21	4.0	0.09	0.36
11-12-16-23B	-3.5400	-3.4930	23	23.31	-3.93	0.39	15.18	14.30	0.88	4.0	0.09	0.36
11-12-16-23B	-3.5337	-3.6550	23	20.44	-3.93	0.40	15.18	14.27	0.91	4.0	0.09	0.36
11-12-16-23A	-3.5037	-2.7810	23	22.99	-3.98	0.48	15.18	13.91	1.27	4.0	0.09	0.36
20-33A	-2.0720	-2.0990	32	23.85	-1.31	-0.76	19.30	19.77	-0.47	5.0	0.14	0.70
20-33A	-1.9020	-2.1300	32	21.66	-1.31	-0.59	19.30	18.93	0.37	5.0	0.14	0.70
20-33A	-2.1430	-2.5610	32	22.34	-1.31	-0.83	19.30	20.12	-0.82	5.0	0.14	0.70
20-33A	-1.9020	-2.3920	32	17.33	-1.31	-0.59	19.30	18.93	0.37	5.0	0.14	0.70
20-33A	-1.9850	-1.8050	32	16.52	-1.31	-0.68	19.30	19.34	-0.04	5.0	0.14	0.70
20-33A	-2.0123	-2.0470	32	14.90	-1.31	-0.70	19.30	19.47	-0.17	5.0	0.14	0.70
20-33A	-2.0860	-2.2160	32	17.88	-1.31	-0.78	19.30	19.84	-0.54	5.0	0.14	0.70
20-33A	-1.9760	-1.8920	32	13.95	-1.31	-0.67	19.30	19.29	0.01	5.0	0.14	0.70
20-33A	-1.9010	-2.1510	32	12.46	-1.31	-0.59	19.30	18.92	0.38	5.0	0.14	0.70
20-33B	-1.8070	-1.5930	32	26.51	-1.31	-0.50	19.30	18.46	0.84	5.0	0.14	0.70
20-33B	-1.9630	-2.4380	32	27.55	-1.31	-0.65	19.30	19.23	0.07	5.0	0.14	0.70
20-33B	-1.8123	-1.6860	32	21.00	-1.31	-0.50	19.30	18.49	0.81	5.0	0.14	0.70
20-33B	-2.0150	-2.5680	32	20.77	-1.31	-0.71	19.30	19.49	-0.19	5.0	0.14	0.70
20-33B	-1.8330	-2.3800	32	18.99	-1.31	-0.52	19.30	18.59	0.71	5.0	0.14	0.70
20-33B	-1.6510	-1.2370	32	21.34	-1.31	-0.34	19.30	17.71	1.59	5.0	0.14	0.70
20-33B	-1.9930	-2.4530	32	15.27	-1.31	-0.68	19.30	19.38	-0.08	5.0	0.14	0.70
11-12-20-33B	-2.2150	-3.3970	32	27.41	-1.56	-0.66	19.34	19.24	0.10	4.0	0.14	0.56
11-12-20-33B	-2.2140	-3.1920	32	19.67	-1.56	-0.65	19.34	19.23	0.11	4.0	0.14	0.56
11-12-20-28A	-3.4720	-3.5860	28	21.59	-2.66	-0.81	19.34	20.02	-0.68	4.0	0.14	0.56
11-12-20-28B	-3.4470	-3.2463	28	17.96	-2.72	-0.73	19.34	19.59	-0.25	4.0	0.14	0.56
11-12-20-28B	-3.3460	-3.0803	28	18.71	-2.72	-0.63	19.34	19.10	0.24	4.0	0.14	0.56
11-12-20-28A	-3.0690	-3.2950	28	25.82	-2.66	-0.41	19.34	18.04	1.30	4.0	0.14	0.56
11-12-20-23A	-4.5350	-4.1360	23	21.73	-3.88	-0.66	19.34	19.24	0.10	4.0	0.14	0.56
11-12-20-23B	-4.4590	-4.5050	23	19.70	-3.80	-0.66	19.34	19.26	0.08	4.0	0.14	0.56
11-12-20-23B	-4.4300	-4.1750	23	19.86	-3.80	-0.63	19.34	19.11	0.23	4.0	0.14	0.56
11-12-20-23A	-4.3980	-4.2780	23	15.15	-3.88	-0.52	19.34	18.57	0.77	4.0	0.14	0.56
11-12-20-23B	-4.2330	-4.1130	23	22.94	-3.80	-0.43	19.34	18.15	1.19	4.0	0.14	0.56

Appendix B:

SUPPLEMENTARY DATA FOR CHAPTER 3

Table B.1. Information for each column [1-16] is shown here: collection location / age class [1], sample ID [2], culture temperature (°C) [3], culture salinity (PSU) [4], shell $\delta^{13}\text{C}$ ‰ (VPDB) [5], shell $\delta^{18}\text{O}$ ‰ (VPDB) [6], water $\delta^{18}\text{O}$ ‰ (VSMOW) [7], $\delta^{18}\text{O}$ ‰ shell – water (VPBD-VSMOW) [8], shell length (mm) [9], growth rate (mm/month) [10], linear shell removed (mm) [11], predicted temperature (°C) [12], temperature deviation (°C) [13], estimated $\delta^{13}\text{C}$ DIC ‰ (VPDB) [14], predicted shell equilibrium $\delta^{13}\text{C}$ ‰ (VPDB) [15], estimated shell disequilibrium $\delta^{13}\text{C}$ ‰ (VPDB) [16].

1	2	3	4	5	6	7	8	9	10	11	12	13	14	15	16
Greenland/Juvenile	4-33A	4.0	32	-5.043	1.459	-1.40	2.86	18.41	0.30	0.07	4.2	-0.2	0.21	1.21	-6.25
Greenland/Juvenile	4-33A	4.0	32	-5.721	1.226	-1.40	2.63	17.73	0.30	0.15	5.0	-1.1	0.21	1.21	-6.93
Greenland/Juvenile	4-33A	4.0	32	-5.386	1.554	-1.40	2.95	18.46	0.30	0.19	3.8	0.1	0.21	1.21	-6.59
Greenland/Juvenile	4-33A	4.0	32	-4.810	1.563	-1.40	2.96	18.25	0.30	0.11	3.8	0.2	0.21	1.21	-6.02
Greenland/Juvenile	4-33A	4.0	32	-5.560	1.427	-1.40	2.83	19.04	0.30	0.24	4.3	-0.3	0.21	1.21	-6.77
Greenland/Juvenile	4-33A	4.0	32	-4.982	1.528	-1.40	2.93	19.4	0.30	0.10	3.9	0.0	0.21	1.21	-6.19
Greenland/Juvenile	4-33A	4.0	32	-5.723	1.437	-1.40	2.84	18.6	0.30	0.13	4.3	-0.3	0.21	1.21	-6.93
Greenland/Juvenile	4-33A	4.0	32	-5.289	1.503	-1.40	2.90	15.21	0.30	0.37	4.0	-0.1	0.21	1.21	-6.50
Greenland/Juvenile	4-33A	4.0	32	-4.700	1.556	-1.40	2.96	19.43	0.30	0.11	3.8	0.1	0.21	1.21	-5.91
Greenland/Juvenile	4-33A	4.0	32	-5.951	1.100	-1.40	2.50	16.82	0.30	0.22	5.5	-1.6	0.21	1.21	-7.16
Greenland/Juvenile	4-33A	4.0	32	-5.190	1.329	-1.40	2.73	16.94	0.30	0.31	4.7	-0.7	0.21	1.21	-6.40
Greenland/Juvenile	4-33A	4.0	32	-5.429	1.505	-1.40	2.90	18.92	0.30	0.12	4.0	-0.1	0.21	1.21	-6.64
Greenland/Juvenile	4-33A	4.0	32	-4.960	1.391	-1.40	2.79	15.82	0.30	0.38	4.4	-0.5	0.21	1.21	-6.17
Greenland/Juvenile	4-33A	4.0	32	-6.382	1.335	-1.40	2.73	19.53	0.30	0.40	4.6	-0.7	0.21	1.21	-7.59
Greenland/Juvenile	4-33A	4.0	32	-5.536	1.373	-1.40	2.77	19.72	0.30	0.69	4.5	-0.5	0.21	1.21	-6.74
Greenland/Juvenile	4-23B	4.0	23	-4.961	-0.382	-3.10	2.72	19.87	0.36	0.13	4.7	-0.7	-5.33	-4.33	-0.63
Greenland/Juvenile	4-23B	4.0	23	-5.051	-0.518	-3.10	2.58	20.94	0.36	0.28	5.2	-1.3	-5.33	-4.33	-0.72
Greenland/Juvenile	4-23B	4.0	23	-5.196	-0.372	-3.10	2.73	18.14	0.36	0.35	4.7	-0.7	-5.33	-4.33	-0.87
Greenland/Juvenile	4-23B	4.0	23	-4.684	-0.228	-3.10	2.87	22.86	0.36	0.18	4.1	-0.2	-5.33	-4.33	-0.36
Greenland/Juvenile	4-23B	4.0	23	-4.670	-0.259	-3.10	2.84	14.36	0.36	0.29	4.2	-0.3	-5.33	-4.33	-0.34
Greenland/Juvenile	4-23B	4.0	23	-4.757	-0.280	-3.10	2.82	17.3	0.36	0.28	4.3	-0.4	-5.33	-4.33	-0.43
Greenland/Juvenile	4-23B	4.0	23	-5.091	-0.469	-3.10	2.63	19.31	0.36	0.16	5.0	-1.1	-5.33	-4.33	-0.76
Greenland/Juvenile	4-23B	4.0	23	-5.198	-0.384	-3.10	2.72	20.72	0.36	0.42	4.7	-0.8	-5.33	-4.33	-0.87
Greenland/Juvenile	4-23B	4.0	23	-5.433	-0.305	-3.10	2.80	17.69	0.36	0.46	4.4	-0.5	-5.33	-4.33	-1.11
Greenland/Juvenile	4-23B	4.0	23	-5.282	-0.446	-3.10	2.65	21.49	0.36	0.25	4.9	-1.0	-5.33	-4.33	-0.96
Greenland/Juvenile	4-23B	4.0	23	-4.861	-0.195	-3.10	2.91	22.03	0.36	0.10	4.0	0.0	-5.33	-4.33	-0.53
Greenland/Juvenile	4-23B	4.0	23	-6.620	-0.420	-3.10	2.68	18.86	0.36	0.31	4.8	-0.9	-5.33	-4.33	-2.29
Greenland/Juvenile	4-23B	4.0	23	-5.541	-0.421	-3.10	2.68	16.76	0.36	0.29	4.8	-0.9	-5.33	-4.33	-1.21
Greenland/Juvenile	4-23B	4.0	23	-4.155	-0.306	-3.10	2.79	17.71	0.36	0.24	4.4	-0.5	-5.33	-4.33	0.17
Greenland/Juvenile	4-23B	4.0	23	-5.078	-0.254	-3.10	2.85	19.48	0.36	0.27	4.2	-0.3	-5.33	-4.33	-0.75
Greenland/Juvenile	4-23B	4.0	23	-5.366	-0.391	-3.10	2.71	18.2	0.36	0.20	4.7	-0.8	-5.33	-4.33	-1.04

Table B.1. (cont.) Information for each column [1-16] is shown here: collection location / age class [1], sample ID [2], culture temperature (°C) [3], culture salinity (PSU) [4], shell $\delta^{13}\text{C}$ ‰ (VPDB) [5], shell $\delta^{18}\text{O}$ ‰ (VPDB) [6], water $\delta^{18}\text{O}$ ‰ (VSMOW) [7], $\delta^{18}\text{O}$ ‰ shell – water (VPDB-VSMOW) [8], shell length (mm) [9], growth rate (mm/month) [10], linear shell removed (mm) [11], predicted temperature (°C) [12], temperature deviation (°C) [13], estimated $\delta^{13}\text{C}$ DIC ‰ (VPDB) [14], predicted shell equilibrium $\delta^{13}\text{C}$ ‰ (VPDB) [15], estimated shell disequilibrium $\delta^{13}\text{C}$ ‰ (VPDB) [16].

1	2	3	4	5	6	7	8	9	10	11	12	13	14	15	16
Greenland/Juvenile	8-28B	8.0	28	-6.986	-0.210	-1.96	1.75	17.17	0.36	0.20	8.5	-0.5	-2.25	-1.25	-5.73
Greenland/Juvenile	8-28B	8.0	28	-8.197	-0.310	-1.96	1.65	18.33	0.36	0.14	8.9	-0.9	-2.25	-1.25	-6.94
Greenland/Juvenile	8-28B	8.0	28	-8.189	-0.459	-1.96	1.50	18.5	0.36	0.30	9.5	-1.5	-2.25	-1.25	-6.94
Greenland/Juvenile	8-28B	8.0	28	-6.921	0.151	-1.96	2.11	20.2	0.36	0.22	7.0	1.0	-2.25	-1.25	-5.67
Greenland/Juvenile	8-28B	8.0	28	-8.298	-0.239	-1.96	1.72	19.97	0.36	0.29	8.6	-0.6	-2.25	-1.25	-7.05
Greenland/Juvenile	8-28B	8.0	28	-9.145	-0.256	-1.96	1.70	18.99	0.36	0.10	8.7	-0.7	-2.25	-1.25	-7.89
Greenland/Juvenile	8-28B	8.0	28	-8.032	-0.093	-1.96	1.87	18.48	0.36	0.18	8.0	0.0	-2.25	-1.25	-6.78
Greenland/Juvenile	8-28B	8.0	28	-8.686	-0.248	-1.96	1.71	19.2	0.36	0.18	8.7	-0.6	-2.25	-1.25	-7.43
Greenland/Juvenile	8-28B	8.0	28	-7.483	-0.172	-1.96	1.79	18.98	0.36	0.24	8.3	-0.3	-2.25	-1.25	-6.23
Greenland/Juvenile	8-28B	8.0	28	-7.826	-0.135	-1.96	1.83	17.58	0.36	0.32	8.2	-0.2	-2.25	-1.25	-6.57
Greenland/Juvenile	8-28B	8.0	28	-7.317	0.049	-1.96	2.01	15.77	0.36	0.38	7.5	0.6	-2.25	-1.25	-6.06
Greenland/Juvenile	8-28B	8.0	28	-8.004	-0.310	-1.96	1.65	16.45	0.36	0.22	8.9	-0.9	-2.25	-1.25	-6.75
Greenland/Juvenile	8-28B	8.0	28	-8.553	-0.248	-1.96	1.71	17.12	0.36	0.17	8.7	-0.6	-2.25	-1.25	-7.30
Greenland/Juvenile	8-28B	8.0	28	-8.519	-0.212	-1.96	1.75	17.21	0.36	0.31	8.5	-0.5	-2.25	-1.25	-7.27
Greenland/Juvenile	8-28B	8.0	28	-8.222	-0.211	-1.96	1.75	19.48	0.36	0.16	8.5	-0.5	-2.25	-1.25	-6.97
Greenland/Juvenile	8-28B	8.0	28	-7.654	-0.044	-1.96	1.92	17.39	0.36	0.30	7.8	0.2	-2.25	-1.25	-6.40
Greenland/Juvenile	8-33B	8.0	32	-7.180	0.156	-1.36	1.52	23.11	0.71	0.10	9.5	-1.4	0.21	1.21	-8.39
Greenland/Juvenile	8-33B	8.0	32	-6.645	0.277	-1.36	1.64	19.54	0.71	0.40	9.0	-0.9	0.21	1.21	-7.85
Greenland/Juvenile	8-33B	8.0	32	-5.357	0.163	-1.36	1.52	20.66	0.71	0.32	9.4	-1.4	0.21	1.21	-6.56
Greenland/Juvenile	8-33B	8.0	32	-6.659	0.334	-1.36	1.69	16.71	0.71	0.20	8.7	-0.7	0.21	1.21	-7.87
Greenland/Juvenile	8-33B	8.0	32	-6.365	0.420	-1.36	1.78	20.16	0.71	0.18	8.4	-0.3	0.21	1.21	-7.57
Greenland/Juvenile	8-33B	8.0	32	-6.665	0.408	-1.36	1.77	20.91	0.71	0.30	8.4	-0.4	0.21	1.21	-7.87
Greenland/Juvenile	8-33B	8.0	32	-7.276	0.424	-1.36	1.78	22.18	0.71	0.38	8.4	-0.3	0.21	1.21	-8.48
Greenland/Juvenile	8-33B	8.0	32	-7.411	0.444	-1.36	1.80	22.01	0.71	0.21	8.3	-0.2	0.21	1.21	-8.62
Greenland/Juvenile	8-33B	8.0	32	-6.707	0.417	-1.36	1.78	24.33	0.71	0.27	8.4	-0.4	0.21	1.21	-7.91
Greenland/Juvenile	8-33B	8.0	32	-6.246	0.631	-1.36	1.99	18.08	0.71	0.18	7.5	0.5	0.21	1.21	-7.45
Greenland/Juvenile	8-33B	8.0	32	-6.567	0.535	-1.36	1.89	17.10	0.71	0.29	7.9	0.1	0.21	1.21	-7.77
Greenland/Juvenile	8-33B	8.0	32	-7.132	0.442	-1.36	1.80	19.91	0.71	0.21	8.3	-0.3	0.21	1.21	-8.34
Greenland/Juvenile	8-33B	8.0	32	-6.550	0.523	-1.36	1.88	19.83	0.71	0.23	8.0	0.1	0.21	1.21	-7.76
Greenland/Juvenile	8-33B	8.0	32	-7.051	0.505	-1.36	1.86	20.50	0.71	0.14	8.0	0.0	0.21	1.21	-8.26
Greenland/Juvenile	8-33B	8.0	32	-6.352	0.506	-1.36	1.87	17.91	0.71	0.38	8.0	0.0	0.21	1.21	-7.56
Greenland/Juvenile	12-28B	11.9	28	-6.169	-1.066	-1.97	0.90	18.55	0.61	0.20	12.1	-0.2	-2.25	-1.25	-4.92
Greenland/Juvenile	12-28B	11.9	28	-6.820	-1.143	-1.97	0.83	21.02	0.61	0.25	12.4	-0.5	-2.25	-1.25	-5.57
Greenland/Juvenile	12-28B	11.9	28	-6.255	-0.944	-1.97	1.03	15.23	0.61	0.24	11.6	0.3	-2.25	-1.25	-5.00
Greenland/Juvenile	12-28B	11.9	28	-6.214	-0.791	-1.97	1.18	20.65	0.61	0.17	10.9	1.0	-2.25	-1.25	-4.96
Greenland/Juvenile	12-28B	11.9	28	-6.575	-0.994	-1.97	0.98	17.45	0.61	0.22	11.8	0.1	-2.25	-1.25	-5.32
Greenland/Juvenile	12-28B	11.9	28	-7.317	-0.926	-1.97	1.04	18.31	0.61	0.28	11.5	0.4	-2.25	-1.25	-6.06

Table B.1. (cont.) Information for each column [1-16] is shown here: collection location / age class [1], sample ID [2], culture temperature (°C) [3], culture salinity (PSU) [4], shell $\delta^{13}\text{C}$ ‰ (VPDB) [5], shell $\delta^{18}\text{O}$ ‰ (VPDB) [6], water $\delta^{18}\text{O}$ ‰ (VSMOW) [7], $\delta^{18}\text{O}$ ‰ shell – water (VPDB-VSMOW) [8], shell length (mm) [9], growth rate (mm/month) [10], linear shell removed (mm) [11], predicted temperature (°C) [12], temperature deviation (°C) [13], estimated $\delta^{13}\text{C}$ DIC ‰ (VPDB) [14], predicted shell equilibrium $\delta^{13}\text{C}$ ‰ (VPDB) [15], estimated shell disequilibrium $\delta^{13}\text{C}$ ‰ (VPDB) [16].

1	2	3	4	5	6	7	8	9	10	11	12	13	14	15	16
Greenland/Juvenile	12-28B	11.9	28	-5.741	-0.753	-1.97	1.22	19.2	0.61	0.11	10.7	1.1	-2.25	-1.25	-4.49
Greenland/Juvenile	12-28B	11.9	28	-6.906	-0.983	-1.97	0.99	21.19	0.61	0.14	11.7	0.2	-2.25	-1.25	-5.65
Greenland/Juvenile	12-28B	11.9	28	-7.131	-0.831	-1.97	1.14	19.84	0.61	0.24	11.1	0.8	-2.25	-1.25	-5.88
Greenland/Juvenile	12-28B	11.9	28	-7.403	-0.852	-1.97	1.12	15.9	0.61	0.20	11.2	0.7	-2.25	-1.25	-6.15
Greenland/Juvenile	12-28B	11.9	28	-7.564	-1.045	-1.97	0.92	22.14	0.61	0.13	12.0	-0.1	-2.25	-1.25	-6.31
Greenland/Juvenile	12-28B	11.9	28	-6.740	-0.951	-1.97	1.02	17.54	0.61	0.28	11.6	0.3	-2.25	-1.25	-5.49
Greenland/Juvenile	12-28B	11.9	28	-6.907	-0.839	-1.97	1.13	18.09	0.61	0.25	11.1	0.8	-2.25	-1.25	-5.65
Greenland/Juvenile	12-28B	11.9	28	-7.107	-0.859	-1.97	1.11	19.09	0.61	0.23	11.2	0.7	-2.25	-1.25	-5.85
Greenland/Juvenile	12-28B	11.9	28	-6.924	-0.883	-1.97	1.09	14.95	0.61	0.21	11.3	0.6	-2.25	-1.25	-5.67
Greenland/Juvenile	12-28B	11.9	28	-6.766	-1.097	-1.97	0.87	19.55	0.61	0.35	12.2	-0.3	-2.25	-1.25	-5.51
Greenland/Juvenile	12-23B	11.9	23	-7.722	-2.416	-3.13	0.71	19.45	0.57	0.33	12.9	-1.0	-5.33	-4.33	-3.40
Greenland/Juvenile	12-23B	11.9	23	-8.593	-2.266	-3.13	0.86	18.4	0.57	0.35	12.3	-0.4	-5.33	-4.33	-4.27
Greenland/Juvenile	12-23B	11.9	23	-8.382	-2.162	-3.13	0.97	21.36	0.57	0.34	11.8	0.1	-5.33	-4.33	-4.06
Greenland/Juvenile	12-23B	11.9	23	-8.535	-1.934	-3.13	1.20	19.84	0.57	0.34	10.8	1.1	-5.33	-4.33	-4.21
Greenland/Juvenile	12-23B	11.9	23	-8.319	-2.104	-3.13	1.03	16.89	0.57	0.3	11.6	0.3	-5.33	-4.33	-3.99
Greenland/Juvenile	12-23B	11.9	23	-9.314	-2.214	-3.13	0.92	23.32	0.57	0.42	12.0	-0.2	-5.33	-4.33	-4.99
Greenland/Juvenile	12-23B	11.9	23	-8.654	-2.155	-3.13	0.97	23.3	0.57	0.39	11.8	0.1	-5.33	-4.33	-4.33
Greenland/Juvenile	12-23B	11.9	23	-9.218	-2.034	-3.13	1.10	18.93	0.57	0.23	11.3	0.6	-5.33	-4.33	-4.89
Greenland/Juvenile	12-23B	11.9	23	-8.735	-2.063	-3.13	1.07	19.4	0.57	0.27	11.4	0.5	-5.33	-4.33	-4.41
Greenland/Juvenile	12-23B	11.9	23	-8.563	-2.124	-3.13	1.01	20.53	0.57	0.12	11.6	0.2	-5.33	-4.33	-4.24
Greenland/Juvenile	12-23B	11.9	23	-9.855	-2.012	-3.13	1.12	20.32	0.57	0.22	11.2	0.7	-5.33	-4.33	-5.53
Greenland/Juvenile	12-23B	11.9	23	-9.412	-2.038	-3.13	1.09	15.96	0.57	0.29	11.3	0.6	-5.33	-4.33	-5.09
Greenland/Juvenile	12-23B	11.9	23	-8.990	-2.048	-3.13	1.08	17.72	0.57	0.29	11.3	0.6	-5.33	-4.33	-4.66
Greenland/Juvenile	12-23B	11.9	23	-8.256	-2.050	-3.13	1.08	20.43	0.57	0.1	11.3	0.6	-5.33	-4.33	-3.93
Greenland/Juvenile	12-23B	11.9	23	-8.820	-1.921	-3.13	1.21	18.29	0.57	0.16	10.8	1.1	-5.33	-4.33	-4.49
Greenland/Juvenile	12-23B	11.9	23	-8.450	-2.059	-3.13	1.07	19.59	0.57	0.18	11.4	0.5	-5.33	-4.33	-4.12
Greenland/Juvenile	16-23A	15.2	23	-6.249	-2.695	-2.90	0.21	21.52	0.64	0.07	15.2	0.0	-5.33	-4.33	-1.92
Greenland/Juvenile	16-23A	15.2	23	-5.606	-2.670	-2.90	0.23	22.22	0.64	0.52	15.1	0.1	-5.33	-4.33	-1.28
Greenland/Juvenile	16-23A	15.2	23	-6.707	-2.759	-2.90	0.14	17.6	0.64	0.11	15.5	-0.3	-5.33	-4.33	-2.38
Greenland/Juvenile	16-23A	15.2	23	-6.113	-2.660	-2.90	0.24	20.13	0.64	0.37	15.1	0.1	-5.33	-4.33	-1.79
Greenland/Juvenile	16-23A	15.2	23	-6.596	-2.571	-2.90	0.33	17.18	0.64	0.38	14.7	0.5	-5.33	-4.33	-2.27
Greenland/Juvenile	16-23A	15.2	23	-5.943	-2.977	-2.90	-0.08	22.29	0.64	0.35	16.6	-1.4	-5.33	-4.33	-1.62
Greenland/Juvenile	16-23A	15.2	23	-7.058	-2.779	-2.90	0.12	15.43	0.64	0.07	15.6	-0.4	-5.33	-4.33	-2.73
Greenland/Juvenile	16-23A	15.2	23	-6.475	-2.614	-2.90	0.29	19.01	0.64	0.19	14.9	0.3	-5.33	-4.33	-2.15
Greenland/Juvenile	16-23A	15.2	23	-6.459	-2.609	-2.90	0.29	18.82	0.64	0.16	14.8	0.4	-5.33	-4.33	-2.13
Greenland/Juvenile	16-23A	15.2	23	-6.725	-2.592	-2.90	0.31	20.04	0.64	0.18	14.8	0.4	-5.33	-4.33	-2.40
Greenland/Juvenile	16-23A	15.2	23	-6.412	-2.424	-2.90	0.48	18.82	0.64	0.73	14.0	1.2	-5.33	-4.33	-2.09
Greenland/Juvenile	16-23A	15.2	23	-6.563	-2.661	-2.90	0.24	20.02	0.64	1.00	15.1	0.1	-5.33	-4.33	-2.24
Greenland/Juvenile	16-23A	15.2	23	-6.251	-2.653	-2.90	0.25	19.01	0.64	0.09	15.0	0.2	-5.33	-4.33	-1.92

Table B.1. (cont.) Information for each column [1-16] is shown here: collection location / age class [1], sample ID [2], culture temperature (°C) [3], culture salinity (PSU) [4], shell $\delta^{13}\text{C}$ ‰ (VPDB) [5], shell $\delta^{18}\text{O}$ ‰ (VPDB) [6], water $\delta^{18}\text{O}$ ‰ (VSMOW) [7], $\delta^{18}\text{O}$ ‰ shell – water (VPDB-VSMOW) [8], shell length (mm) [9], growth rate (mm/month) [10], linear shell removed (mm) [11], predicted temperature (°C) [12], temperature deviation (°C) [13], estimated $\delta^{13}\text{C}$ DIC ‰ (VPDB) [14], predicted shell equilibrium $\delta^{13}\text{C}$ ‰ (VPDB) [15], estimated shell disequilibrium $\delta^{13}\text{C}$ ‰ (VPDB) [16].

1	2	3	4	5	6	7	8	9	10	11	12	13	14	15	16	
Greenland/Juvenile	16-23A	15.2	23	-6.432	-2.539	-2.90	0.36	17.16	0.64	0.20	14.5	0.7	-5.33	-4.33	-2.11	
Greenland/Juvenile	16-23A	15.2	23	-7.084	-2.699	-2.90	0.20	16.15	0.64	0.26	15.3	-0.1	-5.33	-4.33	-2.76	
Greenland/Juvenile	16-28A	15.2	28	-7.010	-1.635	-1.95	0.32	21.52	0.83	0.33	14.7	0.5	-2.25	-1.25	-5.76	
Greenland/Juvenile	16-28A	15.2	28	-7.143	-1.519	-1.95	0.43	16.6	0.83	0.12	14.2	1.0	-2.25	-1.25	-5.89	
Greenland/Juvenile	16-28A	15.2	28	-7.177	-1.685	-1.95	0.27	21.56	0.83	0.36	15.0	0.2	-2.25	-1.25	-5.92	
Greenland/Juvenile	16-28A	15.2	28	-7.205	-1.794	-1.95	0.16	21.58	0.83	0.23	15.5	-0.3	-2.25	-1.25	-5.95	
Greenland/Juvenile	16-28A	15.2	28	-6.687	-1.578	-1.95	0.37	17.08	0.83	0.24	14.5	0.7	-2.25	-1.25	-5.43	
Greenland/Juvenile	16-28A	15.2	28	-6.699	-1.519	-1.95	0.43	15.85	0.83	0.13	14.2	1.0	-2.25	-1.25	-5.45	
Greenland/Juvenile	16-28A	15.2	28	-6.697	-1.822	-1.95	0.13	21.27	0.83	0.13	15.6	-0.4	-2.25	-1.25	-5.44	
Greenland/Juvenile	16-28A	15.2	28	-6.939	-1.604	-1.95	0.35	22.24	0.83	0.54	14.6	0.6	-2.25	-1.25	-5.69	
Greenland/Juvenile	16-28A	15.2	28	-7.058	-1.622	-1.95	0.33	17.18	0.83	0.36	14.7	0.5	-2.25	-1.25	-5.81	
Greenland/Juvenile	16-28A	15.2	28	-6.703	-1.461	-1.95	0.49	18.33	0.83	0.34	13.9	1.3	-2.25	-1.25	-5.45	
Greenland/Juvenile	16-28A	15.2	28	-6.765	-1.630	-1.95	0.32	18.73	0.83	0.33	14.7	0.5	-2.25	-1.25	-5.51	
Greenland/Juvenile	16-28A	15.2	28	-7.181	-1.631	-1.95	0.32	21.15	0.83	0.45	14.7	0.5	-2.25	-1.25	-5.93	
Maine/Adult		1	4.1	23	-4.723	-0.367	-3.10	2.73	44.09	0.11	0.10	4.64	-0.56	-5.33	-4.33	-0.39
Maine/Adult		2	4.1	23	-3.559	-0.326	-3.10	2.77	42.14	0.08	0.05	4.49	-0.41	-5.33	-4.33	0.77
Maine/Adult		3	4.1	23	-3.600	-0.397	-3.10	2.70	42.20	0.06	0.06	4.75	-0.67	-5.33	-4.33	0.73
Maine/Adult		4	4.1	23	-3.444	-0.389	-3.10	2.71	42.31	0.15	0.07	4.73	-0.65	-5.33	-4.33	0.89
Maine/Adult		5	4.1	23	-4.847	-0.335	-3.10	2.76	41.38	0.14	0.08	4.52	-0.44	-5.33	-4.33	-0.52
Maine/Adult		6	4.1	28	-4.376	0.752	-1.94	2.69	53.17	0.29	0.02	4.80	-0.72	-2.25	-1.25	-3.13
Maine/Adult		8	4.1	28	-3.472	1.014	-1.94	2.95	54.08	0.13	0.09	3.82	0.26	-2.25	-1.25	-2.22
Maine/Adult		9	4.1	28	-3.535	0.732	-1.94	2.67	51.11	0.04	0.04	4.87	-0.79	-2.25	-1.25	-2.29
Maine/Adult		10	4.1	28	-3.778	1.079	-1.94	3.02	49.10	0.07	0.05	3.58	0.50	-2.25	-1.25	-2.53
Maine/Adult		11	4.1	32	-4.335	1.509	-1.42	2.93	49.73	0.27	0.06	3.91	0.17	0.21	1.21	-5.54
Maine/Adult		12	4.1	32	-2.369	1.434	-1.42	2.85	49.79	0.03	0.04	4.19	-0.11	0.21	1.21	-3.58
Maine/Adult		13	4.1	32	-3.549	1.519	-1.42	2.94	43.19	0.15	0.04	3.87	0.21	0.21	1.21	-4.76
Maine/Adult		14	4.1	32	-4.704	1.548	-1.42	2.97	42.06	0.35	0.09	3.77	0.31	0.21	1.21	-5.91
Maine/Adult		15	4.1	32	-3.998	1.507	-1.42	2.93	43.08	0.33	0.07	3.92	0.16	0.21	1.21	-5.21
Maine/Adult		16	8.0	23	-4.507	-1.322	-3.02	1.70	57.35	0.04	0.01	8.72	-0.70	-5.33	-4.33	-0.18
Maine/Adult		17	8.0	23	-5.184	-1.310	-3.02	1.71	65.13	0.18	0.02	8.67	-0.65	-5.33	-4.33	-0.85
Maine/Adult		18	8.0	23	-4.908	-1.023	-3.02	2.00	62.77	0.02	0.03	7.50	0.52	-5.33	-4.33	-0.58
Maine/Adult		19	8.0	23	-5.347	-1.413	-3.02	1.61	54.89	0.03	0.02	9.09	-1.07	-5.33	-4.33	-1.02
Maine/Adult		20	8.0	23	-4.857	-1.236	-3.02	1.78	53.13	0.09	0.03	8.37	-0.35	-5.33	-4.33	-0.53
Maine/Adult		21	8.0	28	-5.212	0.099	-1.98	2.08	54.52	0.05	0.40	7.17	0.85	-2.25	-1.25	-3.96
Maine/Adult		26	8.0	32	-3.740	0.212	-1.57	1.78	62.97	0.02	0.10	8.37	-0.35	0.21	1.21	-4.95
Maine/Adult		30	8.0	32	-6.539	0.300	-1.57	1.87	54.04	0.16	0.13	8.01	0.01	0.21	1.21	-7.75
Maine/Adult		31	11.5	23	-5.467	-1.921	-3.05	1.13	59.71	0.10	0.09	11.11	0.40	-5.33	-4.33	-1.14
Maine/Adult		33	11.5	23	-6.226	-2.085	-3.05	0.97	58.42	0.03	0.05	11.82	-0.31	-5.33	-4.33	-1.90
Maine/Adult		34	11.5	23	-5.930	-1.982	-3.05	1.07	59.72	0.04	0.05	11.37	0.14	-5.33	-4.33	-1.60

Table B.1. (cont.) Information for each column [1-16] is shown here: collection location / age class [1], sample ID [2], culture temperature (°C) [3], culture salinity (PSU) [4], shell $\delta^{13}\text{C}$ ‰ (VPDB) [5], shell $\delta^{18}\text{O}$ ‰ (VPDB) [6], water $\delta^{18}\text{O}$ ‰ (VSMOW) [7], $\delta^{18}\text{O}$ ‰ shell – water (VPDB-VSMOW) [8], shell length (mm) [9], growth rate (mm/month) [10], linear shell removed (mm) [11], predicted temperature (°C) [12], temperature deviation (°C) [13], estimated $\delta^{13}\text{C}$ DIC ‰ (VPDB) [14], predicted shell equilibrium $\delta^{13}\text{C}$ ‰ (VPDB) [15], estimated shell disequilibrium $\delta^{13}\text{C}$ ‰ (VPDB) [16].

1	2	3	4	5	6	7	8	9	10	11	12	13	14	15	16
Maine/Adult	35	11.5	23	-2.378	-1.989	-3.05	1.06	57.29	0.03	0.07	11.41	0.10	-5.33	-4.33	1.95
Maine/Adult	36	15.0	28	-5.406	-1.503	-1.89	0.39	62.76	0.13	0.03	14.40	0.60	-2.25	-1.25	-4.16
Maine/Adult	38	15.0	28	-5.514	-1.572	-1.89	0.32	59.07	0.10	0.11	14.72	0.28	-2.25	-1.25	-4.26
Maine/Adult	40	15.0	28	-5.372	-1.611	-1.89	0.28	63.63	0.05	0.01	14.90	0.10	-2.25	-1.25	-4.12
Maine/Adult	41	11.5	32	-5.237	-0.608	-1.58	0.97	65.58	0.04	0.04	11.79	-0.28	0.21	1.21	-6.45
Maine/Adult	42	11.5	32	-6.041	-0.322	-1.58	1.26	66.32	0.03	0.05	10.56	0.95	0.21	1.21	-7.25
Maine/Adult	43	11.5	32	-4.884	-0.158	-1.58	1.42	59.28	0.06	0.05	9.86	1.65	0.21	1.21	-6.09
Maine/Adult	44	11.5	32	-5.005	-0.402	-1.58	1.18	69.71	0.02	0.05	10.90	0.61	0.21	1.21	-6.21
Maine/Adult	59	15.0	32	-6.702	-1.235	-1.51	0.28	57.34	0.09	0.11	14.91	0.09	0.21	1.21	-7.91
Maine/Adult	60	15.0	32	-6.938	-1.232	-1.51	0.28	48.12	0.05	0.14	14.90	0.10	0.21	1.21	-8.15
Greenland/Adult	61	4.1	23	-5.984	-0.425	-3.10	2.68	36.91	0.13	0.08	4.86	-0.78	-5.33	-4.33	-1.65
Greenland/Adult	63	4.1	23	-3.737	-0.331	-3.10	2.77	34.64	0.08	0.11	4.51	-0.43	-5.33	-4.33	0.59
Greenland/Adult	64	4.1	23	-3.608	-0.481	-3.10	2.62	32.71	0.05	0.10	5.07	-0.99	-5.33	-4.33	0.72
Greenland/Adult	65	4.1	23	-3.409	-0.420	-3.10	2.68	32.45	0.08	0.12	4.84	-0.76	-5.33	-4.33	0.92
Greenland/Adult	66	4.1	23	-5.987	-0.353	-3.10	2.75	32.20	0.17	0.10	4.59	-0.51	-5.33	-4.33	-1.66
Greenland/Adult	67	4.1	28	-4.261	0.661	-1.94	2.60	38.80	0.06	0.04	5.14	-1.06	-2.25	-1.25	-3.01
Greenland/Adult	68	4.1	28	-5.195	0.640	-1.94	2.58	32.10	0.14	0.02	5.22	-1.14	-2.25	-1.25	-3.95
Greenland/Adult	69	4.1	28	-4.218	0.645	-1.94	2.58	37.23	0.06	0.12	5.20	-1.12	-2.25	-1.25	-2.97
Greenland/Adult	72	4.1	28	-4.856	0.841	-1.94	2.78	39.74	0.14	0.10	4.46	-0.38	-2.25	-1.25	-3.61
Greenland/Adult	73	4.1	32	-5.178	1.260	-1.42	2.68	29.57	0.29	0.06	4.84	-0.76	0.21	1.21	-6.39
Greenland/Adult	74	4.1	32	-3.384	1.425	-1.42	2.85	39.19	0.04	0.03	4.22	-0.14	0.21	1.21	-4.59
Greenland/Adult	75	4.1	32	-4.336	1.206	-1.42	2.63	47.46	0.05	0.05	5.05	-0.97	0.21	1.21	-5.55
Greenland/Adult	76	4.1	32	-4.321	1.279	-1.42	2.70	38.17	0.21	0.13	4.77	-0.69	0.21	1.21	-5.53
Greenland/Adult	77	4.1	32	-3.921	1.297	-1.42	2.72	38.67	0.02	0.07	4.70	-0.62	0.21	1.21	-5.13
Greenland/Adult	79	8.0	23	-6.971	-1.223	-3.02	1.80	31.04	0.23	0.05	8.31	-0.29	-5.33	-4.33	-2.64
Greenland/Adult	80	8.0	23	-5.696	-1.319	-3.02	1.70	29.78	0.34	0.05	8.71	-0.69	-5.33	-4.33	-1.37
Greenland/Adult	82	8.0	23	-7.186	-1.143	-3.02	1.88	31.29	0.64	0.06	7.99	0.03	-5.33	-4.33	-2.86
Greenland/Adult	83	8.0	23	-6.781	-1.138	-3.02	1.88	28.08	0.17	0.07	7.97	0.05	-5.33	-4.33	-2.45
Greenland/Adult	84	8.0	23	-5.408	-1.326	-3.02	1.69	28.65	0.03	0.05	8.73	-0.71	-5.33	-4.33	-1.08
Greenland/Adult	85	8.0	28	-6.423	-0.151	-1.98	1.83	30.26	0.15	0.16	8.18	-0.16	-2.25	-1.25	-5.17
Greenland/Adult	86	8.0	28	-6.659	-0.116	-1.98	1.86	44.09	0.06	0.09	8.04	-0.02	-2.25	-1.25	-5.41
Greenland/Adult	88	8.0	28	-5.487	0.106	-1.98	2.09	44.76	0.07	0.04	7.15	0.87	-2.25	-1.25	-4.24
Greenland/Adult	89	8.0	28	-5.337	0.001	-1.98	1.98	47.09	0.05	0.08	7.57	0.45	-2.25	-1.25	-4.09
Greenland/Adult	90	8.0	28	-6.011	-0.157	-1.98	1.82	44.08	0.03	0.08	8.21	-0.19	-2.25	-1.25	-4.76
Greenland/Adult	91	8.0	32	-6.706	0.539	-1.57	2.11	38.25	0.08	0.05	7.05	0.97	0.21	1.21	-7.92
Greenland/Adult	92	8.0	32	-4.693	0.342	-1.57	1.91	35.03	0.05	0.07	7.84	0.18	0.21	1.21	-5.90
Greenland/Adult	93	8.0	32	-6.118	0.412	-1.57	1.98	31.45	0.08	0.03	7.56	0.46	0.21	1.21	-7.33
Greenland/Adult	94	8.0	32	-5.502	0.448	-1.57	2.02	37.09	0.03	0.04	7.42	0.60	0.21	1.21	-6.71
Greenland/Adult	95	8.0	32	-7.606	0.396	-1.57	1.97	29.52	0.09	0.10	7.63	0.39	0.21	1.21	-8.82
Greenland/Adult	98	11.5	23	-7.109	-1.943	-3.05	1.11	35.33	0.07	0.06	11.21	0.30	-5.33	-4.33	-2.78

Table B.1. (cont.) Information for each column [1-16] is shown here: collection location / age class [1], sample ID [2], culture temperature (°C) [3], culture salinity (PSU) [4], shell $\delta^{13}\text{C}$ ‰ (VPDB) [5], shell $\delta^{18}\text{O}$ ‰ (VPDB) [6], water $\delta^{18}\text{O}$ ‰ (VSMOW) [7], $\delta^{18}\text{O}$ ‰ shell – water (VPDB-VSMOW) [8], shell length (mm) [9], growth rate (mm/month) [10], linear shell removed (mm) [11], predicted temperature (°C) [12], temperature deviation (°C) [13], estimated $\delta^{13}\text{C}$ DIC ‰ (VPDB) [14], predicted shell equilibrium $\delta^{13}\text{C}$ ‰ (VPDB) [15], estimated shell disequilibrium $\delta^{13}\text{C}$ ‰ (VPDB) [16].

1	2	3	4	5	6	7	8	9	10	11	12	13	14	15	16
Greenland/Adult	99	11.5	23	-6.855	-2.027	-3.05	1.02	36.43	0.05	0.10	11.57	-0.06	-5.33	-4.33	-2.52
Greenland/Adult	100	11.5	23	-6.226	-1.765	-3.05	1.29	35.57	0.05	0.16	10.44	1.07	-5.33	-4.33	-1.90
Greenland/Adult	101	11.5	23	-6.077	-1.898	-3.05	1.15	39.83	0.02	0.04	11.01	0.50	-5.33	-4.33	-1.75
Greenland/Adult	102	11.5	23	-7.845	-1.900	-3.05	1.15	31.51	0.30	0.05	11.02	0.49	-5.33	-4.33	-3.51
Greenland/Adult	104	15.0	28	-5.412	-1.467	-1.89	0.42	30.54	0.07	0.10	14.24	0.76	-2.25	-1.25	-4.16
Greenland/Adult	105	15.0	28	-5.474	-1.465	-1.89	0.43	36.03	0.05	0.04	14.23	0.77	-2.25	-1.25	-4.22
Greenland/Adult	107	15.0	28	-6.311	-1.496	-1.89	0.39	29.34	0.10	0.08	14.37	0.63	-2.25	-1.25	-5.06
Greenland/Adult	108	15.0	28	-6.942	-1.480	-1.89	0.41	29.01	0.11	0.07	14.29	0.71	-2.25	-1.25	-5.69
Greenland/Adult	109	11.5	32	-6.435	-0.644	-1.58	0.94	33.79	0.03	0.07	11.95	-0.44	0.21	1.21	-7.64
Greenland/Adult	110	11.5	32	-6.617	-0.563	-1.58	1.02	34.67	0.07	0.06	11.60	-0.09	0.21	1.21	-7.83
Greenland/Adult	111	11.5	32	-6.885	-0.632	-1.58	0.95	31.18	0.33	0.15	11.90	-0.39	0.21	1.21	-8.09
Greenland/Adult	112	11.5	32	-5.837	-0.540	-1.58	1.04	28.96	0.10	0.11	11.50	0.01	0.21	1.21	-7.05
Greenland/Adult	113	11.5	32	-6.787	-0.530	-1.58	1.05	26.20	0.08	0.04	11.45	0.06	0.21	1.21	-8.00
Greenland/Adult	114	11.5	32	-6.085	-0.397	-1.58	1.18	30.92	0.03	0.30	10.88	0.63	0.21	1.21	-7.29
Greenland/Adult	115	15.0	23	-6.929	-2.731	-3.02	0.29	31.12	0.05	0.11	14.85	0.15	-5.33	-4.33	-2.60
Greenland/Adult	116	15.0	23	-6.945	-2.567	-3.02	0.45	36.09	0.09	0.11	14.10	0.90	-5.33	-4.33	-2.62
Greenland/Adult	117	15.0	23	-8.436	-2.817	-3.02	0.20	28.22	0.10	0.16	15.24	-0.24	-5.33	-4.33	-4.11
Greenland/Adult	118	15.0	23	-8.205	-2.928	-3.02	0.09	34.78	0.06	0.07	15.76	-0.76	-5.33	-4.33	-3.88
Greenland/Adult	119	15.0	23	-7.954	-2.752	-3.02	0.27	30.80	0.05	0.10	14.94	0.06	-5.33	-4.33	-3.62
Greenland/Adult	120	15.0	23	-5.203	-2.822	-3.02	0.20	32.46	0.09	0.07	15.27	-0.27	-5.33	-4.33	-0.87
Greenland/Adult	122	15.0	28	-7.453	-1.698	-1.81	0.11	30.87	0.17	0.12	15.67	-0.67	-2.25	-1.25	-6.20
Greenland/Adult	123	15.0	28	-7.766	-1.708	-1.81	0.10	28.24	0.19	0.10	15.71	-0.71	-2.25	-1.25	-6.52
Greenland/Adult	124	15.0	28	-7.324	-1.695	-1.81	0.12	41.12	0.17	0.07	15.65	-0.65	-2.25	-1.25	-6.07
Greenland/Adult	125	15.0	28	-7.234	-1.606	-1.81	0.20	33.42	0.16	0.16	15.24	-0.24	-2.25	-1.25	-5.98
Greenland/Adult	126	15.0	28	-8.824	-1.671	-1.81	0.14	36.20	0.13	0.06	15.54	-0.54	-2.25	-1.25	-7.57
Greenland/Adult	127	15.0	32	-8.305	-1.318	-1.51	0.19	38.10	0.17	0.10	15.30	-0.30	0.21	1.21	-9.52
Greenland/Adult	128	15.0	32	-7.959	-1.312	-1.51	0.20	37.49	0.12	0.08	15.27	-0.27	0.21	1.21	-9.17
Greenland/Adult	129	15.0	32	-5.119	-1.221	-1.51	0.29	39.02	0.03	0.08	14.85	0.15	0.21	1.21	-6.33
Greenland/Adult	130	15.0	32	-7.791	-1.197	-1.51	0.31	42.99	0.09	0.06	14.74	0.26	0.21	1.21	-9.00
Greenland/Adult	131	15.0	32	-6.859	-1.082	-1.51	0.43	39.95	0.03	0.07	14.21	0.79	0.21	1.21	-8.07
Greenland/Adult	132	15.0	32	-8.854	-1.242	-1.51	0.27	31.95	0.22	0.05	14.95	0.05	0.21	1.21	-10.06

Appendix C:

SUPPLEMENTARY TEXT AND FIGURES FOR CHAPTER 6

High-resolution oxygen isotope profiles from bivalve shells (and corals) provide a method for investigating subannual changes in hydrographic conditions (water temperature and salinity). Specifically, if the sampling resolution allows for at least four carbonate samples to be extracted between annual growth layers, changes in seasonality of shell growth can be determined (Figs. C.1., C.2.). Further, maximum and minimum in shell $\delta^{18}\text{O}_c$ values provide valuable information about the severity of extreme seasons such as winter and summer. Although marine sediment records (e.g., alkenones, $\delta^{18}\text{O}$ and Sr/Ca ratios of biogenic material, % abundance of environmentally sensitive taxa, etc.) can provide valuable information about low-frequency changes in the ocean, they lack the ability to document high-frequency changes because sedimentation rates are generally too low in most oceanographic settings. Thus bivalves and corals are better suited to document sub-annual to annual changes in ocean conditions, although these records tend to be much shorter than marine sediment records. Currently, it is possible to develop sub-annual $\delta^{18}\text{O}_c$ records for centuries by overlapping shells of varying ages with modern shell samples that were collected alive.

Distinct changes in seasonality are noted in each shell record (Figs. C.1., C.2.). Most notably, $\delta^{18}\text{O}_c$ values from shell SBVC9609-30cm (ca. 1357 \pm 40 AD) demonstrate an attenuation of the seasonal cycle (near sample 100) for approximately 5-6 years. $\delta^{18}\text{O}_c$ values from shell SBVC9609-40cm (ca. 1320 \pm 45 AD) indicate a strong seasonal cycle (samples 100-250) for about four years, followed by decreased seasonality. $\delta^{18}\text{O}_c$ values from shell SBVC9609-48cm show decreasing mean water temperatures (more positive $\delta^{18}\text{O}_c$ values) for the first 250 micro-samples, followed by decreased seasonality and steady mean water temperatures. The modern shell (SF1; ca. 1864) includes \sim 20

years of seasonality information, and $\delta^{18}\text{O}_c$ values from SF1 indicate highly variable oceanographic conditions throughout the record. Combined, the shell records noted here offer an insight to seasonal changes in hydrographic conditions in the Western Gulf of Maine for windows of time during the late Holocene. Currently, these shell $\delta^{18}\text{O}_c$ profiles are the only records of seasonality from the Gulf of Maine prior to 1905. These data offer a significant advance in high-resolution paleoceanographic applications. A more thorough description of these data will follow this dissertation. Additionally, I will investigate the seasonal timing of annual growth bands using oxygen isotope profiles from *Arctica islandica* L. from around the North Atlantic. This will facilitate a better understanding of the timing of growth cessation, and hence the formation of annual growth bands. This future study will ultimately aid in the development of assigning monthly to seasonal values (spring, summer, fall, winter) to shell $\delta^{18}\text{O}_c$ values.

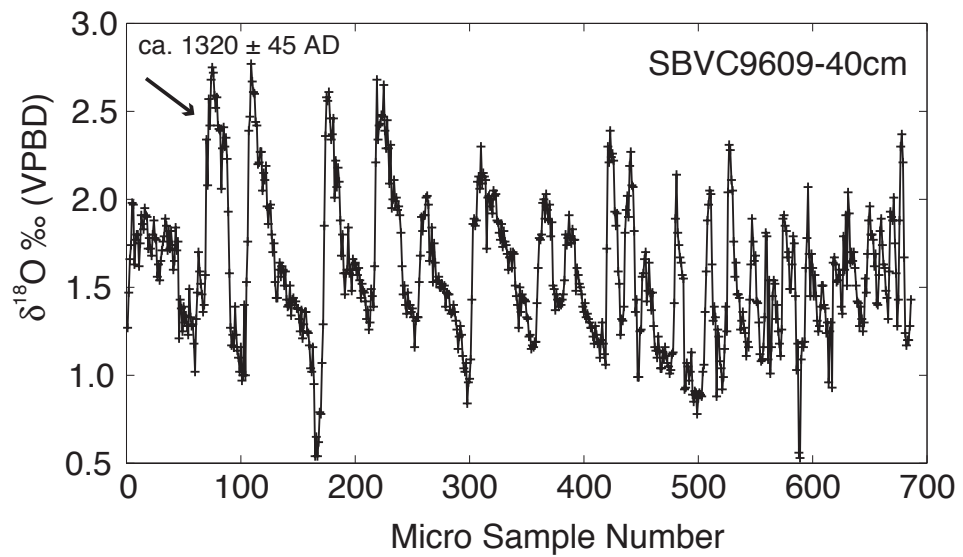
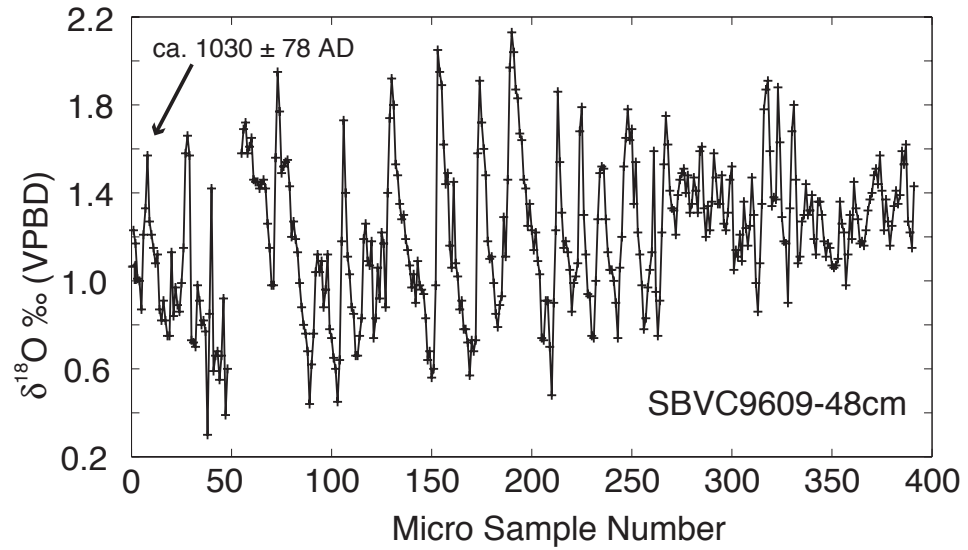


Figure C.1. High-resolution oxygen isotope profiles for shells SBVC9609-48cm (top) and SBVC9609-40cm (bottom) are shown with an approximate calendar age. Data shown here represents at least four carbonate samples per annual cycle.

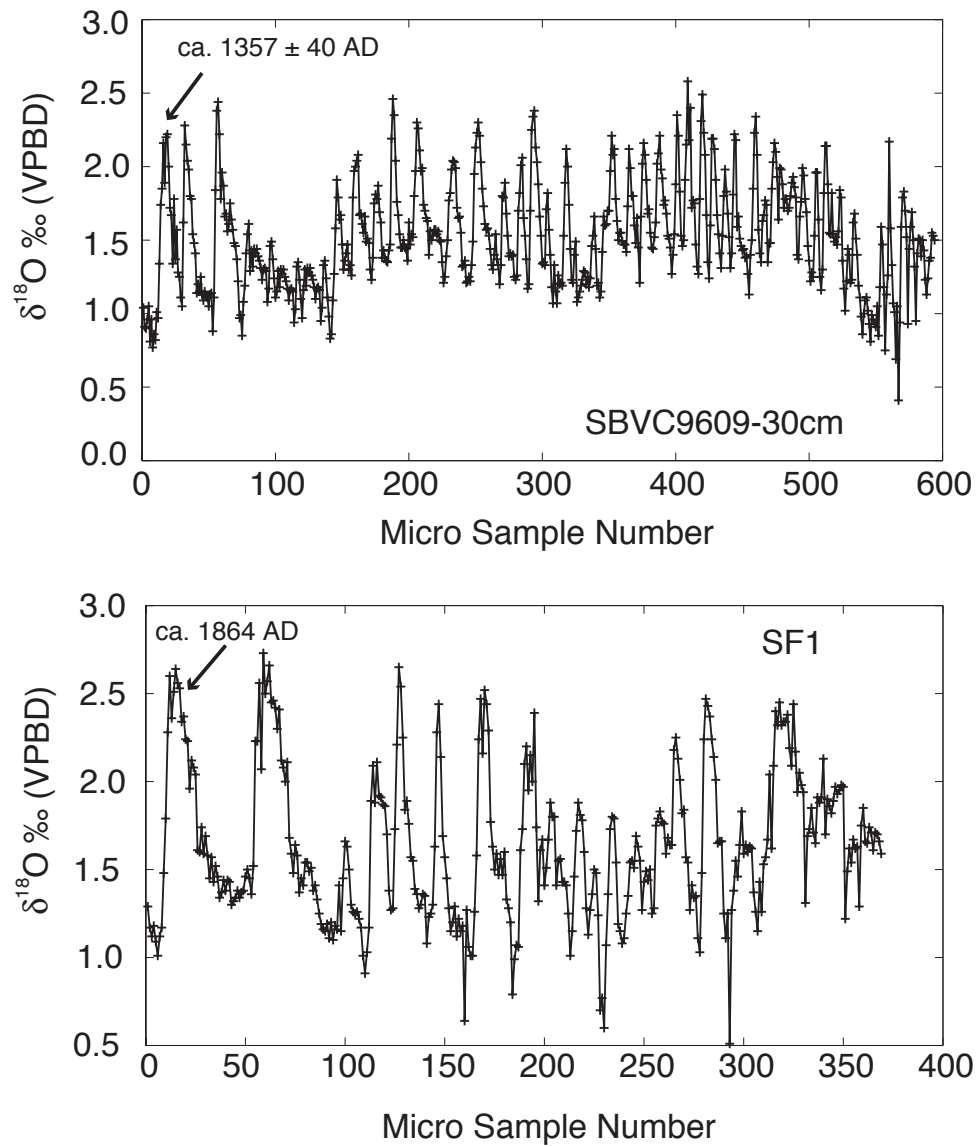


Figure C.2. High-resolution oxygen isotope profiles for shells SBVC9609-30cm (top) and SF1 (bottom) are shown with an approximate calendar age. Data shown here represents at least four carbonate samples per annual cycle.

BIOGRAPHY OF THE AUTHOR

Alan D. Wanamaker Jr. was born in Lowell, Massachusetts on January 24, 1970. He grew up in Billerica, MA, and he graduated from high school (Shawsheen Valley Regional Technical High School - Electronics Program) in 1988. For the next two years, he studied Electrical Engineering at the University of Massachusetts. In 1990, the author joined the United States Marine Corps, where he served from 1990 – 1995 as a secure electronics technician. While serving in the Marine Corps, he earned an Associate in Science degree from Quincy College in 1995. After departing from military service, the author enrolled at the University of New Hampshire. He earned a Bachelor of Arts in Earth Science Teaching in 1997, and a Master of Arts in Secondary Education in 1998. From 1997 to 2002, the author taught high school science in New Hampshire and Maine. In 2002, he joined the Department of Earth Sciences at the University of Maine. He is a candidate for the Doctor of Philosophy degree in Earth Sciences in May, 2007.